D. Kranzlmüller • H. Brüchle • M. Brehm *EDITORS*

High Performance Computing

– on the Tier-2 System CoolMUC –

in Science and Engineering
Garching/Munich 2018

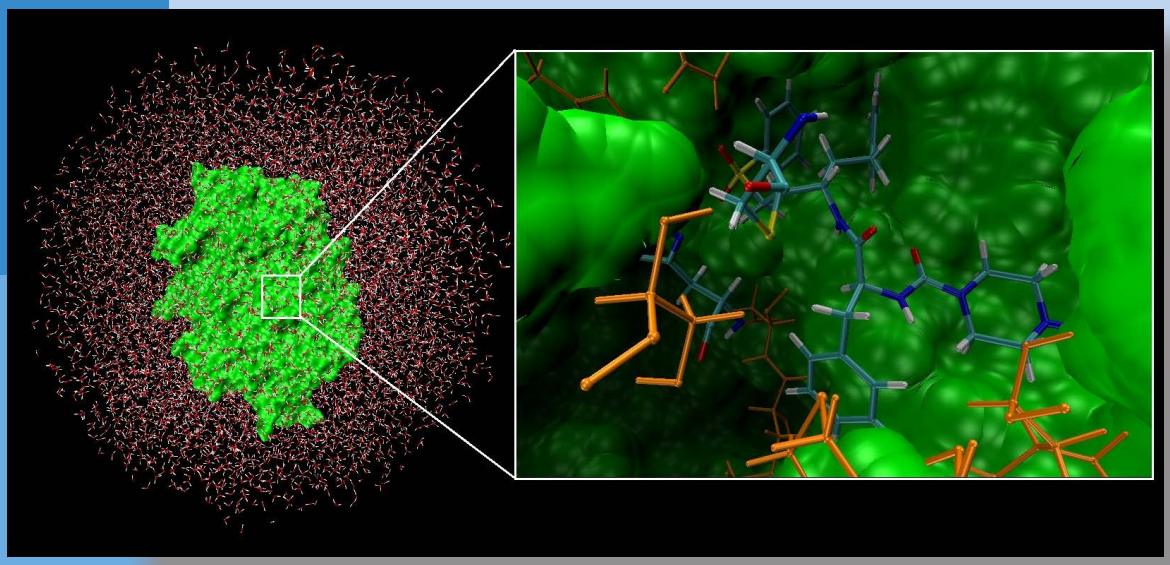

lrz Leibniz Supercomputing Centre
of the Bavarian Academy of Sciences and Humanities
BAdW

Impressum:

Bayerische Akademie der Wissenschaften
Alfons-Goppel-Str. 11, D-80539 München
info@badw.de, www.badw.de

Leibniz-Rechenzentrum (LRZ)
Boltzmannstraße 1, D-85748 Garching bei München
lrzpost@lrz.de, www.lrz.de

Herausgeber: Dieter Kranzlmüller, Helmut Brüchle, Matthias Brehm
Redaktion: Helmut Brüchle
Gestaltungskonzept: Tausendblauwerk, Konrad-Adenauer-Straße 22, 85221 Dachau, www.tausendblauwerk.de
Druck und Bindung: Mayr & Abel Druck GmbH, Marktplatz 2, 87764 Legau.

Das Titelbild zeigt das Enzym Rhodesain (grün) in einer Wasserbox. Der Inhibitor ist Kovalent-Irreversibel an das CYS25-Residuum gebunden. Unterschiedliche, interessante Aminosäuren für weitergehende quantenmechanische Berechnungen sind Orange eingefärbt.
Siehe Seite 32 für weitere Informationen.
Bild Vorwort: Andreas Heddergott; Bilder Umschlag-Rückseite: Megware (CoolMUC-1), Michael Klinksik (CoolMUC-2), LRZ (CoolMUC-3).

Bezugsadresse:

Leibniz-Rechenzentrum (LRZ)
Boltzmannstraße 1, D-85748 Garching bei München
https://www.lrz.de/hpcbooks

ISBN 978-3-9816675-3-0

D. Kranzlmüller • H. Brüchle • M. Brehm *EDITORS*

High Performance Computing

– on the Tier-2 System CoolMUC –

in Science and Engineering Garching/Munich 2018

Leibniz Supercomputing Centre
of the Bavarian Academy of Sciences and Humanities

Table of Contents

Chapter 03 - Computer Science and Mathematics

Chapter 04 - Earth Climate Environmental Sciences

Chapter 05 - High Engergy Physics

Chapter 06 - Life Sciences

Appendix

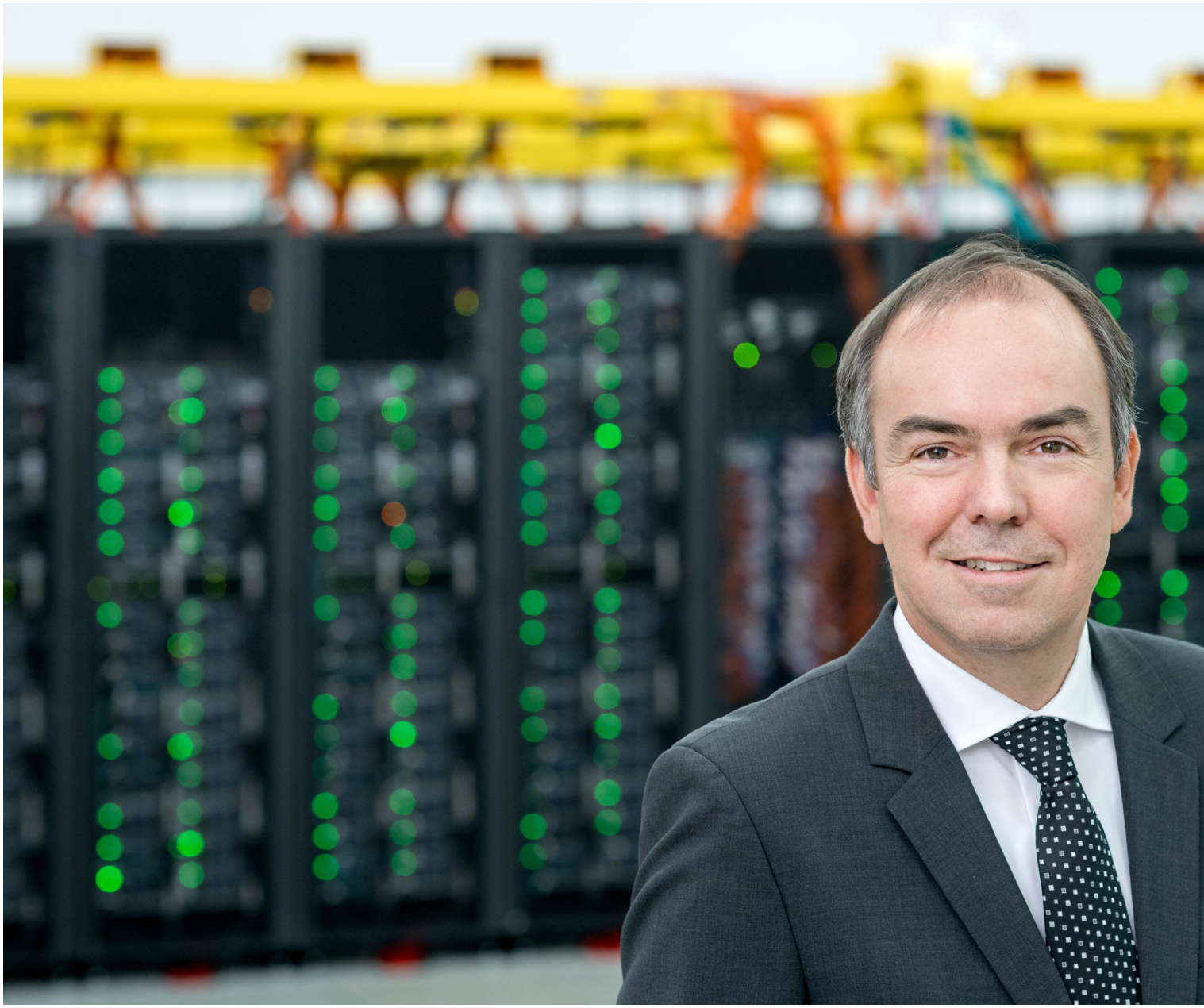

Prof. Dr. Dieter Kranzlmüller is Chairman of the Board of Directors at the Leibniz Supercomputing Centre.

CoolMUC: The Bavarian Tier-2 HPC Resource

The Leibniz Supercomputing Centre has a long tradition of offering HPC resources to Bavarian Universities. The latest embodiments of Tier-2 systems are:

- CoolMUC-1: The first cluster worldwide that used direct warm water cooling, and also the prototype system for the Tier-1 HPC system SuperMUC.
- CoolMUC-2: A cluster offering the same architecture as SuperMUC Phase 2 and ranked 261 in the TOP500 list in 2015.
- CoolMUC-3: A prototype system featuring Intels Many-Core architecture and the first 100% warm water cooled cluster.

In 2012, CoolMUC-1 received the German datacenter award 2012 in the category energy and resource efficient datacenter for its innovative cooling using warm water, which makes the cooling much more efficient and makes additional chillers redundant. In 2018, CoolMUC-3 received the German datacenter award in the category datacenter air conditioning and cooling.

Tier-2 systems at LRZ: CoolMUC-1, CoolMUC-2, and CoolMUC-3

CoolMUC-1 was installed in the summer of 2011. It had 178 dual socket compute nodes with AMD Magny Cours processors (2.0 GHz, 16GB memory) and Infiniband QDR interconnect using a fat tree topology. The system had 2,848 Cores, 2.8 TByte memory, and a peak performance of 22.7 TFLOP/s. Two Gbit Ethernet ports were used for IPMI and a service network, which was used to boot the diskless nodes and to provide the root file system over NFS. A network bridge component connected the Infiniband network to the upstream Ethernet services at LRZ.

In June 2015, the LRZ started user operation of the CoolMUC-2. The system was ranked 315 in the TOP500 list in June 2015 with a peak performance of 230.8 TFLOP/s. The machine had 252 nodes and 7,056 cores (Intel Haswell EP, FDR14 Infiniband interconnect). In November 2015, CoolMUC-2 was extended to 400 nodes and 11,200 cores, achieving a peak performance of 366.4 TFLOP/s, which resulted in rank 261 of the TOP500 list.

Early 2017, CoolMUC-3 started user operation with 148 nodes, 9,472 cores, Intel Knights Landing, 14.2 TByte, Intel Omnipath interconnect, and a peak performance of 383 TFLOP/s.

Advancing science by using LRZ computing resources

The Leibniz Supercomputing Centre supplies its Tier-2 high performance computing resources to students, researchers and research teams from Bavarian Universities.

Twice a year, users can submit proposals to KONWIHR, the Bavarian Competence Network for Technical and Scientific High Performance Computing. KONWIHR has a strong focus on porting, optimizing, and increasing the parallelization of user applications and libraries. Applicants with KONWIHR funding bring their own codes into the project and work closely together with application experts from the LRZ, spending a significant amount of time at the LRZ, to be able to work closely together with LRZ staff.

In this book, we present 44 reports from projects that used the LRZ Tier-2 HPC resources in the 2015-2018 period and consumed 138 mio core hours on CoolMUC-2. In the 2015-2018 period, the TOP 50 projects that used CoolMUC produced 8 B.Sc. thesis, 27 M.Sc. thesis, 17 PhD thesis, and one Habilitation thesis. Additionally, 15 students used the CoolMUC systems for internship programs. The TOP 50 projects published 82 papers in peer reviewed journals, used the CoolMUC systems in 31 third-party funded projects, had 11 collaborations within their university, and participated in 30 collaborations with external partners.

Acknowledgments

We gratefully acknowledge the continued support of the Free State of Bavaria and the German Research Foundation (DFG) for funding of infrastructure, high performance computing hardware, and the funding of staff to operate the systems and provide application support to our users. We thank the Bavarian Competence Network for Technical and Scientific High Performance Computing (KONWIHR) for funding research projects on CoolMUC.

Garching near Munich, December 2018

Dieter Kranzlmüller
Helmut Brüchle
Matthias Brehm

Chemistry and Material Sciences

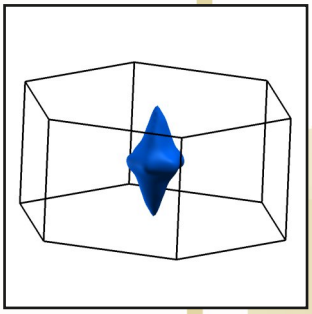

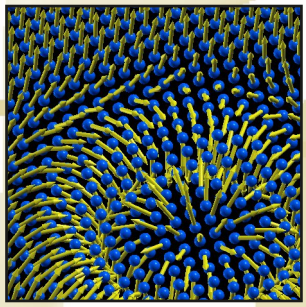

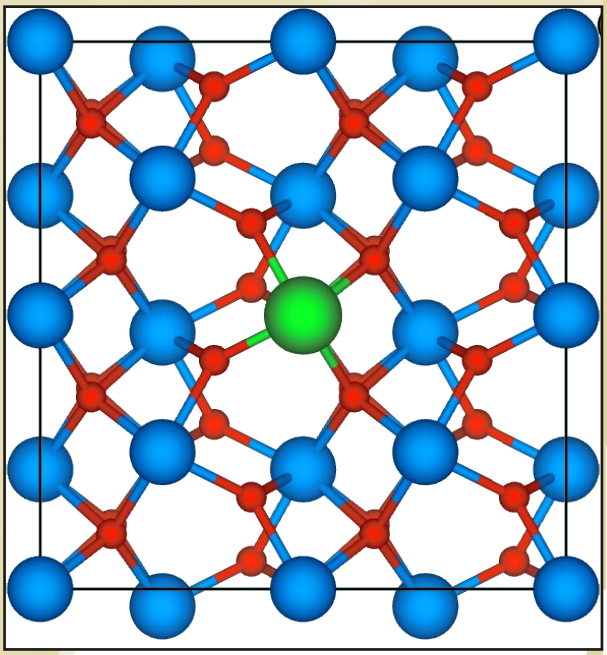

Mechanism of Ferroelectric and Antiferroelectric HfO2 from doping

1

Research Institution
Modeling and Simulation Lab, Department of Applied Sciences and Mechatronics, University of Applied Sciences Munich

Principal Investigator
Alfred Kersch

Researchers
Christopher Künneth, Robin Materlik, Max Falkowski

Project Partners
NamLab gGmbH Dresden, Electronic Materials Research Lab RWTH Aachen

Linux Cluster Project ID: p6001

Introduction

Hafnia (HfO2) is well-known and extensively studied for its high dielectric constant ("high-k dielectrics"), making it an excellent replacement for conventional SiO2 dielectrics and facilitating miniaturization of microelectronic devices. However, the recent unexpected observations of ferroelectricity in thin films of pure and doped hafnia have generated renewed excitement in this material [2]. Stable ferroelectric behavior along with excellent Si-compatibility, easy complementary metal oxide semiconductor (CMOS) integration, and high scalability make hafnia a promising candidate for future non-volatile memory applications. Other applications, including pyroelectric energy harvesting and electrocaloric cooling, are based on the antiferroelectric behavior and have also been proposed. Research directed at understanding the underlying origins of ferroelectricity and antiferroelectricity have intensified.

Funded by the DFG, there has been an extensive computational investigation of the material properties [1]. Apart from identifying the potential polar phase in hafnia, attempts have been made to understand factors that lead to the emergence of these polar phases in thin films, which would otherwise be metastable. One important stabilization factor is extrinsic doping on the level of a few percent. Interestingly, ferroelectric as well as the transition to antiferroelectric (field induced ferroelectricity) behaviour can be induced with some dopants in specific concentrations. Experimentally, such a transition has been found for Si doping and Al doping. Other dopants like Y or La show only ferroelectric behavior.

The effect of doping and a transition from ferroelectric to antiferroelectric behaviour can in principle be understood with the Landau–Devonshire model of ferroelectricity, see Fig. 1.

The free energy G(x) as a function of the reaction coordinate x (representing the polarization P as well,

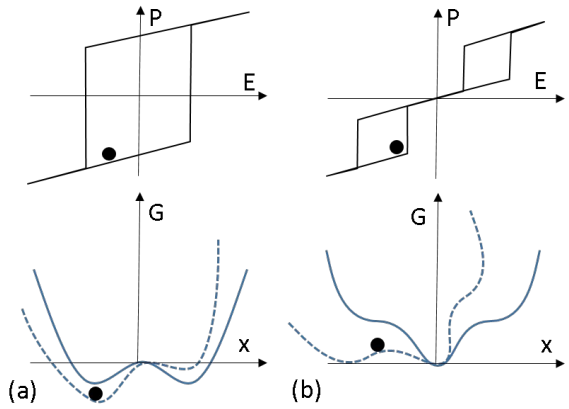

Figure 1: Landau-Devonshire model of the (a) ferroelectric and (b) antiferroelectric characteristics.

x=P) interpolating between a non-polar phase (x=0) and a polar phase (x=±x0) may be represented by Figure 1 (a) where the polar phase is below the non-polar phase in free energy G(x0)<G(0) leading to ferroelectric behaviour, or by Figure 1 (b) with a non-polar phase lower in free energy than the polar phase G(x0)>G(0) leading to antiferroelectric behaviour. The question raised here is if the various dopants act on the free energy in a way consistent with experiments (validation) and if by simulation new dopants with a better functionality could be found (material design).

A problem with the simulation of the influence of dopants in a crystal concerns the incorporation of the defect in the structure. Figure 2 shows the replacement of a III-valent dopant with a IV-valent Hf atom as example. In Figure 2(a), the dopant may preserve the lattice bonds, but then there must be an electronic charge compensation. In Figure 2(b), the defect may be electrically neutral, but then the lattice bonds have to rearrange and include an oxygen vacancy for two dopants. Or there is an intermediate case including defect charges and a vacancy for a single dopant. The concentration of the various defects depends on the processing conditions as

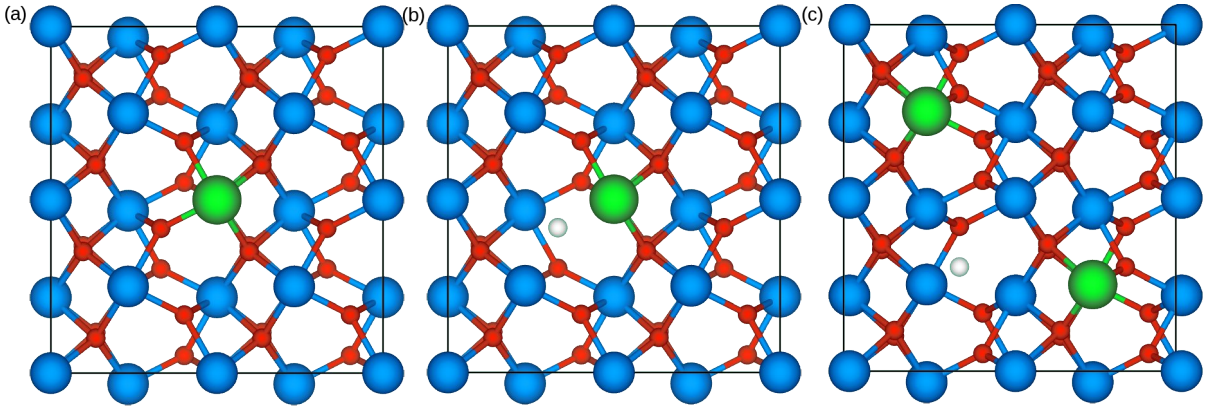

Figure 2: Supercell of a (a) electronically compensated, (b) mixed compensated and (c) ionically compensated defect. Blue: Hf, red: O, green:dopant M, white: vacancy.

there are temperature and especially oxygen partial pressure. The large number of possible defect structures (Figure 2 (a) is unique, but each defect type (b) or (c) has many different configurations) has the consequence, that all have to be calculated to assess the situation. After the defect structure is decided (which is experimentally almost impossible), the free energy can be determined.

Results and Methods

The crystal structures are simulated on the atomic scale, on the level of quantum mechanics with the simulation package Aims [3] or Abinit [4]. The electron distribution in the crystal is calculated with density functional theory (DFT). Afterwards, the forces between the atoms are derived and new positions of the atoms closer to the equilibrium is searched iteratively until a convergence is reached. For doping and defects on the percent level, structures up to 100 atoms have to be investigated. Each calculation is scaled on up to 1000 cores and runs for 12 h – 48 h. Due to the large amount of competing crystallographic structures and several relevant conditions that may contribute to the stabilization of the phases, two millions of CPU-hours have been used for the results shown below.

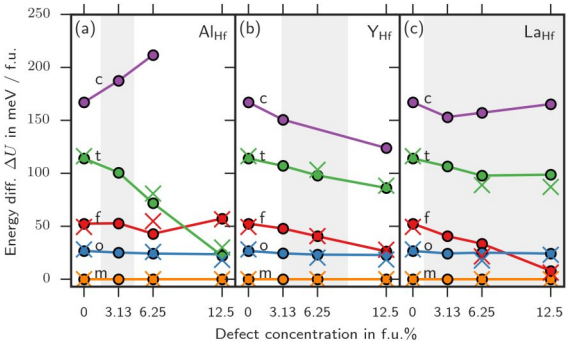

Figure 3: Effect of electronically compensated substitutional defects MHf on the total energy differences of HfO2 polymorphs relative to the m-phase.

The III-valent dopants Al, Y and La were explored. It was found that under the thin film processing conditions (with atomic layer deposition(ALD)) the creation of electronically compensated structures were the most likely. The results for these kind of defects are shown for the dopants Al, Y and La in Figure 3. The diagrams show the total energy of the competing crystallographic phases (m=monoclinic, o=non-polar orthorhombic, f=polar orthorhombic, t=tetragonal, c=cubic). For Al the t-phase energy is below the f-phase energy, and for increasing concentration of Al, antiferroelectric behavior is possible. For Y and La this behavior is not possible.

The results do not explain why in thin films in a thickness range of a few 10 nm the o-phase and the m-phase do not always appear. To a part, this has been explained by surface energy contributions to the Gibbs energy. To another part, it could be related to the crystallization kinetics.

On-going Research / Outlook

The surface energy contribution as well as the crystallization kinetics is determined from interface energies. It is planned to determine values with different simulation methods to establish a basis for a multiscale model.

References and Links

[1] M. Park et al., Advanced Materials 27, 1811 (2015)
[2] V. Blum et al., Comput. Phys. Commun., vol. 180, no. 11, pp. 2175–2196, 2009.
[3] X. Gonze et al., Comput. Phys. Commun., vol. 180, no. 12, pp. 2582–2615, 2009.
[4] R. Materlik, C. Künneth, T. Mikolajick, and A. Kersch, Appl. Phys. Lett. 111, 082902 (2017)
[5] C. Künneth, R. Materlik,, M. Falkowski, A. Kersch, ACS Appl. Nano Mater. 1, 254-264 (2017)
[6] R. Materlik, C. Künneth, M. Falkowski, A. Kersch, J Appl. Phys. 123 (16), 164101 (2018)

Optimization of Nanodiamond Based Dielectric

1

Single-Photon Sources

Research Institution
Department für Physik, Ludwig-Maximilians-Universität München

Principal Investigator
Harald Weinfurter

Researchers
Martin Zeitlmair, Lars Liebermeister, Wenjamin Rosenfeld

Linux Cluster Project ID: pr23nu

Introduction

Both quantum information science as well as novel schemes for unbreakable cryptography require carriers of information at the fundamental level. For the implementation of novel information processing schemes based on quantum effects and communication over long distances using light as the carrier of information, single photons have become a valuable resource. Efficient and reliable single-photon sources are thus of utmost importance. In this context, single-photon source means that the light source by definition emits only one single quantum of light at a time (in contrast to, e.g., attenuated laser light, where the number of photons is described by a Poissonian distribution).

Our single-photon sources are based on single colour centers in nanodiamonds, a system comprising of a dopant atom in the diamond host lattice accompanied by one or more vacancy sites. Due to its position in the large energetic band gap of diamond, it is well isolated and emits single photons even at ambient temperatures.

For controlling the propagation of photons and efficient extraction of the emitted light, additional waveguiding structures for light confinement and redirection are needed. As the emission linewidth of colour centers can be significantly broadened due to the influence of phonon coupling, the nanophotonic structures should provide strong coupling of the emitted light over a broad spectral range. Here, purely dielectric waveguide structures are advantageous as their working principle, the high contrast of the refractive index between the employed materials and the surrounding, is subject to very little dispersion. In addition, for strong coupling of light emitted by colour centers to the waveguide, the electric field of the guided mode should be well concentrated at the position of the emitter.

We use tantalum pentoxide (Ta_2O_5) as the waveguide material, as it offers both a high refractive index and very low autofluorescence. Figure 1 shows the working principle of such structures: The guided mode of the waveguide is strongly confined in the air slot between the two part waveguides. Placing a single-photon emitter in this region, therefore, promises strong coupling to the guided mode.

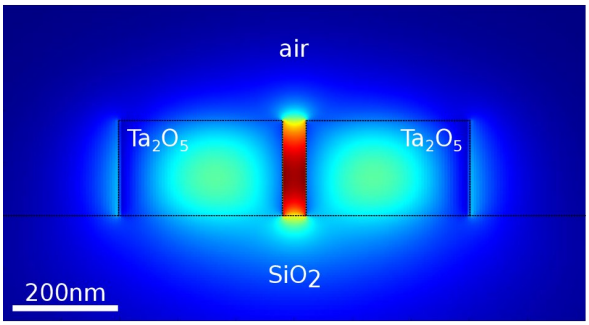

Figure 1: Simulated guided mode of a slot waveguide made of Ta2O5 positioned on a fused silica (SiO2) substrate. Strong confinement of the mode is visible in the air slot region between the two part waveguides.

Results and Methods

Finite-difference time-domain (FDTD) methods are one of the most important tools for modeling dynamic electromagnetic phenomena on the nanoscale. By discretizing the studied geometry, the electrodynamic properties can be calculated in sequential timesteps. However, accurately modeling both nanometer- and micrometer-scaled objects in one simulation (as we require for the study of our single-photon sources) requires a large amount of both computing power and memory. Luckily, the underlying FDTD algorithm allows for parallel computing, which makes the use of a computer cluster like the CoolMUC-2 very advantageous. We employed two open-source FDTD programs for investigating the coupling of colour centers hosted in nanodiamonds to dielectric slot waveguides, namely MEEP [1] and openEMS [2]. Both of them are licensed under the GPL permitting the adaption and customization of the source code for our needs.

The typical setup simulated by these means is presented in Figure 2a: A dipole emitter (represented by the yellow sphere) is placed in the middle of a slotted waveguide structure. By dynamically simulating

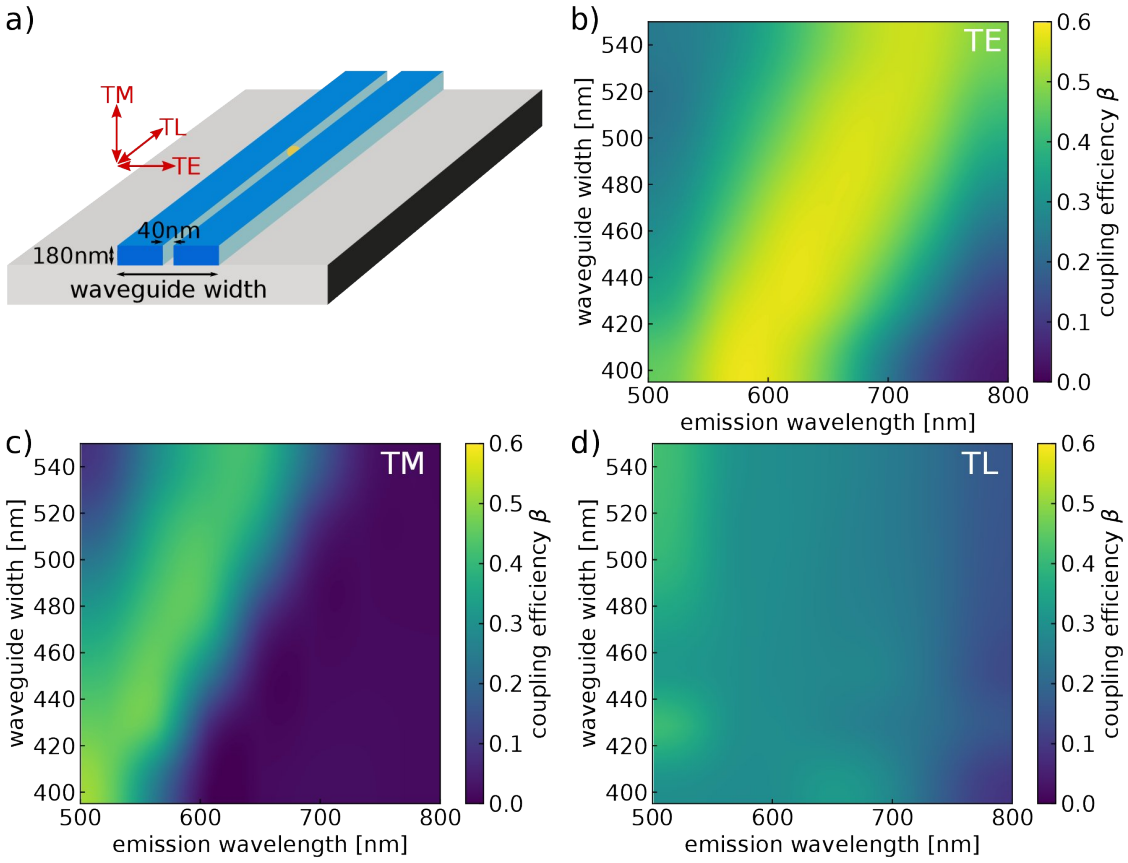

Figure 2: Results for typical FDTD simulations of dielectric slot waveguides for different waveguide widths. a) Schematic of a nanodiamond (yellow) positioned inside the dielectic slot waveguide. The different dipole orientations TE, TM and TL are illustrated by red arrows. b), c) and d) show simulated coupling efficiencies for different emission wavelengths in dependence of the overall waveguide width with a fixed height of 180nm and a slot width of 40nm for b) TE, c) TM and d) TL polarized light. The simulations for transverse-electric (TE) polarized light in b) show strong broadband coupling to the guided mode.

the emission, the coupling strength to the surrounding dielectric structure can be extracted. The figure of merit for this coupling is the coupling efficiency β, which is the ratio of the amount of light emitted into the guided mode of the waveguide to the amount of all emitted light.

For a complete understanding of such a system, different geometries of the slot waveguide as well as different orientations of the emitting dipole have to be investigated. Figures 2b, 2c and 2d exemplarily show the results of such an investigation, where the influence of the waveguide width on the coupling efficiency in dependence of the emission wavelength is simulated for TE- (transverse-electric), TM- (transverse-magnetic) and TL- (transverse-longitudinal) orientated dipole emitters.

The strong influence of the dipole orientation as well as the influence of the waveguide width is clearly visible. TE-polarized emission (figure 2b) experiences strong coupling efficiencies to the guided mode over a broad spectral region. Furthermore, this strong broadband coupling can be tuned to different wavelengths by adjusting the waveguide parameters. Simulating variations of multiple parameters allows for a thorough investigation of the whole system.

Ideal smooth nanophotonic structures like slot waveguides can be quite easily implemented and simulated with FDTD. Real structures, however, are always subject to surface roughnesses at the small nanometer scale. This can be investigated by FDTD as well, but at a cost: The discretization steps have to be very small, thereby boosting the demand for computation power and memory even further. Only with powerful computation clusters like the CoolMUC-2, this roughness modeling could be done accurately leading to much more realistic simulation results.

Outlook

Combining powerful open-source FDTD packages with the large computation power provided by the CoolMUC-2 cluster facilitated the simulation of realistic single-photon sources based on nanodiamonds coupled to dielectric slot waveguides. After thoroughly investigating the principal coupling mechanism for different structural parameters of the slot waveguide itself, other parts of a whole integrated optical circuit chip like waveguide couplers or the coupling of the waveguide based single-photon source to optical fibers can be examined allowing for the design of novel integrated photonic devices.

References and Links

[1] http://xqp.physik.uni-muenchen.de/
[2] https://meep.readthedocs.io/en/latest/
[3] http://openems.de/start/index.php

1 Spontaneous charge carrier localization in extended one-dimensional systems

Research Institution
Bayerisches Geoinstitut, Universität Bayreuth, 95440 Bayreuth

Principal Investigator
Gerd Steinle-Neumann

Researchers
Vojtěch Vlček, Helen Eisenberg, Roi Baer

Linux Cluster Project ID: pr28yi

Introduction

Quasi-one-dimensional polymer systems are at the forefront as charge donors in the development of organic photovoltaic and electronic technology, and for such systems performance depends strongly on charge mobility and localization which in turn is strongly affected by the presence of polarons, bipolarons or solitons. It is therefore of crucial importance to understand, predict and successfully model these quasiparticles and the possible localization of charge density. Until recently, such understanding has only been possible by use of expensive many-body methods. Here we consider positive charge localization in large quasi-one-dimensional polymer strands of trans-polyacetylene (tPA) and polythiophene (PT). While it is known that charge localization occurs in conjugated systems via distortion of the lattice, it remains an open question whether localization can occur in disorder-free translationally invariant systems (Figure 1).

Results and Methods

We use various computational approaches to describe quantum effects of electron interaction in order to explore this type of behavior for tPA and PT: Hartree-Fock and density functional theory using standard local density approximation, the hybrid B3LYP and range-separated BNL* functionals. The latter contains a system-dependent range separation parameter which is chosen such that the energy of the highest occupied eigenstate coincides with the electron removal energy, i.e., it enforces the ionization potential theorem and we can regard the eigenvalue of the highest occupied state to truly represent the quasiparticle energy. Finally, we also employ many-body perturbation theory within the GW approximation.

Using these calculations, we are indeed able to observe localization of the quasiparticles (holes) for very large polymer chains if Hartree-Fock or BNL* functionals are used (Figure 2) and we find that the localization is governed by the non-local exchange interaction. Hence it cannot occur when (semi-)local density functional approximations are used. Furthermore, BNL* provides an accurate description of the optical gap in comparison to experiments, with GW calculations corroborating this result.

Since we consider the underlying ionic geometry to be fully periodic, we conclude that it represents a case of spontaneous, purely electronic, symmetry breaking in charge density. It is an open question whether symmetry restored solution would be obtained by higher level methods and whether the locality would thus be preserved only in the structure of the density matrix.

The observed spontaneous quasiparticle localization can moreover explain the fast formation of polarons in the polymers in which the hole can serve as a precursor for the geometric distortion of the ionic lattice.

Within this project, three types of calculations were performed on the CoolMUC-2 cluster:

(i) Structural optimization with Hartree-Fock and density functional theory computations reported in Ref [2] were performed with the NWChem software package [3] using varying basis sets and different chain lengths. Systems with less than 10 monomer units (Figure 1) were run on a single node (28 cores). Calculations for larger systems were parallelized over up to eight nodes with variable efficiency, depending on the basis set and method. Wall time did not exceed 24 hrs. This task consumed ~1M core hours; storing

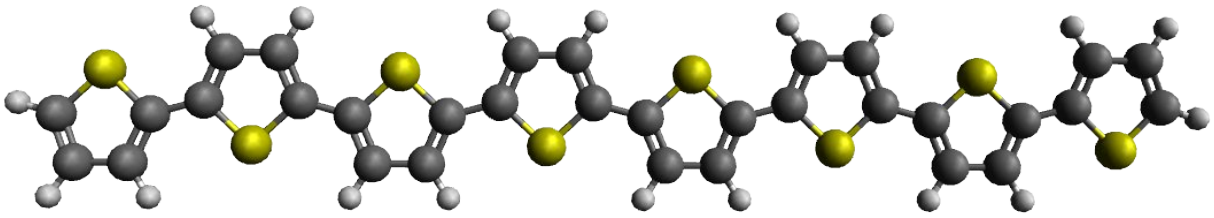

Figure 1: An example of a planar polythiophene molecule is shown with four repeat units (containing two thiophene rings each). Yellow, black and while spheres represent sulphur, carbon and hydrogen atoms, respectively.

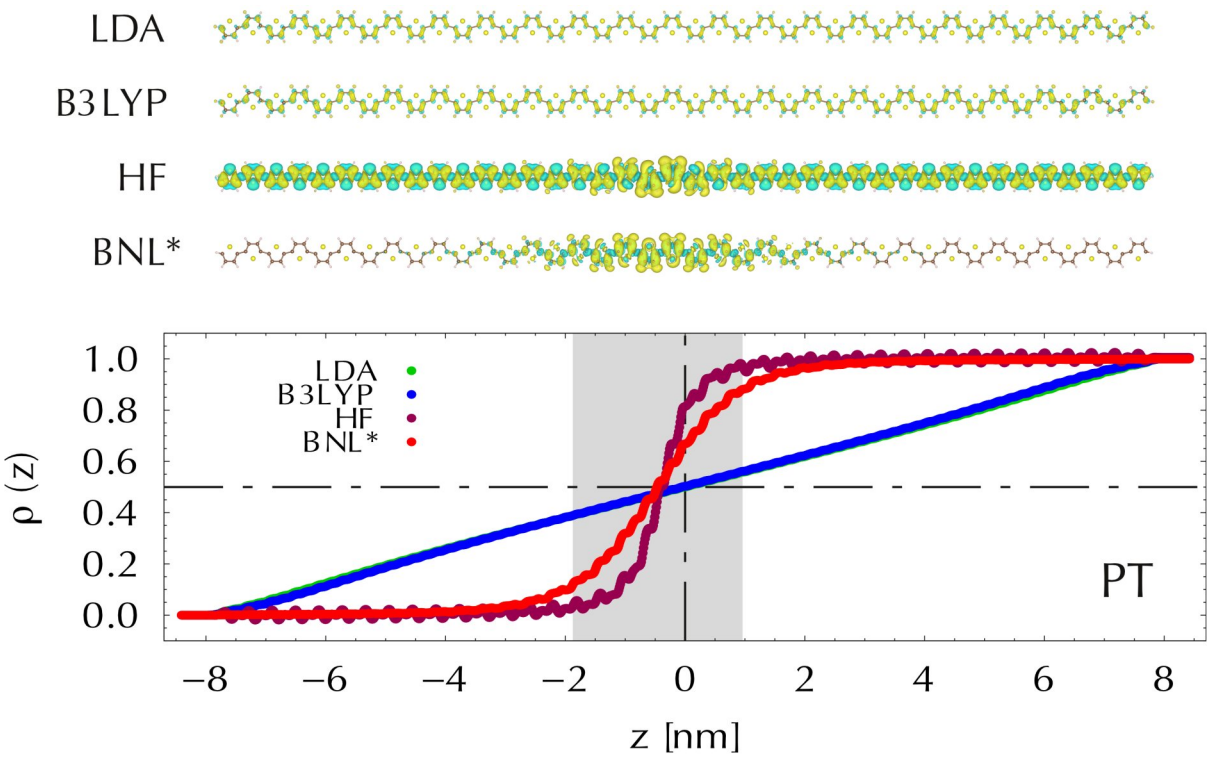

Figure 2: Difference in charge density of a neutral and a charged (cation) polythiophene with 20 repeat units. Density differences are computed by Hartree-Fock (HF) and density functional theory based methods on various levels. The charge density hole is shown by the yellow isosurface (top). The cumulative curve (bottom) reveals the localization of the charge density difference at the center of the chain in the HF and BNL* computations.

results (wave function and charge densities) required ~500 GB of disk space.

(ii) Excited state computations within time-dependent DFT were also performed with NWChem. Employing non-local (Fock) exchange for the BNL* functional significantly increases computational costs. Several tests were required to find an optimal balance between basis set size, accuracy and resource requirements. Calculations were parallelized over up to 20 nodes using 10-14 cores per node due to memory reqirement, with up to 48 hours of wall time. For 12 molecular systems we spent ~200k core hours in total and used ~200 GB of disk space.

(iii) Finally, we computed the ionization potential of PT chains with many-body perturbation theory (GW approximation). A new framework employing stochastic sampling of the Hilbert space permitted calculations even for the largest system. Due to the nature of the method, a statistical average over multiple stochastic samples is evaluated. Individual samples were run on single cores, and the results are averaged in a post-processing step. In total, between 6,000 and 10,000 stochastic samples were required to converge the quasiparticle energies for each system considered. The GW calculations required ~280k core hours and 500 GB of disk space.

On-going Research / Outlook

Range-separated hybrids, such as the BNL* approach discussed above, depend on a tuning parameter to mix non-local Fock exchange to local exchange and correlation in density functional theory. For finite systems, such as the ones discussed above, the separation parameter can be determined through the piecewise linearity condition of the ionization potential. For crystals, i.e., systems with periodic boundary conditions, we have recently determined a criterion for functional construction [4] (using earlier incarnations of the linux cluster at LRZ). We now apply this criterion to construct a range-separated potential for a prototypical Mott insulator, CdO, in order to investigate both the electronic band gap and the band structure. CdO is of particular interest as standard GW approaches to perturbation theory fail to open a band gap if the starting band structure is metallic, while some approaches to exchange and correlation are capable of opening the bandgap within a density functional theory scheme [5].

References and Links

[1] https://en.wikipedia.org/wiki/Organic_solar_cell
[2] Vojtěch Vlček, Helen R. Eisenberg, Gerd Steinle-Neumann, Daniel Neuhauser, Eran Rabani, and Roi Baer. 2016. Spontaneous Charge Carrier Localization in Extended One-Dimensional Systems. Phys. Rev. Lett. 116, 186401. DOI: 10.1103/PhysRevLett.116.186401
[3] http://www.nwchem-sw.org
[4] Vojtěch Vlček, Helen R. Eisenberg, Gerd Steinle-Neumann, Leeor Kronik, and Roi Baer. 2015. J. Chem. Phys. 142, 034107. DOI: 10.1063/1.4905236
[5] Vojtěch Vlček, Gerd Steinle-Neumann, Linn Leppert, Rickard Armiento, and Stephan Kuemmel. 2015. Improved ground-state electronic structure and optical dielectric constants with a semilocal exchange functional. Phys. Rev. B 91, 035107. DOI: 10.1103/PhysRevB.91.035107

Mapping Chemical Space with High-Throughput Quantum Chemistry

1

Research institution
Chair of Theoretical Chemistry, TU Munich

Principal Investigator
Karsten Reuter

Researchers
Johannes T. Margraf

Linux Cluster Project ID: pr47fo

Introduction

The goal of this project is to study the complex reaction networks that connect molecules in chemical space. Here, the "chemical space" concept refers to the totality of possible forms of matter (i.e. all possible molecules and solids). Studying the whole of chemical space is obviously intractable, but more limited subsets (e.g. all organic molecules with up to x atoms, all binary solids, etc.) can be enumerated exhaustively.

In recent years, much research has focused on studying the components of chemical space, e.g. by constructing and analyzing extensive molecular databases.[1] In contrast to this, we are systematically studying the topology of chemical space. This can be compared to going from a list of cities (which might contain some information on each city) to a map (which tells you how to get from A to B).

The central object of interest is the chemical reaction network (see Fig. 1). A reaction network visualizes how molecules are connected via chemical reactions. In this project, we will develop tools to automatically and systematically generate and explore such networks. Since the reaction network in principle contains all the information about the mechanism of any chemical process, this has important implications for the rational design of catalysts and allows novel insights into biochemical processes.

Results and Methods

We recently developed an algorithm for the exhaustive and systematic enumeration of reactions and intermediates in chemical space.[2] This gives us information about how molecules are connected to each other by chemical reactions. However, not every chemical reaction occurs with the same probability. This is because the reaction path is generally characterized by an energetic barrier, which must be overcome in order for a chemical transformation to occur.

This activation energy (along with the reaction energy see Fig. 2) therefore governs which parts of the reaction network are relevant for a given process.

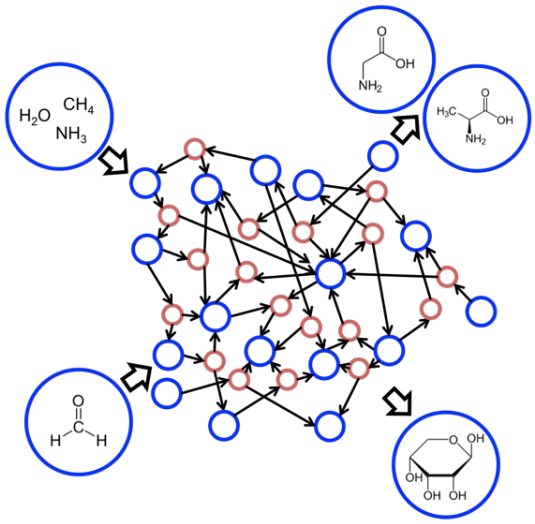

Figure 1: Illustration of a chemical reaction network. We are particularly interested in how complex industrially or biologically relevant molecules such as aminoacids or carbohydrates (right) emerge from simple precursors like water, methane or formaldehyde (left).

These quantities can be determined via first-principles simulations using density functional theory.

Computationally, this is associated with two challenges. Firstly, the reaction networks can easily encompass tens of thousands of molecules and millions of reactions. Secondly, the effect of different catalyst surfaces on the activation energy can be quite costly to model even for a single reaction (ca. 20k core hours per reaction).

The brute force exploration of all possible reactions on all catalysts of interest is therefore simply not feasible. Luckily, the calculation of reaction energies in the absence of a catalyst can be done quite efficiently (ca. 20-50 core hours per intermediate). Additionally, these results for each intermediate can be 'reused' for several reactions.

Consequently, we are currently generating a comprehensive database of gas-phase (i.e. uncatalyzed) reaction energies for tens of millions of reactions, associated with ca. 27k intermediates. This

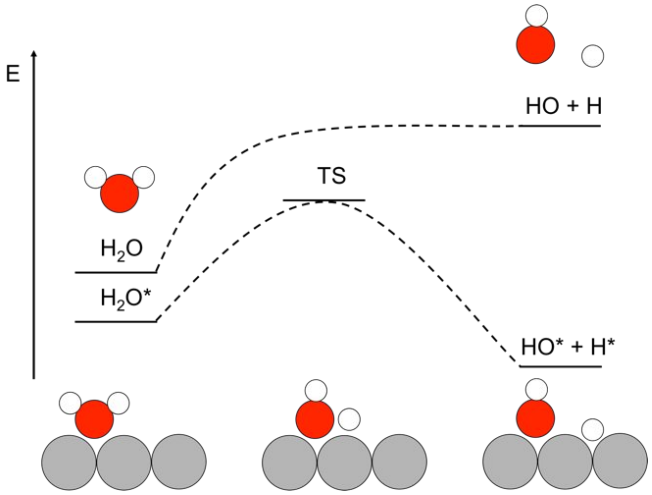

Figure 2: Schematic reaction pathways for the dissociation of water in the gas-phase and on a catalyst surface. A reaction is characterized by its activation energy (energy difference between the educt and the transition state, TS) and the reaction energy (difference between educt and product). A catalyst can affect both by changing the relative stabilities of transition states and reactands.

already provides important information about what parts of the reaction network are thermodynamically accessible from a given set of educts.

On-going Research / Outlook

Given these reaction energies, the next challenge lies in the full description of reaction paths on a catalyst surface. As mentioned above, this cannot be done for the full network. However, for a process of interest, the relevant parts of a network can be preselected on thermodynamic grounds, so that the full computational effort only has to be spent for the most relevant reactions.

For such a pre-screening to be effective, the influence of the catalyst on the reaction energetics has to be estimated (i.e. the difference between the top and bottom curves in Fig. 2). This should occur based on a cheap-to-compute descriptor, which can be done because transition metal surfaces are known to interact very systematically with organic molecules.

Indeed, simple physical approaches like the “d-band model” can already provide a qualitative picture.[3] Machine-learning methods offer a promising route for a more sophisticated “semi-quantitative” description, though they require sufficiently representative training data. The generation of this data is the subject of a LRZ “Summer of Simulation” project granted to our group.

References and Links

[1] L. Ruddigkeit, R. Van Deursen, L.C. Blum, and J.L. Reymond, J. Chem. Inf. Model. 52, 2864 (2012).
[2] J. T. Margraf, K. Reuter, to be submitted.
[3] B. Hammer, J. Nørskov, Nature 376, 238 (1995).

Understanding Morphological Changes of Plasmonic Nanoparticles

1

Research Institution
[1]Chair for Photonics and Optoelectronics, LMU Munich

Principal Investigator
Jochen Feldmann[1], Theo Lohmüller[1]

Researchers
Paul Kühler[1], Christoph Maier[1], Ana-Maria Huergo[2]

Project Partners
[2]Universidad Nacional de La Plata

Linux Cluster Project ID: pr86ze

Introduction

Metal nanoparticles made from gold and silver display fascinating optical properties. The most prominent example is the occurrence of strong plasmonic resonances due to collective oscillations of free electrons upon interaction with light. The high absorption and scattering cross-sections of gold nanoparticles allow to investigate them on a single particle level by dark-field microscopy and also to effectively heat and manipulate them with laser light. The particles do not blink or bleach and their extinction spectrum is highly sensitive to the refractive index of the surrounding medium, enabling a wide range of applications for sensing and spectroscopy. Most importantly, the plasmon resonance can be shifted over a wide spectral range by changing the particle size, shape or composition.

Results and Methods

Optical Sorting of Plasmonic Nanotriangles. In the near-infrared (NIR) window, light absorption in biological tissue is minimal. Noble metal nanoparticles with a plasmon resonance in the NIR are thus interesting tools for applications in biomedical imaging and cancer therapy. One of the methods to synthesize particles with extremely strong and tunable extinction in the NIR region is the reduction of gold salt by sodium sulfide. However, the origin of the observed resonance and its temporal development during synthesis were a subject of debate for many years. Several reports claimed that either different particle morphologies or the formation of particle aggregates may be the cause of the NIR resonance.

In the first project [1], we employed an all-optical method in combination with numerical calculations to answer this outstanding argument. In our experiment, we arrested the nanoparticle synthesis at different time points, such that the resonance positions of the particle dispersions were fixed at values between 700 and 1000nm. By using a focused laser beam with a wavelength tuned to the plasmon resonances observed in the UV-Vis spectra, we were able optically print individual particles from solution onto a substrate

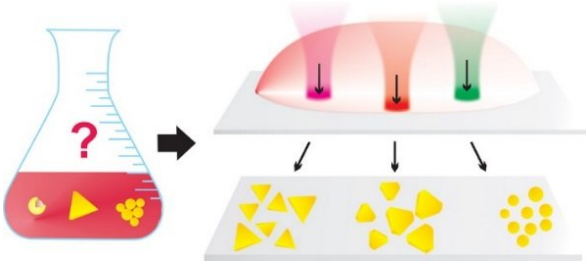

Figure 1: Wavelength selective deposition of individual plasmonic nanoparticles enabled an understanding of the spectral behavior of a nanoparticle dispersion during synthesis.

and thus to separate them according to their spectral properties (Figure 1). Following this strategy, we were able to determine the optical and morphological properties of the nanoparticles present at all times during the synthesis. Subsequently dark-field Rayleigh-scattering and electron microscopy imaging revealed that the NIR resonance is caused by thin gold nanotriangles and therefore a result of the nanoparticles' shape.

Computational methods were employed to support our findings, showing that the occurrence of nanotriangles can completely explain the optical properties of the particle dispersion. By performing numerical calculations, we were able to correctly assign the optically printed nanoparticles to peaks found in the spectrum of the stock solution, which turned out to be a mixture of small spheres and nanotriangles (Figure 2). Furthermore, due to the quantitative nature of the

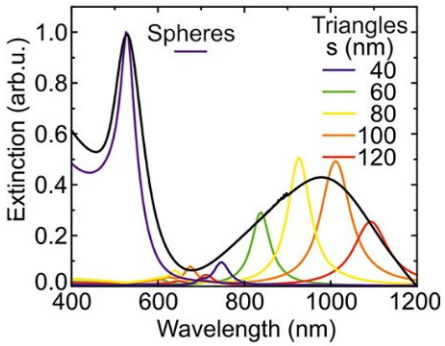

Figure 2: Numerical calculations of the different components (colored lines) of the nanoparticle dispersion are in very good agreement with the measured spectrum of the entire solution (black line). Reprinted with permission from [1]. Copyright 2016 American Chemical Society.

calculations, we could exclude contributions from other particles through a statistical analysis of the particles' shapes by electron microscopy.

The nanotriangles with their strong and narrow, tunable cross sections hold great promise for bio-(chemical) sensing and cancer therapy applications. Additionally, this method of all-optical sorting is applicable to virtually any synthesis of nanoparticles and shows how complex nanostructures can be built up out of individual nanoparticles that are all present in a dispersion at the same time, by tuning the printing laser wavelength to the desired nanoparticle type.

Bending Gold Nanorods with Light. Plasmonic V-shaped nanoantennas are important building blocks for the rational design of optical metamaterials and flat optical devices. The fabrication of V-shaped antenna arrays, however, is not a simple task. Electron-beam lithography is widely used, yet shows limitations when it comes to the fabrication of very small gold nanostructures with high crystallinity and purity. The controlled assembly of gold nanoparticles from solution would be a preferred alternative, yet to date the chemical synthesis of V-shaped nanoparticles itself is not possible.

In the second project [2] we investigated the possibility to use laser manipulation to controllably bend single gold nanorods in solution into a V-shaped geometry (Figure 3). We could show that optical forces, which emerge during the bending process, can be utilized to optically pattern the V-shaped particles onto an underlying substrate.

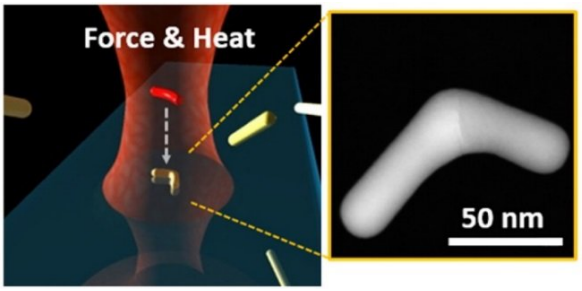

Figure 3: Sketch of the laser-induced bending of gold nanorods together with a high resolution electron microscopy image of such a rod. Reprinted with permission from [2]. Copyright 2016 American Chemical Society.

This approach simultaneously leverages two modes of light-matter interactions, namely plasmonic heating and optical forces, to achieve a previously impossible feat for nanofabrication. With the help of numerical calculations, we were able to devise a mechanism how nanorod bending can be controlled by tuning the laser conditions. Furthermore, we have investigated how the optical properties of bent nanorods change depending on the bending angle (Figure 4).

For both projects, we employed the finite difference time domain (FDTD) method implemented in Lumerical FDTD Solutions (Lumerical, Canada) to solve the Maxwell equations and hence the electromagnetic response of a complex system, by using a fine rectangular mesh for both E and H fields.

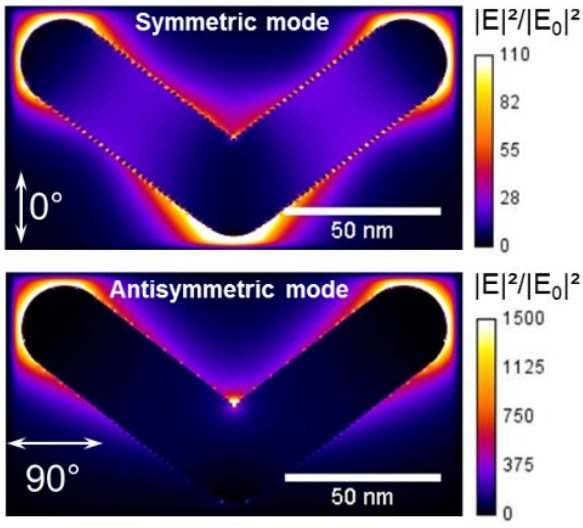

Figure 4: Calculated field enhancement around a bent nanorod revealing a symmetric and an antisymmetric mode. Reprinted with permission from [2]. Copyright 2016 American Chemical Society.

This was done by first modelling the particle geometry and then monitoring the amplitude of the absorbed and scattered electromagnetic field to find the resonance condition. Putting the entire geometry on a fine mesh (typically a mesh size of 0.1Å was required to ensure convergence) is computationally very demanding. We therefore performed the main part of the calculations related to our projects on the CoolMUC-2 cluster.

In total, we used about 900,000 core hours, generating ~90GB of data and 250 files. Simulations were usually run on 1-2 nodes (depending on the load of the cluster) which corresponds to 28 or 56 cores.

On-going Research / Outlook

In the future, we will intensify our research efforts on light-nanoparticle manipulation and extend our investigations towards hybrid nanosystems and new materials. Here, numerical simulations and modelling are important for interpreting and understanding the consequences of light-matter interaction at the nanoscale.

References and Links

[1] Maria Ana Huergo, Christoph Matthias Maier, Marcos Federico Castez, Carolina Vericat, Spas Nedev, Roberto C. Salvarezza, Alexander S. Urban and Jochen Feldmann. 2016. Optical Nanoparticle Sorting Elucidates Synthesis of Plasmonic Nanotriangles. ACS Nano. 10, 3 (Mar. 2016), 3614–3621. DOI: 10.1021/acsnano.5b08095

[2] Anastasia Babynina, Michael Fedoruk, Paul Kühler, Alexander Meledin, Markus Döblinger and Theobald Lohmüller. 2016. Bending Gold Nanorods with Light. Nano Lett. 16, 10 (Oct. 2016), 6485–6490. DOI: 10.1021/acs.nanolett.6b03029

1 Molecular simulations for complexes in metalorganic frameworks

Research Institution
Department of Chemistry, Chair of Inorganic and Metalorganic Chemistry

Principal Investigator
Roland A. Fischer

Researchers
Markus Drees, Christian Jandl, Benjamin Hofmann

Linux Cluster Project ID: t3331

Introduction

In our project, we use quantum chemical calculation to gain insights of molecular properties, spectroscopical simulation, mechanisms and reactivities. Due to its huge development in the recent years, density functional theory algorithms are the methods of choice especially in organic and metalorganic calculations. Together with high-standard computer systems like CoolMUC-2, the systems to be dealt with may be growing or the methods used might be improving in quality.

Results and Methods

We used mostly the software package Gaussian, that is available as either Gaussian09 or Gaussian16 in the last years. Gaussian has a scaling problem, using cores in different physical nodes, but shared memory nodes can significantly speed up the calculations (4-8 nodes are recommended) Gaussian is the advantage, that multiple algorithms are available in one software package. Ranging from DFT, Hartree-Fock and post-HF methods, and also there are a lot of calculation types starting of a simple geometry optimization to vibration analyses and thermochemical data, exited states descriptions for UV-VIS spectroscopy, population analysis for electronic distributions and even NMR simulations can be applied.

Figure 1: Simplified potential energy surface for the Pd-migration in imidazolium-substituted η^3-cycloheptatrienide- Pd complexes (left). Interconversion of different dihalocycloheptatriene isomers via a halotropylium halide intermediate (right). Gaussian stores two types of files. In scratch it uses sometimes very large “read-write files” during a program run that are usually deleted upon end. Important for the user are the log files that record all the steps and can be visualized for analysis and a machine- coded “checkpoint file” that you can use to continue some calculation without starting from scratch (e.g. re-using of already calculated properties like geometry and wavefunctions generated by the DFT or other computational methods). For the storage of log and checkpoint files, our project just needs 100 GB, while the scratch files can be growing up tp several 10 to 100 GB per run.

Here is the first example of a DFT project that was run on CoolMUC-2 by Christian Jandl.

Gaining insights into dynamic molecules is a challenging task with experimental techniques. For example, X-ray crystal structure analysis only provides a static picture of the most favourable species, while many spectroscopic methods yield information that is averaged over all present species. In our studies, density functional theory (DFT) calculations proved to

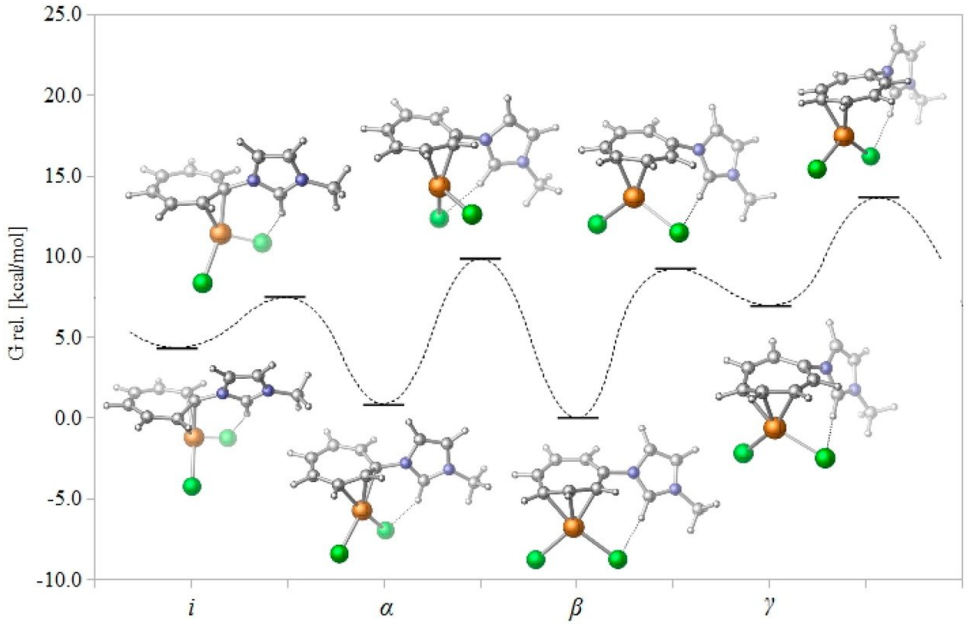

Figure 1: Simplified potential energy surface for the Pd-migration in imidazolium-substituted η^3-cycloheptatrienide- Pd complexes (left). Interconversion of different dihalocycloheptatriene isomers via a halotropylium halide intermediate (right).

be a valuable tool to gain detailed information about all relevant isomers and their interconversion in two highly dynamic systems.

All simulations were carried out with the Gaussian09 software package using the ωB97X-D functional and the basis sets TZVP for first and second row elements, def2- TZVPD for higher non-metals and def2-TZVP (with a corresponding effective core potential) for metals as implemented in Gaussian09 [1].

As the first example, the class of imidazolium-substituted η3-cycloheptatrienide-Pd complexes features a constant migration of the Pd atom along the seven-membered ring of the ligand, which effects an interconversion between different regioisomers (Figure 1, left) [2]. In agreement with crystallographic data, the β-isomer was predicted to be most favourable. The calculations also show that the internal hydrogen bond from the imidazolium-substituent to the halide ligand is maintained in all species and features a high binding energy of ca. 13.5 kcal/mol. In the other case, it was shown that the compounds which exist as halotropylium halides in the solid state form a dynamic equilibrium between different dihalocycloheptatriene isomers in solution, where the ionic halotropylium halide only exists as an intermediate (Figure 1, right) [3]. In both cases, the activation barriers for the interconversion of different isomers were calculated to be very low (mostly <10 kcal/mol), confirming the very fast dynamic at room temperature.

Another subject is the search for catalytic mechanisms. This time conducted by Markus Drees, DFT methods were used to follow the oxygen transfer of an iron-oxo complex to oxidize benzene to phenol. [4] Experimentalist were also working on this study. Iron-oxo compounds bearing cyclic ligands are especially interesting, because they mimic iron systems similar to the haemoglobin that is a content of our blood and plays a similar role in transporting oxygen through a human body.

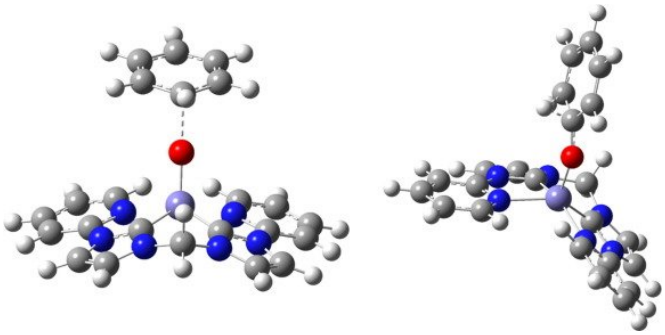

Figure 2: Two calculated transition states for the oxygen transfer from the complex to benzene.

In this reaction, H_2O_2 is used as the oxygen source and building up the Fe-O bond. The most crucial part is then, how the oxygen atom is transported to a stable molecule like benzene to get it reacted. In Figure 2, the two crucial transition states are shown. On the left, the transition state structure Is shown during the addition of the benzene to the oxygen. On the right, the structure represents a hydrogen shift to the neighbour carbon atom.

The search of transition states require especially skills and calculation time. With the identification of such states, one can determine the kinetic behaviour of a given reaction (e.g. how fast it will be).

On-going Research / Outlook

Problems were sometimes, that the queuing system has been too overcrowded with jobs of new users who in the SLURM system were “over-advantaged” in comparison to users that even already successfully run jobs on the machines. Sometimes, the individual users sometimes as to wait for several days at times with high job loads.

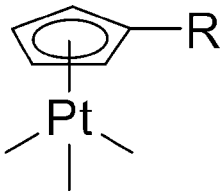

Figure 3: Chemical formula of Cp-functionalized platinum complexes.

In an ongoing project, Ben Hofmann is dealing with Cp- functionalized metal complexes (Figure 3). How he deals with the project shows how typically an investigation with DFT calculation is stepwise conducted. First you calculate the geometry and the electronic structure of the desired compounds. Further focus is now put to decomposition pathways of these compounds upon light excitation and the influence of different alkyl groups R and the electron density of the Cp moiety on the UV/Vis spectrum. From this, an assessment is made of the possibility of a stabilization of reactive intermediates by functionalized Cp moieties (-R e.g. –Si(Me_2)allyl or Si(Me2)ethyleneamine). In the end, it should be also proven by experiment in the real-world laboratories.

References and Links

[1] M. J. Frisch et al., Gaussian 09, Revisions C.01/D.01/E.01; Gaussian, Inc., Wallingford, CT, 2013. Further computational details can be found in the respective publications.
[2] C. Jandl, K. Öfele, F. E. Kühn, W. A. Herrmann, A. Pöthig, Organometallics 2014, 33,
[3] C. Jandl, D. C. Mayer, A. Pöthig, Eur. J. Org. Chem. 2017, 4255–4259.
[4] A.C. Lindhorst, M. Drees, W. Bonrath, J. Schuetz, T. Netscher, F.E. Kühn,, J. Catal., 2017, 352, 599-605.

1

Density Functional Modeling of Multinuclear Actinide Hydrolysis Complexes

Research Institution
Fachgebiet Theoretische Chemie, Department Chemie, Technische Universität München

Principal Investigator
Notker Rösch

Researchers
on Chiorescu, Andrew Gray, Sven Krüger

Linux Cluster Project ID: t3831

Introduction

The early actinide (An) elements are highly hazardous due to their toxicity and radioactivity, which contributes to the long-term activity of highly active nuclear waste. For assessing the safety of geological waste repositories, one needs to understand the solution chemistry and the solid state chemistry of An elements. Accurate information on the composition of An compounds and their properties is a prerequisite for modeling the retention of these elements by technical or geological barriers and the migration behavior in a repository and the environment. Regarding the transport of actinides, their complexes in aqueous solutions are especially of concern.

The chemistry of actinide ions in pure water is already rather intricate; it increases in complexity when typical components of natural waters such as carbonate, other salts, and natural organic matter are considered. In pure water, metal ions undergo hydrolysis, i.e., they form hydroxo complexes $M(OH)_n^{q-n}$ with the number of hydroxo ligands increasing with pH. Some actinide ions, like U(VI) and Th(IV), show a rich variety of hydrolysis complexes, including multinuclear species at nearly neutral to basic pH [1,2]. For U(VI), which forms the uranyl ion UO_2^{2+}, the formal composition of these complexes is $(UO_2)_m(OH)_n^{2m-n}$ while one finds the simpler species $Th_m(OH)_n^{4m-n}$ for Th(IV). Only a few mononuclear hydrolysis species of the other common oxidation states V and III of actinide ions have been accepted in thermodynamic data bases. For U(VI) di- to tetranuclear hydrolysis complexes are widely accepted [2], but the actual compositions and structures are not known for most of these species. On the other hand, such a detailed knowledge, beyond the bare number of species involved, is necessary for describing chemical equilibria as a basis of a predictive thermodynamic model of hydrolysis. For a thorough understanding of the thermodynamics of hydrolysis, the number and the type of isomers of these complexes also needs to be determined. For Np(VI), which should behave similar to U(VI), even the number and the type of species is largely unexplored. Using an accurate quantum chemistry method, determing the composition, structure, and stability of trinuclear hydrolysis complexes of U(VI) and Np(VI), including pertinent isomers, our computational project contributes to understanding the complex An(VI) hydrolysis chemistry and to verifying current thermochemical models [2].

Results and Methods

We apply a first-principles scalar relativistic all-electron density functional (DF) approach without empirical parameters specific to actinide complexes to determine electronic structures and energies for given atomic structures of the complexes by solving the Schrödinger equation in an iterative, self-consistent manner. As the actinides are very heavy elements, a relativistic treatment of the electronic structure is necessary in all-electron calculations. The in-house developed efficiently parallel code ParaGauss [3] (Fortran, MP2, distributed load balancing) is used for that purpose. The quantum mechanical exchange-correlation interaction between the electrons is treated at the generalized gradient approximation (GGA) level. We tested two GGA, a hybrid type as well as a meta-GGA type representation of this interaction for U and Np aqua complexes and found that the PBE GGA functional performs comparable or better than the others in reproducing structures and nuclear vibrations. Orbitals were represented by flexible Gaussian-type basis sets, contracted in a generalized fashion. The open-shell nature of Np(VI) with one unpaired electron has been taken into account by carrying out spin-unrestricted calculations. Applying a quasi-Newton algorithm with an approximate Hessian matrix, geometry optimizations were carried out without symmetry constraints. Using 28 cores, a typical geometry optimization converged in 3 days. The relative stability of the various isomers of trinuclear An(VI) complexes was determined by comparing Gibbs free energies, ΔG.

The solvation effect of water on An complexes was modeled in a two-fold way. Water molecules in the first coordination sphere of An cations act as ligands and thus are treated explicitly. In addition, we approximated the long-range effects of the bulk water surrounding the complexes as a polarizable continuum (conductor like screening model, COSMO).

Trinuclear An(VI) complexes exhibit a variety of isomeric structures due to variation of the number and

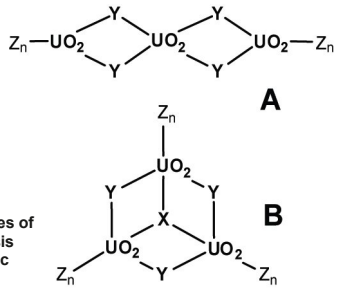

Figure 1: Exemplary structures of trinuclear uranyl(VI) hydrolysis complexes. A: linear, B: cyclic isomer. For details see text.

orientation of the ligands around the actinyl(VI) ion, lying close in energy on the potential energy surface. To validate the results of the geometry optimizations in difficult cases we carried out molecular dynamics (MD) simulations, mainly to check the coordination numbers around the actinyl moieties of the multinuclear complexes. The MD simulations, also based on quantum mechanical DF PBE calculations of inter-atomic forces, were carried out with the software VASP [4]. In this code for periodic systems such as solids, one-electron wave functions are expanded in a plane-wave basis and core electrons are treated by the potential augmented wave approach. An complexes in solution are modeled by means of a periodically repeated box including 160 explicit water molecules, which corresponds to a complex concentration of 0.35 mol/l. Exemplary MD simulations (for 15 ps time) take about 6 days when one uses 224 cores.

We studied isomers of mono-, di- and trinuclear complexes of U(VI) and Np(VI). For the trinuclear species we inspected complexes with overall charges ranging from +3 to -3 *e*. For each charge we found isomers that differed in (i) the relative arrangement of the actinyl ions, linear or cyclic (Fig. 1), (ii) the central ligands X of cyclic species (O^{2-}, OH^-, or missing at all), (iii) the bridging ligands Y (O^{2-}, OH^-, or OH_2), (iv) the positions and the orientations of terminal ligands Z (OH^- or OH_2), and (v) the number of terminal ligands Z which determines the coordination numbers (CNs) of the actinyl ions (Fig. 1). Overall, we inspected about 200 isomers of trinuclear An(VI) complexes.

Comparison of the relative stability of trinuclear U(VI) complexes with charges between +3 to -3 *e* shows that many isomers are lying close in energy (Fig. 2). Cyclic species with a central ligand O^{2-} are the most stable species throughout this series (Fig. 2). For the experimentally and computationally well characterized species with a charge of +1 *e* [5], the other isomers are more than 20 kJ/mol less stable. Most of the species with other charges exhibit smaller energy differences between the more stable isomers, suggesting that they can exist in a dynamic equilibrium. Linear and cyclic species without a central ligand are the next most stable group of isomers, while cyclic complexes with a central OH ligand are the least stable ones (Fig. 2). Current thermodynamic models of U(VI) hydrolysis take into account trinuclear species with charges between +2 to -2 *e*. From the reaction energies between trinuclear and smaller (di- and mononuclear) complexes, one concludes that trinuclear complexes with charge +3 are not stable, in agreement with experiment, while species with charge -3 *e* are suggested to exist.

Characteristic geometry parameters of the complexes, like the average U-ligand bond lengths and the U-U

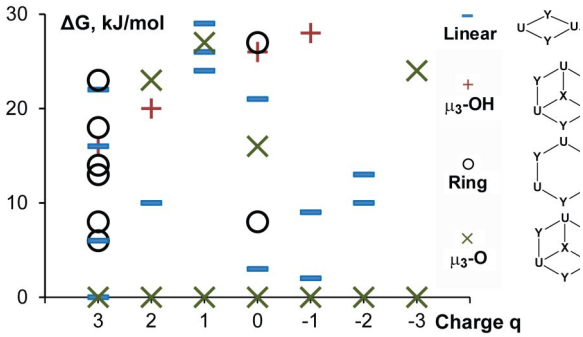

Figure 2: Relative stability of isomers of trinuclear uranyl(VI) hydrolysis complexes with varying charge relative to the most stable cyclic oxo-centered (μ_3-O) isomer. The various structural motifs are given as sketches of the core moiety of the complexes.

distance, vary only slightly between isomers of the same charge. Thus, isomers of trinuclear species can hardly be distinguished experimentally by their structure. With decreasing charge of the complexes, corresponding to increasing pH, we noted increasing uranyl U=O bond lengths and decreasing the U-U distances.

As expected, for Np(VI) we determined an isomer spectrum of trinuclear hydrolysis complexes very similar to that of U(VI). Again, the oxo-centered cyclic isomers were calculated to be the most stable. Compared to U(VI), cyclic isomers without central ligand are somewhat stabilized compared to the other isomers. In agreement with the slightly smaller radius of the Np(VI) ion compared to U(VI), the Np(VI) complexes show a little shorter Np-O bonds and Np-Np distances. All trinuclear Np(VI) complexes are somewhat less stable with respect to decomposition into mono- and dinuclear hydroxo complexes. This finding is traced back to the smaller overall size of these complexes, resulting in an increased repulsion between anionic ligands. In consequence, one expects that for a given concentration of actinyl ions, the concentration of trinuclear hydrolysis species is lower for Np(VI) than for U(VI). The anionic complexes of Np(VI) exhibit a stronger trend to CN = 4, instead of 5, compared to U(VI), which may also be rationalized by the increased ligand repulsion for Np(VI).

In summary, our computational study essentially confirmed the speciation of U(VI) hydrolysis complexes and in addition provided detailed structures and relative energies for all more stable isomers. Also the expected similarity of Np(VI) hydrolysis is confirmed and differences in the behavior of U(VI) and Np(VI) are predicted.

On-going Research / Outlook

Our studies of aqueous actinide complexes, which are supported by Bundesministerium für Wirtschaft und Energie (grant 02E11415E) and Bundesministerium für Bildung und Forschung (grant 02NUK039E), are currently extended to carbonate and hydroxo-carbonate species.

References and Links

[1] M. Altmaier, X. Gaona, T. Fanghänel, Chemical Reviews, 113 (2013) 901.
[2] P. L. Zanonato, P. Di Bernardo, I. Grenthe, Dalton Trans. 43 (2014) 2378.
[3] T. Belling, S. Krüger, M. Mayer, F. Nörtemann, M. Staufer, C. Zenger, N. Rösch In High Performance Scientific and Engineering Computing, Lecture Notes in Computational Science and Engineering; H.-J. Bungartz, F. Durst, C. Zenger, Eds.; Springer: Heidelberg, Germany. Vol. 8, (1999) 439.
[4] G. Kresse, J. Hafner, Physical Review B, 47 (1993) 558.
[5] S. Tsushima, A. Rossberg, A. Ikeda, K. Müller, A.C. Scheinost, Inorganic Chemistry, 46 (2007) 10819.

Photocatalytic water splitting with carbon nitrides: Excited state calculations for heptazine as a model catalyst

1

Research Institution
Technical University of Munich

Principal Investigator
Johannes Ehrmaier

Researchers
Weiwei Xie, Xiuxiu Wu, Xiaojuan Pang, Wolfgang Domcke

Linux Cluster Project ID: t3881

Introduction

Solar-driven water splitting hopefully may provide clean and sustainable energy in the future. Recently, carbon nitride materials, based on triazine or heptazine (tri-s-triazine) building blocks, have attracted vast interest in the field, as they consist of earth abundant materials, are photostable and can split water into hydrogen and oxygen using visible light. Despite a huge amount of experimental work, the underlying mechanism is not understood up to now. The prevailing paradigm for the rationalization of water-splitting with these organic compounds is based on the assumption that an electron hole pair (exciton) is formed by the absorption of a photon. Subsequently, electron and hole separate in the supposedly semiconducting materials and drive the hydrogen generation reaction and the water oxidation reaction, respectively, at solid-liquid interfaces. On the other hand, there are experimental observations which indicate that the water-splitting reaction may rather be a photochemical process within individual molecular chromophores. For example, charge separation in carbon-nitride polymers is energetically quite costly (of the order of eV), which makes it unlikely that charges can efficiently separate in these organic materials. Moreover, carbon nitrides do not form extended two-dimensional crystalline structures, but rather are disordered organic polymers. Lotsch and coworkers have found that small carbon nitride oligomers are more efficient in water splitting than extended polymers [1].

Considering hydrogen-bonded complexes of triazine and heptazine with a single water molecule and using excited-state ab initio electronic-structure calculations, we discovered a new photochemical reaction mechanism for water splitting [2,3]. Two elementary molecular photoreactions are combined to form a catalytic cycle. Scheme 1 gives a short overview of the mechanism for the example of the heptazine-water complex: First, an H-atom is transferred from water to the chromophore after the absorption of a photon, resulting in the formation of a hydroxyl radical and a hydrogenated heptazine molecule. Subsequently, the excess H-atom is detached by the absorption of a second photon, regenerating the catalyst. Both steps have been observed experimentally in a molecular beam experiment, using pyridine as choromophore [4]. Recently, Morawski and co-workers could observe both reaction steps in an experiment using a standard carbon-nitride material in liquid water.[5] The first photoreaction produces OH radicals which have been observed by fluorescence spectroscopy using hydroxyl radical scavengers. Photogenerated H-atoms were also detected by spectroscopic means. Moreover, the evolution of molecular hydrogen was confirmed when Pt was added as co-catalyst [5].

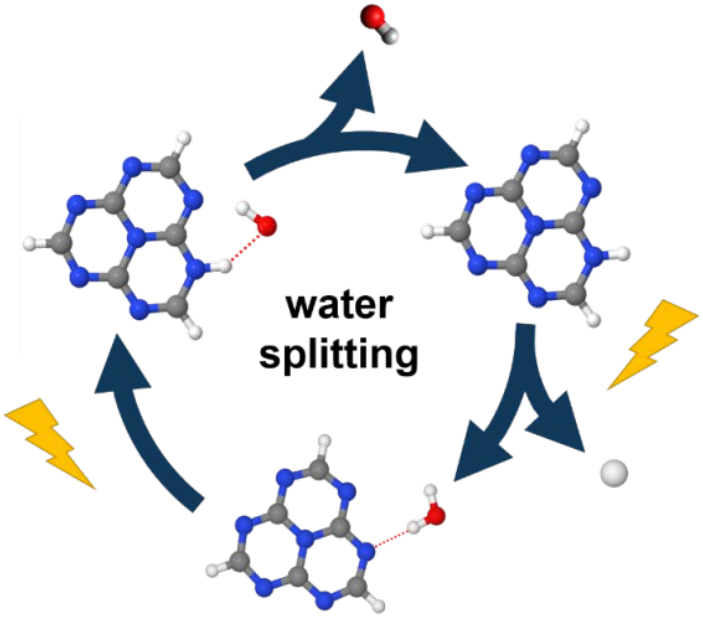

Scheme 1: Photochemical water-splitting cycle with heptazine as model choromophore. After absorption of a photon, an H-atom is transferred from water to heptazine, resulting in the heptazinyl-hydroxyl biradical. Subsequently, the excess H-atom is detached from the chromophore by the absorption of a second photon, which regenerates the catalyst.

Results

H-atom transfer

To understand the atomistic mechanism of the water-splitting reaction with carbon nitrides, calculations of excited-state energies along the relevant reaction coordinates have been performed. Fig. 1 shows a scan along the OH-distance R_{OH} of the water molecule, which is the reaction coordinate for the photoinduced H-atom-transfer reaction. The excited-

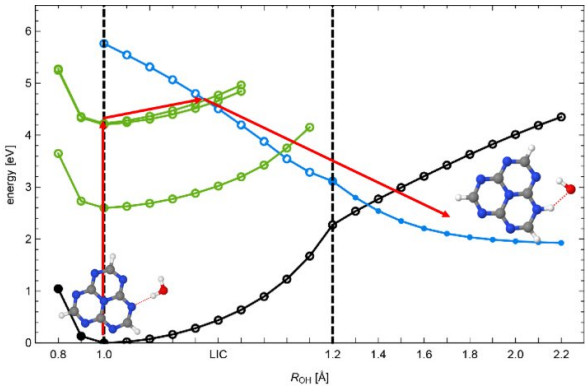

Figure 1: Potential-energy surfaces along the reaction coordinate, R_{OH}, for the photoinduced H-atom transfer reaction. After photoexcitation to one of the upper bright states (green) the system may reach the conical intersection and may be transferred to the charge-transfer state. The charge-transfer state (blue) provides the driving force for the formation of the biradical.

state energy profiles were calculated using the second-order algebraic-diagrammatic construction scheme ADC(2). Møller-Plesset second-order perturbation theory was used for ground-state calculations. All calculations were performed with the Turbomole program package. The system is excited in the Franck-Condon region (R_{OH} = 1.0 Å) to one of the bright states (upper green states in Fig. 1) from which it may reach the crossing between the green and blue energy curves (following the red arrows). At the crossing, the system may be transferred to the charge transfer state (blue curve) which exhibits a strong driving force for the formation of the hydroxyl-heptazinyl biradical. At another crossing, involving the energy curves of the charge transfer state (blue) and the ground state (black), the biradical formation has to compete with relaxation back to the equilibrium position.

Fig. 2 shows the two orbitals which are most important for the charge-transfer state. An electron is transferred from the p_z orbital of water to a virtual (π^*) orbital of the heptazine molecule. The electronic charge transfer from water to heptazine explains the strong driving force for the ensuing proton-transfer reaction (the proton follows the electron).

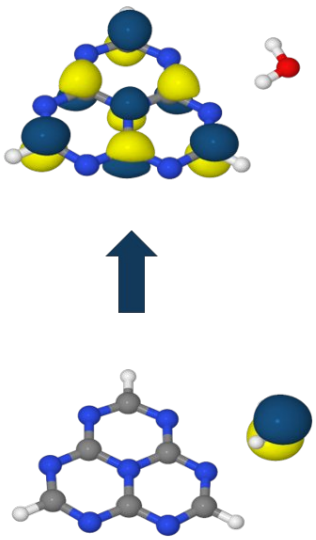

Figure 2: Hartree-Fock orbitals which characterize the charge-transfer state. The lower orbital is the p_z orbital of water, the upper one is an unoccupied π^* orbital of heptazine.

Liquid water

In large-scale density functional theory calculations, we investigated the excitation energies of heptazine molecules solvated in a box of liquid water. Due to the perturbation by the environment, the lowest excited state of heptazine at 2.7 eV can borrow some intensity from higher electronic states, which is fully consistent with the experimental findings. Analyzing the projected density of states, we could identify the mechanism of the H-atom transfer reaction. Photoexcitation of the heptazine molecule leads to a local electron hole pair. The hole in heptazine is filled by an electron from the water molecule, that is, the hole is transferred to the water molecule which, in turn, drives the H-atom transfer reaction from water to heptazine.

Hydrogen evolution

After H-atom transfer to heptazine, the H-atom can be detached from the heptazinyl radical by the absorption of a second photon. The decisive state for the dissociation reaction is a low-lying reactive $\pi\sigma^*$ state, the properties of which have been extensively studied in various heterocyclic compounds. Alternatively to the photodetachment reaction, it is also possible that two heptazinyl radicals can recombine in a dark reaction to form molecular hydrogen and two heptazine molecules. The hydrogen evolution step regenerates the chromophore and thus closes the catalytic cycle.

Outlook

With these first-principles calculations for model systems we have discovered a novel molecular pathway for photocatalytic water-splitting. Our studies are currently extended to investigate larger water clusters and more extended chromophores, e.g. model systems for covalent organic frameworks. Moreover, molecular dynamics simulations will be performed to estimate the time scales and quantum yields of the described photoreactions.

References and Links

[1] V. W.-H. Lau et al., J. Am. Chem. Soc., 2015, 137, 1064-1072.
[2] J. Ehrmaier, T. N. V. Karsili, A. L. Sobolewski and W. Domcke, J. Phys. Chem. A, 2017, 121, 4754-4764.
[3] J. Ehrmaier, M. J. Janicki, A. L. Sobolewski, W. Domcke; Phys. Chem. Chem. Phys., 2018, in press.
[4] N. Estevez-Lopez, S. Coussan, C. Dedonder-Lardeux and C. Jouvet ,Phys. Chem. Chem. Phys., 2016, 18, 25637-25644.
[5] O. Morawski et al., submitted for publication.

Quantitative Aspects of Organic Reactivity

1

Research Institution
Department of Chemistry, LMU Muenchen

Principal Investigator
Hendrik Zipse

Researchers
Harish Jangra

Linux Cluster Project ID: ui271

Introduction

The use of modern quantum chemical methods for the accurate description of the structures, the stabilities, and the spectroscopic characteristics of transient (that is, intrinsically unstable and thus short-lived) molecular systems provides the basis for tightly coupling experimental and computational studies. The accurate prediction of spectroscopic signatures of transient intermediates in solution-phase reactions has been made possible through systematic methodological developments, which have recently been implemented in quantum chemistry program packages supported by the LRZ platforms (Gaussian 16, ORCA, MOLPRO). The most accurate of these methods are characterized by an insatiable appetite for main memory, while exploiting only a comparatively moderate degree of parallelism. The following four projects illustrate in an exemplary fashion, how the prediction of spectroscopic properties integrates into experimental studies on transient molecular systems [1].

Results and Methods

Subproject A: Hunting down unstable peptide conformations
The accurate description of cis/trans peptide structures is of fundamental relevance for the field of protein modeling and protein structure determination. Thermochemical data derived from quantum mechanical calculations and detailed spectroscopic (NMR) studies predict an extended conformation for dipeptide model Ace-Gly-NMe 1 as the preferred conformation in DMSO solution (Figure 1).

Isomerization of the N- or C-terminal amide bonds are both found to be endergonic by 13 kJ/mol at 300 K, leading to the occurrence of the *trans-cis* (**1_tc**) and *cis-trans* (**1_ct**) conformations as detectable species in NMR measurements at almost identical abundance. Supported by theoretical chemical shift calculations, this allowed for the complete assignment of ^{1}H and ^{13}C chemical shift data for these cis/trans isomers. The ability to reproduce the conformational preferences of **1** with common protein force fields is, unfortunately, quite limited [2].

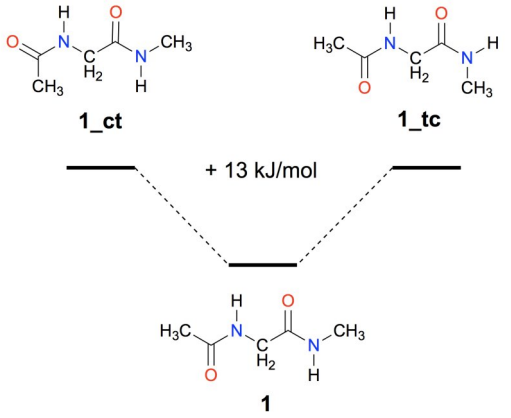

Figure 1. Spectroscopically detected and theoretically characterized conformations of dipeptide model 1.

Subproject B: The unusual chemistry of the TEMPO radical
The reaction of carbon- and oxygen-centered radicals (carrying one unpaired electron each) with each other is commonly believed to occur in a diffusion-controlled manner (that is, without an actual enthalpic barrier). It is the more surprising that recombination reaction of

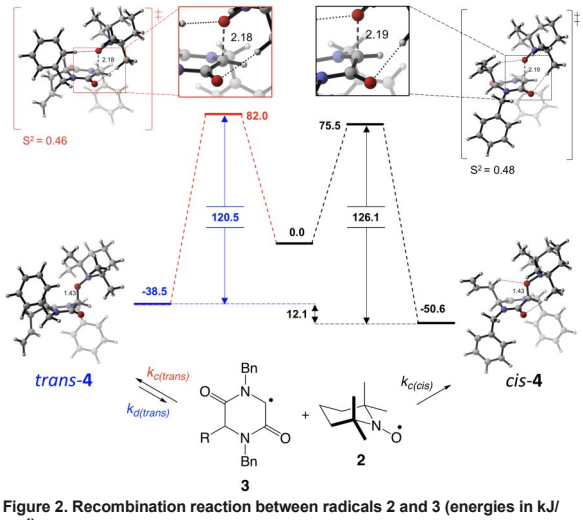

Figure 2. Recombination reaction between radicals 2 and 3 (energies in kJ/mol).

oxygen-centered TEMPO radical (**2**) with cyclic amide radical **3** occurs in a highly selective manner to deliver only product ***cis*-4** (Figure 2). Quantum chemical studies show this to be a consequence of the amide bond distortion in the energetically less favorable ***trans*-4** product. This distortion energy is well reflected already at the stage of the reaction barriers, which are significantly larger in absolute terms as is common for radical recombination reactions.

Subproject C: Electric field effects on peptide radical stability

Carbon-centered radicals derived from amino acid residues in peptides and proteins play a large role in the reaction mechanism of enzymes of the *glycyl radical enzyme* (GRE) family. The name of this enzyme class derives from a backbone glycyl radical positioned in the enzyme active site. How the surrounding protein guides the actual chemistry of this highly reactive intermediate has been a mystery ever since its original discovery. A general control mechanism is elusive mainly because neutral peptide radicals are not expected to respond to electrostatic forces. This hypothesis has now been tested in quantum chemical calculations on the stability of glycine-based dipeptide model **5** in the absence and presence of external monopoles, dipoles and electric fields. Choosing chloride anions (Cl^-) and sodium cations (Na^+) as frequently occurring monovalent ions in protein structures, we find that glycyl radical **5** can be stabilized or destabilized by up to 9 kJ/mol, through appropriate placement of the ions at a distance of 900 pm away from the peptide radical center. Effects of the same magnitude can be observed when using point charges or oriented external electric fields.

Subproject D: Quantification of the Electrophilicity of Michael Acceptors

Alkenes carrying electron-withdrawing substituents are commonly referred to as *Michael acceptors* and play a key role in numerous synthetically important processes. In an effort to establish a system

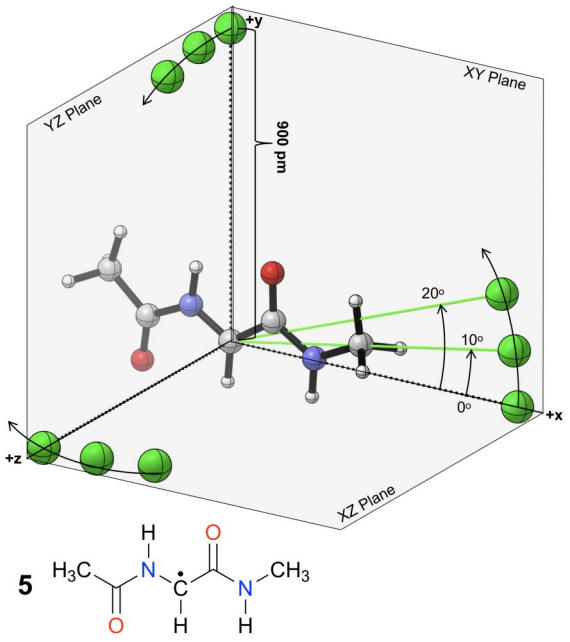

Figure 3. Chloride anions placed at selected grid points around glycyl radical 5.

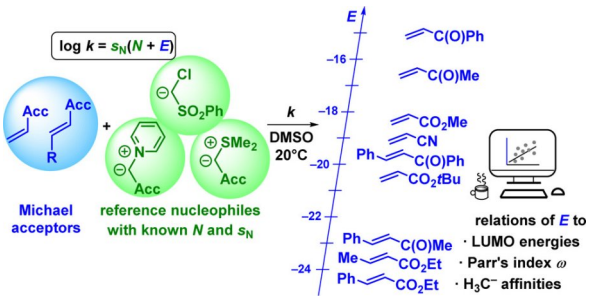

Figure 4. Selected reference nucleophiles and Michael acceptors employed in the determination of electrophilicity parameters E.

describing the rate of reaction of these compounds with electron-rich reaction partners (nucleophiles), the reaction of 44 *Michael acceptors* with clearly defined reference nucleophiles have been studied experimentally and with quantum chemical methods. Using the Mayr-Patz equation ($\log k_2 = s_N(E+N)$), the experimentally determined second-order rate constants k_2 have been converted into electrophilicity parameters E characteristic for each Michael acceptor. These latter parameters correlate surprisingly well with reaction free energies for addition of methyl anions calculated with quantum chemical methods, but not with molecular orbital (MO) energies obtained in the same calculations. This correlation facilitates reactivity predictions for systems not yet studied experimentally. For a smaller number of Michael acceptors quantum chemical calculations have been employed to map the complete reaction pathway for cycloaddition reaction with a reference nucleophile. Despite the fact that concerted as well as stepwise pathways can be located on the potential energy surface, the underlying barrier formation corresponds in all cases to that of nucleophilic attack at the less substituted alkene terminus[3].

On-going Research / Outlook

The projects described here have been initiated and financially supported through the DFG-sponsored SFB 749 on "Dynamics and Intermediates of Molecular Transformations". Ongoing collaborative research projects in the SFB 749 involve the properties of highly sensitive organometallics, zwitterions as transient intermediates of cycloaddition reactions, and radicals in biomolecular transformations[4].

References and Links

[1] http://www.cup.uni-muenchen.de/oc/zipse/
[2] H. Jangra et al., Chem. Eur. J. 2016, 22, 13328.
[3] D. S. Allgäuer, H. Jangra et al., J. Am. Chem. Soc. 2017, 139, 13318.
[4] http://www.sfb749.de/

Electronic and magnetic properties of the TMDC-based materials

Research Institution
LMU Munich

Principal Investigator
Hubert Ebert

Researchers
Svitlana Polesya, Sergiy Mankovsky

Project Partners
Institute of Inorganic Chemistry, Christian-Albrechts University, Kiel

Linux Cluster Project ID: ui461

Introduction

The transition-metal dichalcogenides (TMDCs) have been in a focus of extensive investigations for several decades. Having layered quasi-2D structure TMDCs crystallize in a variety of structure types differing by the stacking sequence of the TX_2 layers (where T is a transition element atom, and X is a chalcogen atom, S, Se or Te) coupled to each other due to rather weak van der Waals interactions [1]. Most of them are nonmagnetic but allow intercalation of magnetic 3d elements. As a result the materials are formed with a great variety of magnetic properties dependent on the host system and on the type and concentration of intercalated element. In recent years a lot of works were devoted to hexagonal TMDC monolayer systems having outstanding properties attractive for spintronic applications.

Results and Methods

The electronic structure properties have been investigated within the framework of density functional theory (DFT) using the general gradient approximation (GGA) with the parametrization for the exchange and correlation pot as given by Perdew, Burke, and Ernzerhof (PBE)]. The Vienna Ab Initio Simulation Package (VASP) has been used for the structure optimization of systems under consideration. The optimization has been performed accounting for the van der Waals corrections treated via the semi-empirical DFT-D3 Grimme's method. A *k* mesh with 21 x 21 x 21 grid points and a kinetic energy cutoff at 440 eV were used for this computational step. For the electronic structure calculations we tave used the SPR-KKR Green function method (Munich code package) as well as full-potential linearized augmented plane wave (LAPW) method as implemented in the ELK code. In ELK calculations a *k*-sampling with 16 x 16 x 8 k-points mesh within the Brillouin zone was used for these calculations. The plane-wave basis set was defined by the cutoff K_{max} = 7/*RMT*, with *RMT* being the average muffin-tin radius. The cutoff l_{max} = 8 for the angular momentum expansion of the wave functions was used inside the MT spheres.

In the 2D systems consisted of 3d-overlayer on top of a TMDC monolayer one can expect strong DM

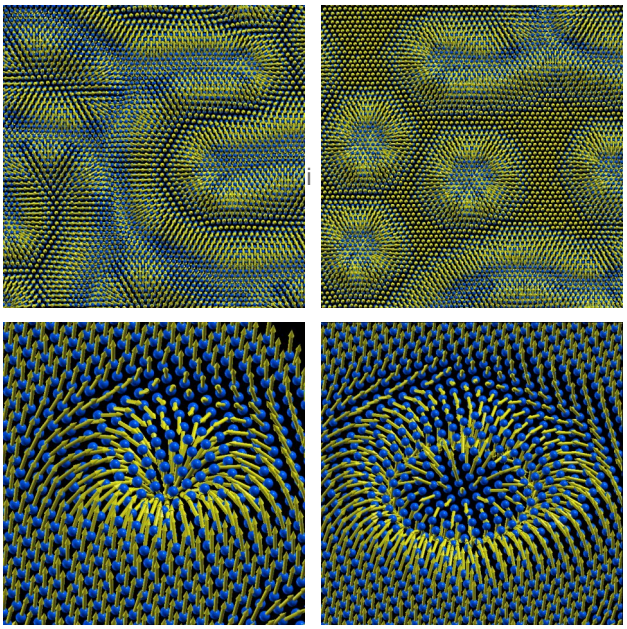

Figure 1: The magnetic texture in the 1T-based Fe/$TaTe_2$ system without (top left) and with (top right) external magnetic field 0.9 T, obtained within MC simulations at T = 0.5 K. Single magnetic skyrmions (bottom) with winding numbers 1 (left) and 2 (right).

nteractions due to the broken inversion symmetry and strong spin-orbit interaction that should result in various types of chiral magnetic texture caused by Dzyaloshinskii-Moriya (DM) interaction. Thus, the first-principles calculations of the exchange parameters have been performed using SPR-KKR code for the Fe monolayer deposited on top of different TMDC monolayers with ^{1}T and ^{1}H polytypes, assuming that Fe atoms create an ordered FM structure [2]. The results of Monte Carlo simulations for Fe/^{1}T-$TaTe_2$ at *T* = 0.5K are shown in Fig. 1. Without external magnetic field the system has rather complicated helimagnetic structure (top left), while the magnetic field results in stabilization of magnetic skyrmions (top right) shown in more details in bottom panels.

The electronic and magnetic properties have been investigated for ^{2}H-NbS_2 compound intercalated by Cr, Mn and Fe [3]. It was found a change of magneto-crystalline anisotropy (MCA) from in-plane in Cr and Mn intercalated systems to an out-of plane in Fe intercalated TMDC due to corresponding modification of electronic structure. It is also shown that for $Cr_{1/3}NbS_2$ and $Mn_{1/3}NbS_2$ the in-plane MCA and DM

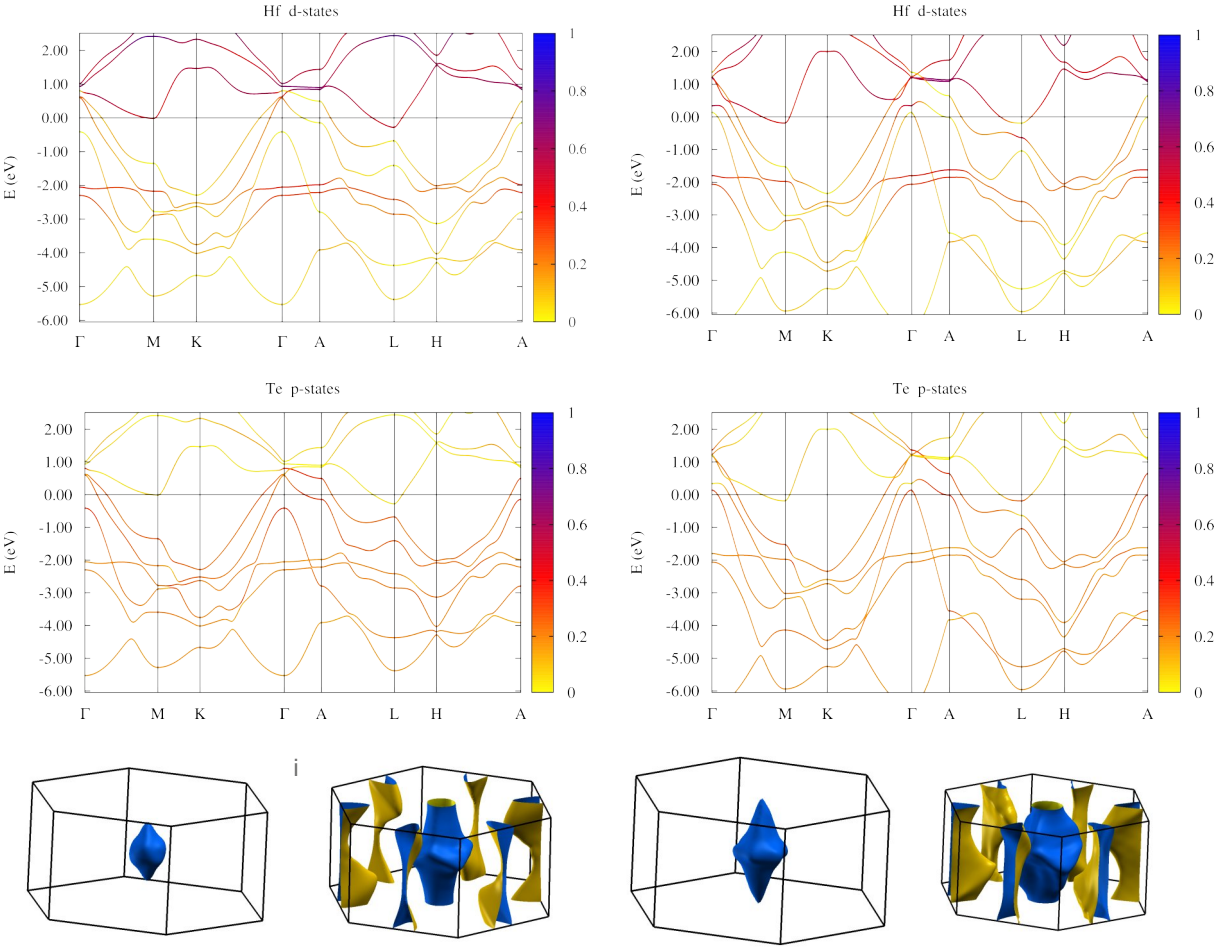

Figure 2: Calculated electronic structure of HfTe2: the calculated band structures for ambient pressure (a) and p = 6.5 Gpa (b) are resolved according to the contributions coming from Hf d and Te p states. Other orbitals are neglected due to their low contributions. In (c, d) plots of the Fermi surface are shown for the respective pressures. The Fermi surface for the innermost energy band at the Γ point is shown separately.

nteractions give rise to a helimagnetic structure along the hexagonal c axis. The negative exchange interactions and strong MCA in the $Fe_{1/3}NbS_2$ compound result in a frustrated magnetic structure referred to as as ordering of the third kind observed experimentally.

The experimental and theoretical study on the layered TMDC $HfTe_2$ that shows a large magnetoresistance (MR) of 1350% at 2K and $_{\mu 0}H$ = 9T, despite the system is different from Weyl semimetals $MoTe_2$ and WTe_2 which both exhibit large MR. Moreover, the structure and electrical resistivity under pressure reveal a unique structural transition. $HfTe_2$ is an appealing platform for future investigations on the interplay of particular band-structure features and their connection to emerging physical properties [4]. The pressure-induced changes of the electronic band structure of $HfTe_2$ have been calculated by optimization of the structural parameters and of the atomic coordinates by minimizing the total energy of the system for each volume decrease with increasing pressure. The electronic band structure of $HfTe_2$ for ground state and for p = 6.5 Gpa is presented in Figure 2.

On-going Research / Outlook

In future we are going to investigate the 3-d-intercalated TMDC materials: electronic structure, magnetic and transport properties dependent on composition and on structure of the intercalated sublattice. Another project is connected with simulation, using VASP package, of Atomic Force Microscopy used for investigation of small magnetic clusters deposited on the metallic or topological insulator surfaces. These calculations will require big amount of RAM memory.

References and Links

[1] http://www.ac.uni-kiel.de/de/bensch/dfg-schwerpunktprogramm-spp-1415
[2] Svitlana Polesya, Sergiy Mankovsky, Diemo Ködderitzsch, Wolfgang Bensch, and Hubert Ebert. 2016. Dzyloshinskii-Moriya interactions and magnetic texture in Fe films deposited on transition-metal dichalcogenides. Phys. Status Solidi RRL 10, 3 (March 2016), 218-221. https://doi.org/10.1002/pssr.201510283
[3] Sergiy Mankovsky, Svitlana Polesya, Hubert Ebert, and Wolfgang Bensch. 2016. Electronic and magnetic properties of 2H-NbS2 intercalated by 3d transition metals. Phys. Rev. B 94, 184430 (2016). hppts://doi.org/10.1103/PhysRevB.94.184430
[4] Sebastian Mangelsen, Pavel G. Naumov, O. I. Barkalov, Sergiy A. Medvedev, Walter Schnelle, Matej Bobnar, Sergiy Mankovsky, Svitlana Polesya, Christian Näther, Hubert Ebert, and Wolfgang Bensch. 2017. Large nonsaturating magnetoresistance and pressure-induced phase transition on the layered semimetal HfTe2. Phys. Rev. B 96, 205148 (2017). hppts://doi.org/10.1103/PhysRevB.96.205148

Insights into the processes of systems with complicated electronic structures using high level quantum chemical approaches

1

Research Institution
Institut für Physikalische und Theoretische Chemie

Principal Investigator
Bernd Engels

Researchers
Paul Schmid, Waldemar Waigel

Linux Cluster Project ID: pr47be

Introduction

Simulation become more and more important in chemistry to understand the outcome of experimental measurements or to predict new compounds. In this report we briefly describe three different projects for which the resource of the LRZ are essential. Protein ligand interactions are of paramount importance in a wide variety of scientific disciplines. This is reflected in the highly interdisciplinary field of drug discovery, where the selective targeting of a disease relevant protein (e.g. Rhodesain) by an inhibitor (e.g. K11777) is one of the central goals. Such covalent-irreversible drug-target reactions have a lot of advantages and disadvantages. A particular interest in our work lies in the exploitation, design and discovery of covalent-reversible building blocks (inhibitors), which would address and invalidate most concerns against covalent drugs.

Solar cells are one of the most promising devices to exploit renewable energy resources. Especially, organic solar cells (OCS) are intensively studied because they possess several advantages with respect to their inorganic counterpart but are still less efficient. The drawbacks arise due to loss process which are not well understood. For an improvement of the efficiencies of OCS's a better understanding of such processes are necessary. To obtain better insights our work focuses on the simulation of the various processes taking place between light absorption and current flow using appropriate quantum chemical approaches.

Biradicals have been in the focus of chemical research for several decades. This great chemical interest results because these systems exhibit unusual physical properties. These molecules contain two unpaired electrons. The resulting open-shell electronic structure leads to small energy gaps and strong intermolecular interactions. The resulting unusual properties make systems with biradical electronic characters to key intermediates in the formation of light-emitting states in optoelectronic materials and interesting starting materials for catalysis. Moreover, biradical systems play an important role in the chemistry of combustion engines, and processes in the atmosphere or in interstellar clouds. It is therefore vital for many areas of chemistry, physics and material science to investigate biradical systems. One of the current research interests includes the investigation of relatively unexplored solvents effects on the singlet and triplet states of biradicals with accurate quantum chemical methods.

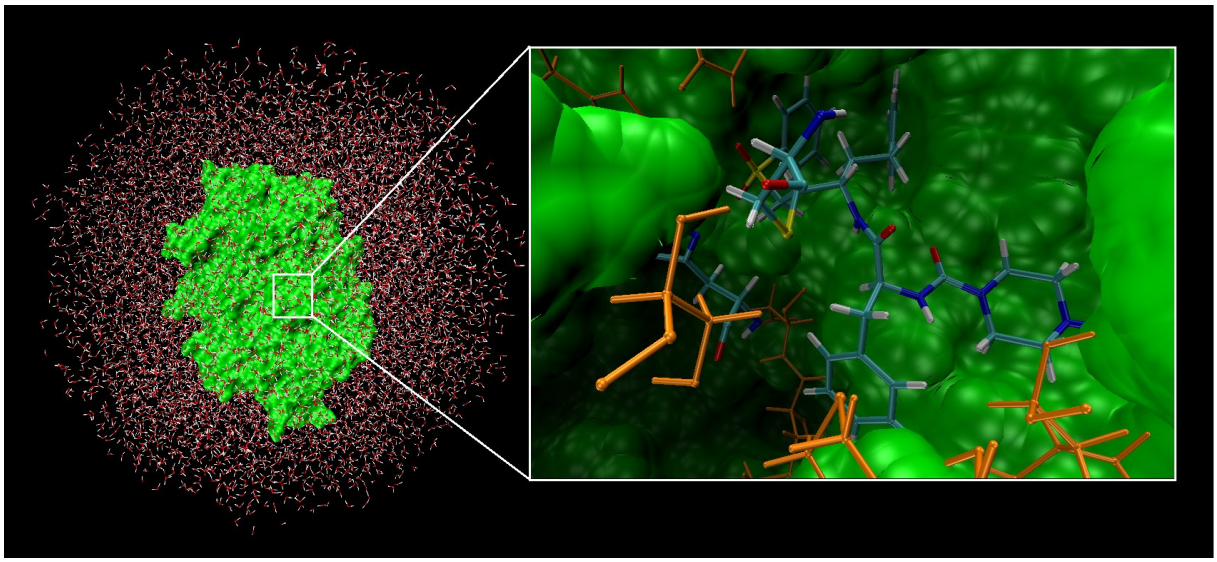

Figure 1: The enzyme Rhodesain (green) solvated in a water cave. The inhibitor is covalently-irreversible bonded to the CYS25 residue. Different interesting amino acids for an additional QM layer or for widen the QM part are colored orange.

Results and Methods

Within our biomedicinal investigations we characterize the inhibition processes of covalent inhibitors. In contrast to standard agents, which only interact non-covalently with an enzyme, covalent ligands chemically react with the enzyme and form a covalent bond. Famous examples are penicillin or aspirin. Despite the success of both famous examples the pharmaceutical companies avoided covalent drugs till 2005 but they currently experience an intensive renaissance in academic and industrial drug development. The design of new covalent ligands with special properties deserves a detailed understanding of the underlying reaction mechanisms, e.g. by simulations. Due to the undergoing chemical reaction the inhibition process cannot be describe by classical approaches as molecular mechanism (MM). However, the size of the systems under consideration (enzyme & ligand & water environment) is too large for quantum mechanical (QM) approaches. Hence, hybrid approaches which use QM methods for the important part (e.g. all atoms which are involved in the chemical reaction) while cheaper mechanics/molecular mechanics methods are used to fold in the influence of the environment (e.g. the enzyme environment) (Fig. 1). The latter cannot be completely neglected because it may hinder the processes due to steric effects but may also accelerate them by polarization effects. We started our investigation on smaller computer clusters but for successful investigations we need resources as they are offered by the LRZ.

In the present investigation we study the reasons which determine if an inhibitor acts irreversibly or

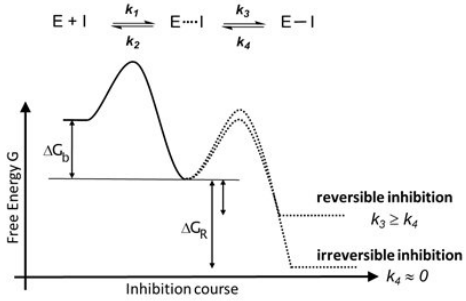

Figure 2: Two-step mechanism of a ligand, which binds covalently to its target. Step1: Formation of a non-covalent ligand-target complex. Step2: Formation of the covalently bound ligand-target complex through a chemical reaction.

reversibly. In an irreversible inhibition the covalent bond is so strong that it does not break again (Fig. 2) Consequently, the enzyme is irreversibly blocked and degraded. Reversible inhibitors form a much weaker covalent bond which is broken again so that only a reversible inhibition results. The very successful drugs penicillin and aspirin are irreversible inhibitors but because reversible inhibitors offer some advantages we investigate which effects govern the reversibility of irreversibility of an inhibitor. We were able to develop a protocol with which we were successful to design a reversible inhibitor starting from a well-known irreversible one [2]. However, while our predictions could be experimentally proven many new questions arise.

The thermodynamic of the chemical reaction represents an important reason because the free reaction energy ΔG_R determines the quotient of k_3 and k_4. Other reasons also seem to be important because the replacement of a hydrogen by a fluorine atom change the mechanism from irreversible to reversible for some inhibitors, however, without changing the thermodynamic of the reaction considerably. Further important reasons which determine reversibility might be relaxation effects of the enzyme along the reaction or the energy dissipation of the reaction energy into the enzyme. To investigate such effects, we will perform QM/MM molecular dynamic (MD) simulations in which these effects are handle on equal footing.

We already mentioned the importance of biradicalic

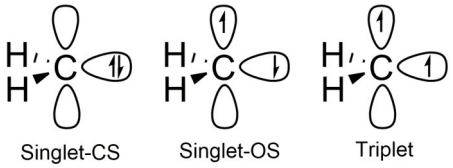

Figure 3: Singlet carbene scheme (left), singlet-open-shell carbene scheme (middle) and triplet carbene scheme (right).

species. Their electronic structure is sketched in Figure 3 using the simplest biradical system carbene as an example. To steer the reactivity of biradicals the energy differences between the two singlet states and their triplet counterpart are important. In our investigation we simulate how this energy differences are influenced by solvent effects. They will be large for the energy difference between the Singlet CS and both other structures because different charge distributions are expected. Their influence on the energy difference between Singlet-OS and Triplet are expected to be smaller. One even may expect that they vanish, but careful studies are missing. Solvation effects are generally taken into account with polarizable continuum models (PCM) in which the solvent molecules are replaced by a homogeneously polarizable medium. Such approaches are expected to be too approximate to grasp the differences between Singlet-OS and Triplet because the effects of the solute-solvent interaction are averaged. Hence, we will simulate the systems more realistically by including explicit solvent molecules. To do so, we will again use QM/MM approaches as described above. They describe so-called bilayer approaches. To increase the accuracy, we will also test so called tri-layer approaches which involve two QM-descriptions with varying accuracies and efforts (QM/QM/MM).

The computations will be performed for boron-containing systems which depending on the ligands form a singlet or a triplet ground state.[3] While less elaborated gas phase computations agree qualitatively with experimental results we will know investigate how solvent effects influence the energy gaps. As a first step we performed the PCM-computations as one limit of the treatments. Computations in which molecular solvent effects are correctly incorporated are under way.

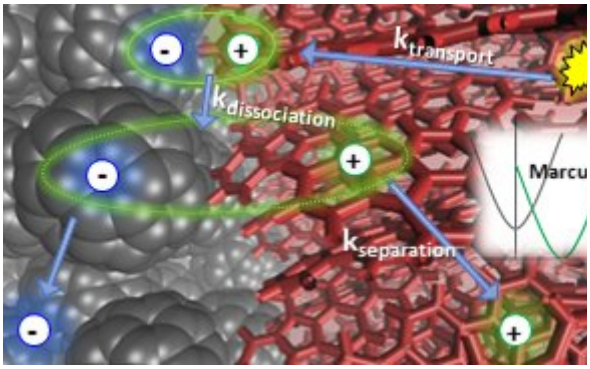

Figure 4: Sketch of the various processes within an OCS.

In our simulations of the interplay of the processes taken place within OSC's we were able to provide some important insights [4] although we used quite rough approximation. To increase our predictive power, we will transfer our computations to the LRZ because this allows us to use improved theoretical approximations.

References and Links

[1] www.phys-chemie.uni-wuerzburg.de/arbeitsgruppen/engels/forschung/
[2] Tanja Schirmeister et al. Quantum Chemical-Based Protocol for the Rational Design of Covalent Inhibitors J. Am. Chem. Soc. 2016, DOI: 10.1021/jacs.6b03052
[3] Marc-Andre Legare et al. Nitrogen fixation and reduction at boron Science 2018 DOI: 10.1126/science.aaq1684
[4] Charlotte Brückner et al. J. Phys. Chem. C. 2017 DOI: 10.1021/acs.jpcc.6b06755 & 10.1021/acs.jpcc.6b11340

Computational Fluid Dynamics and Engineering

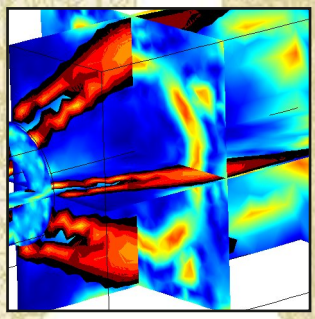

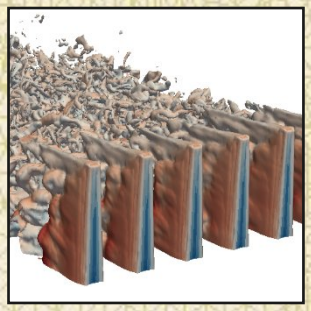

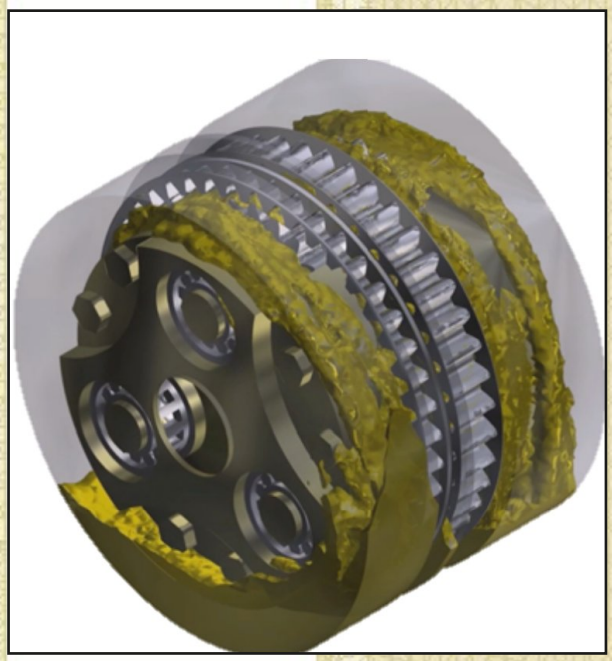

Investigation on Hovering Rotors over Inclined Ground Planes

Research institution
[1]Institute of Helicopter Technology

Principal Investigator
Manfred Hajek[1]

Researchers
Stefan Platzer[1], Jürgen Rauleder[1], Joseph Milluzzo[2]

Project partners
[2]United States Naval Academy

Linux Cluster Project ID: pr47hu

Introduction

Naval helicopters regularly operate under hazardous flight conditions, such as shipboard operations where the helicopter must operate above a moving ship deck. There is a dearth of research examining the effect of ship deck motion on the flow environment below the rotor. Even for rotors in hover over inclined, non-moving ground planes, results are scarce.

Measurements were done at the United States Naval Academy using particle image velocimetry (PIV) to optically measure the flow field. A six-component load cell was used to determine the rotor hub forces and moments. In the experiments, a hovering rotor was investigated out of ground effect (OGE) and in ground effect (IGE) for multiple different ground plane inclination angles. Furthermore, a finite-volume CFD solver (German Aerospace Center - DLR TAU code) was used to solve the unsteady Reynolds-averaged Navier–Stokes (URANS) equations for the same test cases. Modifications to the rotor wake and inflow caused by the influence of different ground plane inclination angles were computed and compared to the experimental results for validation purposes.

Numerical Methodolody

The numerical simulations were performed using the German Aerospace Center - DLR TAU code, a finite-volume based node-centered solver which can be used with unstructured as well as structured grids. A version of the one-equation Spalart-Allmaras (SA) turbulence model was used. It is identical to the standard SA model in regions where the transported variable v is positive and is modified in regions where it becomes negative for numerical reasons. A vortical flow correction was used to improve vortex preservation. In order to decrease dissipation, fully structured grids were created in the vortex path and for the rotor blades. Blade pitch changes and rotation of the domains/blocks relative to each other was achieved using chimera/overset grids. The rotor blades were meshed using an O-O type grid topology. Each blade mesh consisted of about 3.2M points. The rotor mesh consisted of 7.2M points and the background mesh of 27.2M points. Below the rotor a grid spacing of less than 10% of the blade chord length was used. A wall spacing of y+ < 1 was achieved at the blades, allowing to resolve the blade boundary layer rather than using wall functions. The blade surface was assumed to be fully turbulent, i.e., flow transition was not prescribed or calculated.

All simulations used second-order discretization in time and space and unsteady dual-time stepping. A physical time step was considered converged if the

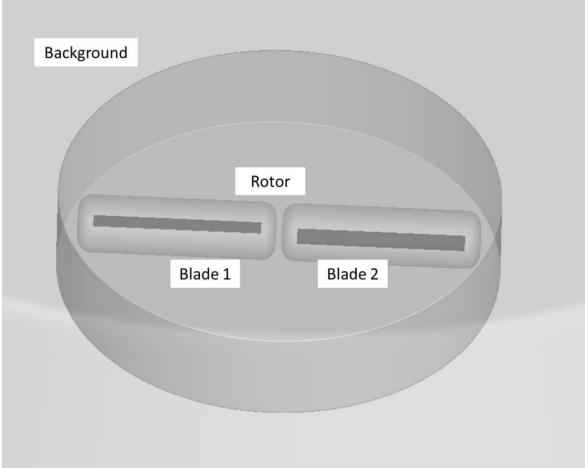

Figure 1: Schematic showing the used chimera setup.

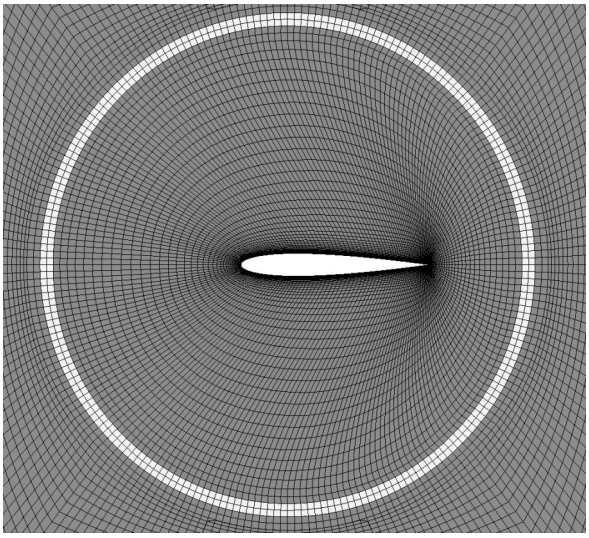

Figure 2: Schematic showing the chimera interpolation region(white) and the blade and rotor grid.

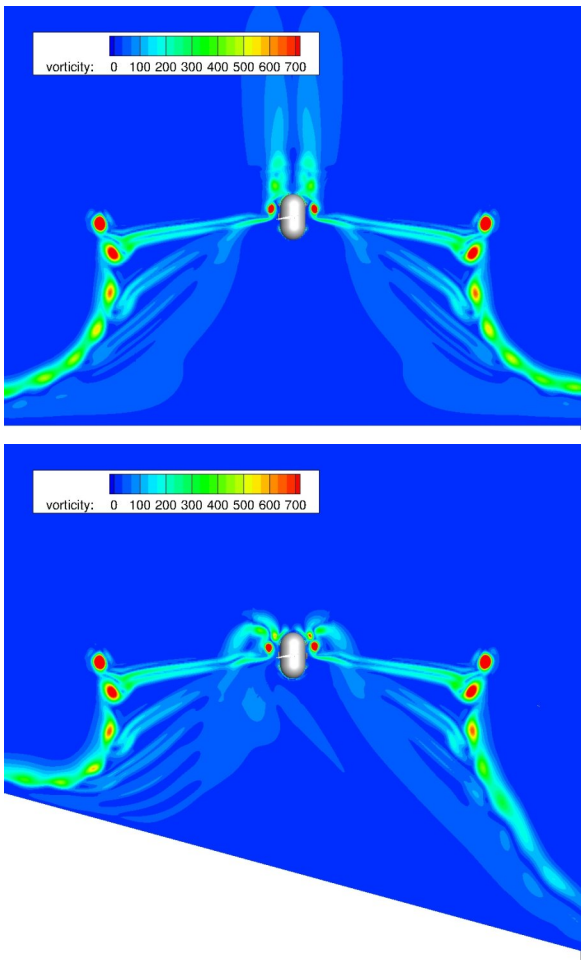

Figure 3: Comparison of vorticity fields from numerical URANS simulations for parallel ground plane (top) and inclined ground plane (bottom, Θ = 15°).

density residual in the time step could at least be reduced to 1e −6 in comparison to the overall first density residual. To rapidly dissipate the starting vortex, relatively large time steps, e.g. $\Delta\Psi = 90°$ for the parallel ground plane, were used to initialize the simulations. The final solutions were generated with significantly smaller time steps in the order of 1°.

Results

For the parallel ground plane (see Fig. 3) it was expected that the flow field is symmetrical for each azimuthal cut through the flow field up to large wake ages. This implies

that the stagnation point is located directly under the rotor hub. Only close to the ground plane the flow symmetry will be impaired, as vortex–vortex interaction and vortex–ground plane interaction will become significant. The currently used time step size in the numerical simulations will suppress these effects to a certain extent.

However, it was expected that the influence on the averaged rotor inflow distribution can be well represented using averaged interactions close to the ground plane. This could be confirmed by the experimental results. Furthermore, due to the symmetry of the flow field, it was expected that two large recirculation vortices form close to the ground plane inside the rotor slipstream, when viewed in a

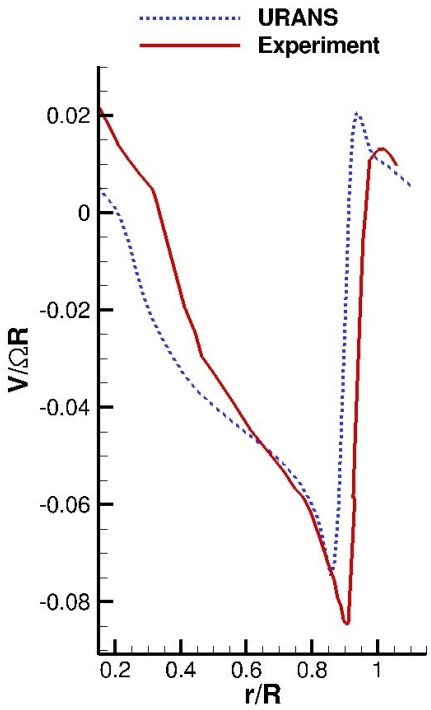

Figure 4: Comparison of calculated and measured inflow velocity distribution for parallel ground plane.

planar cut. A comparison of the measured and computed inflow velocity is shown in Fig. 4 for the parallel ground plane.

Conclusions

Current simulations and experimental results revealed that the structure of the flow field was altered significantly by changing the ground plane inclination angle. Instead of the two symmetric recirculation regions below the rotor for the parallel ground plane (when viewed in a planar cut), one large recirculation region formed and the stagnation point on the ground plane was located far uphill. The strongest effects on the inflow distribution were found to be located at the inboard sections of the blades. The flow field closer to the blade tips was less strongly influenced. Here, the tip vortex was the dominant influence. Its strength is mostly determined by the prescribed rotor thrust and, therefore, the effects of the ground plane-induced altered flow field were less significant. It could be shown that the current grid resolution along with the discretization order already allowed to predict the averaged flow field data and inflow distribution well.

On-going Research / Outlook

The interaction of the vortical structures within the helicopter downwash with the ground is of strong interest for several reasons. Therefore, the Institute of Helicopter Technology at TUM will continue to investigate these effects, also taking into account the helicopter fuselage or additional obstacles. In order to resolve the vortical flow within CFD a high spatial and temporal resolution is required and several rotations need to be taken into account. CoolMUC2 with it's fast interconnect and CPUs provides the capability to investigate the rotor downwash numerically and develop a deeper understanding of the occurring flow phenomena.

Uncertainty Propagation Applied to Multi-Scale Thermal-Hydraulics Coupled Codes: A Step Towards Validation

2

Research Institution
Lehrstuhl für Nukleartechnik, Fakultät für Maschinenwesen

Principal Investigator
Clotaire Geffray

Researchers
Clotaire Geffray, Chunyu Liu, Rafael Macián-Juan

Project Partners
European projects THINS (FP7) and SESAME (H2020)

Linux Cluster Project ID: pr58ca

Introduction

The modeling of complex thermal-hydraulic phenomena is a challenging task. The advanced codes available today include detailed physical models of the physics of interest. The initial and boundary conditions as well as the physical parameters and some physical models are all subject to some sort of uncertainty. The quantification of the effect of this modeling uncertainty on the computer code' predictions are of key importance for assessing the significance of the results.

Methods should therefore be used in order to assess the variability of the output which is due to the variability of the input (uncertainty analysis) and to identify the most important contributors to this variability (sensitivity analysis). The methods used to carry out uncertainty and sensitivity analysis should be carefully selected to account for the problem specific limitations (e.g. computational cost, (im)possibility to access the source code).

Finally, the obtained results can be compared to the experimental data and validation techniques can be applied to assess the quality of the code and model performance. This step is of paramount importance to understand the strengths and weaknesses of the codes and models and to open the way to their future improvement.

The main objectives of the work reported here are the following:

- to provide proof of principle that Uncertainty & Sensitivity Analysis techniques can be applied to coupled 1D and 3D thermal-hydraulics codes;
- to recommend methods that are best suited for the envisioned applications and issue best practice guidelines;
- to perform Uncertainty & Sensitivity Analysis on experiments performed on the TALL-3D facility;
- to assess the performance of the coupled model of the TALL-3D facility against experimental data;
- to conclude on the qualification of the code for application to pool type liquid metal cooled reactors;
- to identify shortcomings of the model and issue recommendations for future code development.

Results and Methods

This work resulted in one of the first applications of uncertainty propagation using coupled codes in the field of thermal-hydraulics. The automated procedure to initialize the stand-alone codes prior to their coupling for the transient calculation proved to be very efficient and versatile. The results from the uncertainty and sensitivity analysis helped quantifying the output variability and identifying the most important contributors to the code outcome variability when accounting for uncertainty in the input data. The added value gained thanks to the application of these methods included motivation for new experimental campaigns and prioritized model improvement strategies.

Three main analyzes were carried out. Each one included about 120 calculations of a given experimental scenario. Each calculation required 28 CPUs during about 2 days. It comprised two parallel jobs: a stand-alone initialization job and a coupled transient job. The coupled codes exchanged data at

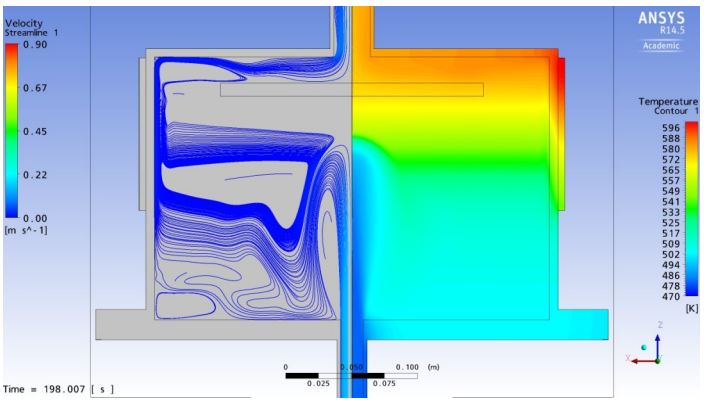

Figure 1: Streamlines (left) and temperature profile (right) in the CFD domain.

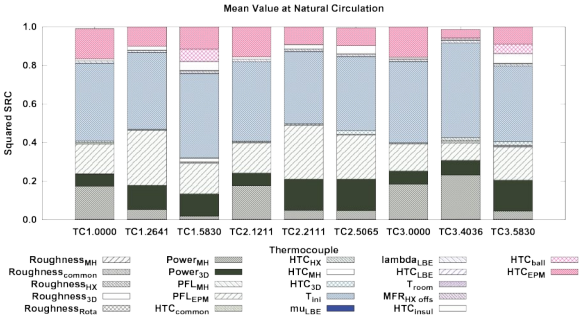

Figure 2: Results of a sensitivity analysis.

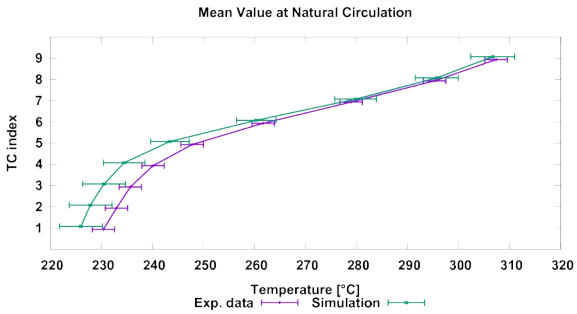

Figure 3: Tolerance limits for a temperature profile comparison with experimental data.

each time step thus allowing a real time feedback between the codes.

This so-called Multi-Scale coupling allows to use the computationally intensive CFD code (here ANSYS CFX) only where 3D phenomena are expected and the 1D code (here ATHLET) elsewhere. Thus the computational cost for the whole system simulation is kept at an affordable level without loss of resolution.

The jobs were submitted as array jobs which allowed to restrict the number of concurrently running jobs to the number of available licenses. In order to reduce the I/O latency, the input decks were transferred on the SCRATCH repository when the jobs were started. All the files were written on the SCRATCH and transferred back to the PROJECT repository at the end of the job. This procedure allowed a significant speed-up. The results were then extracted, processed and the original files were compressed (one run generated about 2 GB of data) and archived.

The calculations carried out for the preparation of [1] (which is available here [2]), had a computational cost of less than 500,000 Core-hours. Earlier analyses and calibration activities were also carried out on CoolMUC-1.

The simulated 3D domain is shown in Figure 1.

Typical results were the tolerance limits which bound a certain portion of the possible code outcomes at a certain level of confidence. In Figure 2 the predictions of the temperature profile (the bounds account for 95% of the cases with 95% confidence) are compared with the experimental data (and their associated error bars). As can be seen a good agreement with the experimental data was achieved with a slight over-cooling at the bottom of the pool (represented in Figure 1).

Additional knowledge can be gained from the calculations' results thanks to sensitivity analysis. In Figure 3, the relative importance of all the considered parameters is plotted. The area occupied by a given parameter on each bar is representative of its importance on the behavior of the monitored system response.

The results can be used to identify the most influential contributors to the output variability. This can advocate for new experimental campaigns aiming at a more accurate measurements or new model developments. If the uncertainty bounds of an influential input parameter can be reduced, the accuracy of the code predictions can be reduced (i.e. improved) as well.

The use of such techniques becomes nowadays essential in the decision making process as systems need to be optimized while strict safety criteria must be met. Nuclear safety authorities require their application for the validation of the codes and the establishment of the safety case.

The present work has demonstrated that uncertainty propagation can be applied to multi-scale thermal-hydraulics code and that a substantial added value can be gained from the application of uncertainty and sensitivity analysis. Thanks to the use of surrogate models, the calculations' results can be further used for calibration and validation purposes.

On-going Research / Outlook

This work was partly funded by the THINS project (grant agreement number 249337) and by the SESAME project (grant agreement number 654935) of the European Commission (EC).

The SESAME project is still ongoing and work is carried out at the institute for nuclear engineering [3] to extend the developed methodology.

Without the computational resources of CoolMUC-2 and the ANSYS CFX licenses of the LRZ, the work reported here would not have been possible. One of the main issues encountered was the limitation on the number of licenses. Future activities might consider using only open source solutions.

References and Link

[1] Geffray, C. (2017). Uncertainty Propagation Applied to Multi-Scale Thermal-Hydraulics Coupled Codes: A Step Towards Validation (Doctoral dissertation, Technische Universität München).
[2] https://mediatum.ub.tum.de/1325469
[3] http://www.ntech.mw.tum.de

SFB TRR40 Summer Program 2017 – Combustion Instabilities in a Multi-Injector GOX-GCH4 Combustion Chamber

Research Institution
Institute for Aerodynamics and Fluid Mechanics

Principal Investigator
Christian Stemmer

Researchers
Bo Zhang, Bing Wang, Xiangyu Hu, Oskar Haidn

Project Partners
School of Aerospace Engineering, Tsinghua University, Beijing, China, Chair for Rocket Propulsion, TUM

Linux Cluster Project ID: pr63ve

Introduction

The particularly high complexity and extreme thermal and mechanical loads of chemical propulsion engines call for intensive fundamental research as prerequisite for radical improvements and innovative technical solutions. Critical, thermally and mechanical highly loaded components of space transportation systems with chemical propulsion engines are the focus of the collaborative research center. The main areas of research are the combustion chamber, the nozzle, aftbody flows around the integrated rocket engine, and structure cooling.

The scientific objective of TRR 40 is to perform fundamental research for accomplishing a significant gain in efficiency and reliability and in reduction of cost of future primary propulsion engines for space transportation systems. The power-to-mass density of the main-stage Ariane 5 engine 'Vulcain 2' is almost 2 MW/kg, a ratio which no other known man-made energy-conversion machine reaches. A single Ariane 5 rocket engine (Vulcain 2) develops up to 1360 kN of thrust – this is equivalent to all four engines on a A380 airbus. The cooling power needed to prevent the nozzle from failure surpasses 100 MW/m2, the power of thrust chamber totals 3 GW and the mass flow of liquid oxygen and hydrogen exceeds 300 kg/s. The sheer numbers underline that novel interdisciplinary technological design procedures are needed to take the development of rocket engines to new levels in reliability and performance. Scientific core subject of all divisions within the collaborative research center TR40 is the multi-disciplinary investigation of nonlinearly coupled thermomechanical systems. Model development is based on experimental findings and validation by detailed numerical simulation in all participating projects.

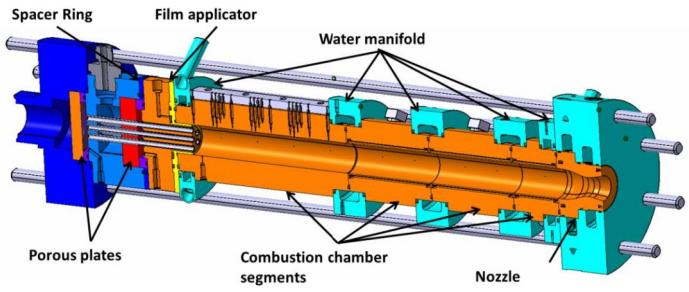

Figure 1: Combustion chamber test facility at TUM.

Innovative cooling concepts are needed for combustion chamber temperatures of about 3500K and multi-scale, multi-physics modelling approaches are developed to handle injection temperatures near the critical point of 50-70K. Dynamic thermomechanical loads, highly unsteady wake flows, new materials and alternative propulsion fuels are among the main focus areas in the interdisciplinary modelling efforts.

Together with the leading universities in Germany in rocket propulsion (RWTH Aachen University, TU Braunschweig, University of Stuttgart, The University of the Armed Forces Munich) the German national aeronautics and space research centre (DLR) and the industrial partner Airbus-Safran Launchers, the TUM is leading the 25 projects in its third (and final) funding period. The German Research Foundation (DFG) has granted another four years and 10 M€ to the TR40, which is the largest research center funded by the DFG in the engineering sciences. The combination of excellent research capabilities and world-class experimental facilities together with an industrial partner is unique among the DFG-funded research centers and receives world-wide attention through its high-level publications and research activities, like the biennial summer research program.

In the presented project, liquid oxygen (LOX) and liquid hydrogen (LH_2) combustion was investigated in a rocket motor setting. LOX/LH_2 has been widely used in liquid rocket engine for transfer into orbit or space exploration due to its high specific impulse. The potential of using hydrocarbon as propellant, in particular methane instead of hydrogen, is one of the most promising solution for the high operational costs. Developing new fuel type rocket engine also brings new challenges to combustion instabilities. To study combustion instabilities in rocket engine using hydrocarbon as fuel, a compressible LES turbulent combustion parallel solver is used to get numerical simulation results. Test cases are based on experimental data of BKS on the LTF high pressure test stand at TUM, which is a multi-element rocket combustion chamber. Both stable and unstable combustion are observed in the experiment and pressure signals at positions along whole chamber are

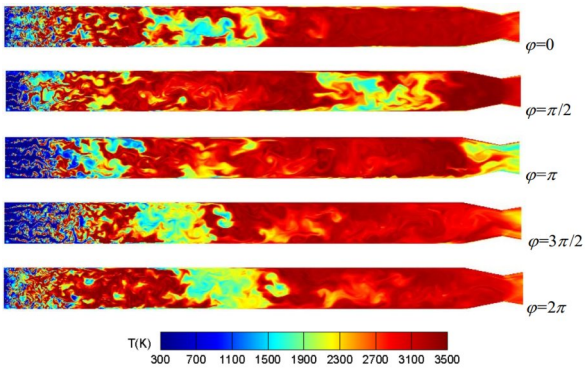

Figure 2: Instant temperature during one cycle (phase: 0,π/2, π,3π/2,2π) for the unstable case.

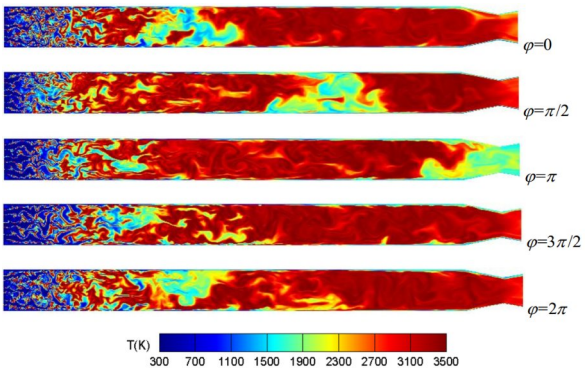

Figure 3: Instant temperature during one cycle (phase: 0,π/2, π,3π/2,2π) for the stable case.

acquired. For unstable case both experiment and simulation show a dominant frequency about 1400Hz, which is the 1st order longitudinal mode of the combustor. For stable case there are also several frequencies but the amplitude is quite small. Several parameters are studied and we find that for unstable case CH_2O (which is mainly involved with ignition process) has the same phase with pressure, OH (which is mainly involved with heat release) has a little phase lag with pressure but less than 90°, meaning that they are still mostly coupled. While for stable case both CH_2O and OH has totally different phase with pressure. Also we find that pressure wave will increase the baroclinic term in vorticity equation, thus increasing fuel oxygen mixing and then promote combustion and heat release.

Results and Methods

The simulations were conducted with RoSimn which is developed by the Spray Combustion and Propulsion Lab in Tsinghua University. RoSim is a compressible LES turbulent combustion parallel solver. The formulation is based on the Favre-filtered conservation equations of mass, momentum, and energy in three dimensions. These equations are obtained by filtering the small-scale dynamics from the resolved scales over a well-defined set of spatial and temporal intervals. geometry. For sub-grid model we use Smagorinsky model and a standard value of 0.7 is used for the turbulent Prandtl number. For advection terms we use 5th order WENO scheme which is more dissipative than the upwind scheme but quite robust for high pressure combustion simulation during our tests. For viscous term we use 6th order central difference scheme. For time iteration we use 3rd order Runge-Kutta method. For reaction source term we use finite rate reaction model with reduced mechanism and we use laminar estimation without turbulent combustion interaction. Also we use point implicit method to solve stiffness of the source term. For boundary conditions we use the NSCBC method.

The hybrid program uses MPI and Openmp. The combustion chamber model depicting the geometric setup is shown in Figure 1. The pressure of the combustion chamber was 20 bar in both cases considered and the inlet temperature was at 300K. for the unstable (first) case, the total mass flux was at 0.3024 kg/s whereas a small reduction of the total mass flux to 0.275 kg/s lead to a stable combustion process (second case). The most typical job was run on 308 CPUs and ran for about 8000 CPUhrs each. Large eddy simulation of a multi-injector GOX/GCH_4 combustor has been used to predict combustion instabilities and pressure distribution along the axis has been compared with experiment data. Both stable and unstable cases are predicted by numerical simulation, and the thermoacoustic coupling has been invested.

For the unstable case (Figure 2), the dominant frequency is close to the experiment, and the flame length increases slowly but decrease quickly. Since the cases work at fuel rich zone, there is still unburnt methane left, causing low temperature field in the product. For the stable case, the pressure amplitude is much smaller and the flame length does not change much during one cycle. For the unstable case, when the pressure wave comes to the head of the chamber, CH_2O reaches its peak value, and vorticity also reaches its peak value because the pressure gradient increases the baroclinic term of the vorticity equation. This vorticity increment will increase fuel oxygen mixing, thus promoting combustion and heat release. OH reaches a high value when pressure wave comes, and there is a phase lag which is less than 90°. Pressure and heat release are mostly coupled, leading to combustion instabilities.

For the stable case (Figure 3), there is no obvious coupling between the pressure and the combustion process, thus the pressure amplitude is much weaker. Further explaining the coupling mechanism requires to understand the relationship among several time scales, which is the mixing time, the cold inflow heating time, ignition delay time, and acoustic propagation time. A theoretical model should be build based on time-lag theory, which is worth being studied in the future.

On-going Research / Outlook

The research within the next 2019 summer program is planned to encourage further international cooperation concerning combustion modelling and instability investigations on the configurations present in the combustion chamber test facilities at TUM and DLR Lampoldshausen.

References and Links

[1] www.sfbtr40.de, www.aer.mw.tum.de
[2] C. Stemmer, N.A. Adams, O.J. Haidn, R. Radespiel, T. sattelmayer, W. Schröder, B. Weigand, Annual report of the SFB TRR40 summer program 2017 available online at http://www.sfbtr40.de/index.php?id=proceedingsofthesummerprogram

High Fidelity CFD Simulation for Wind Turbine Cluster Control

Research Institution
Wind Energy Institute, TUM

Principal Investigator
Jiangang Wang

Researchers
Chengyu Wang, Filippo Campagnolo

Project Partners
Politecnico di Milano

Linux Cluster Project ID: pr85le

Introduction

Wind farms are collections of wind turbines, often operating in close proximity of one another. During operation, several major phenomena take place within a wind farm: there is an interaction between the atmospheric boundary layer and each individual wind turbine, and an interaction among upstream and downstream wind turbines through their wakes. In fact, a wake-affected inflow results in lower power output and increased loading for the downstream wind turbines when compared to an isolated condition. A number of control strategies are currently being investigated to optimize the operation of wind farms, including power derating and wake deflection [2].

Our group has developed scaled wind turbine models, operated in a large boundary layer wind tunnel. The machines are actively controlled (and optionally aeroelastically scaled), and are designed to generate realistic wakes notwithstanding the low Reynolds numbers at which they operate. This unique facility enables experiments to study aeroservoelasticity, turbine wakes, machine-to-machine interactions, and wind farm control for power maximization and load mitigation. The facility is highly instrumented, allowing for the collection of a wide range of high quality data.

A parallel on-going research effort of our group aims at developing a digital copy of this experimental facility, including the wind turbines and the wind tunnel itself. State-of-the-art numerical methods are used to model the wind tunnel generated flow, the wind turbines (including blades, nacelle, tower), and their shed wakes interacting with the other machines and the wind tunnel. The simulation tool also allows for the testing of different wake control strategies and the analysis of floating offshore wind turbines (FOWTs).

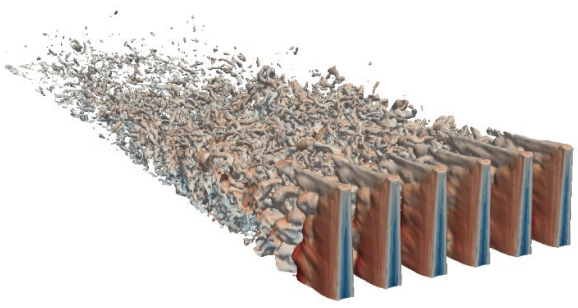

Figure 2: Iso-surface vorticity for turbulence generating spires.

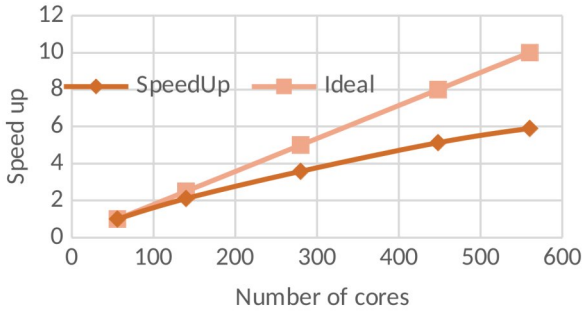

Figure 1: Scaling behavior of the LES framework.

Numerical model

The current simulation framework is developed within SOWFA [5], a simulation tool based on a standard incompressible solver in the OpenFOAM repository. The code uses an actuator line method embedded in a large-eddy simulation (LES) environment, coupled with the aeroservoelastic simulator FAST [5]. An immersed boundary (IB) formulation [3] is used to model the wind turbine nacelle and tower. A blended connective scheme algorithm, coupled with the Gamma and center differencing scheme, is also implemented in the solver to minimize numerical diffusion (Gamma is used at near wake, while center differencing scheme is used at far wake). The employed numerical methods are described in detail in Ref. [3].

Roughly 15 million CPU hours have been used to develop the current simulation framework. A typical production run uses 560~1120 processors and lasts for 72 hours. The storage of each simulation case is kept within 50GB. The current approved overall storage in the LRZ cluster is 2.4 TB. The code package is generated by using the GCC compiler and the Intel MPI library. By loading the Intel MPI module, the runtime performance is enhanced by an extra of 10-20% with respect to the OpenMPI library. Figure 1 presents the scaling behavior of the current solver (parallel efficiency equals to 85%).

Results and analysis

Iso-vorticity surfaces of the precursor and of the wind turbine cluster simulations are visualized in Figs. 2 and 3. The figures show the generation of large vortical structures by the spires placed at the tunnel inlet. Such structures break down into a sheared and turbulent flow that becomes the inflow of the downstream turbines [4].

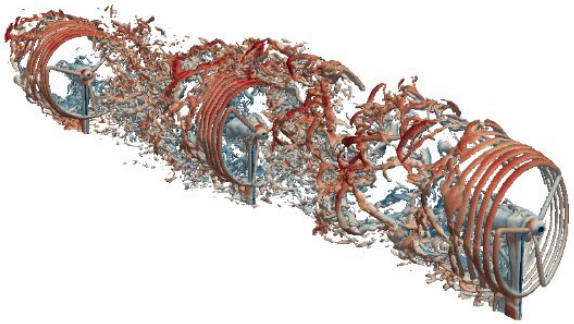

Figure 3: Iso-surface vorticity for three misaligned wind turbines.

Figure 4 shows the streamwise velocity field at a horizontal plane 0.09D above hub-height. The images on the top report LiDAR measurements, the ones in the center are the corresponding numerical simulations, while the ones in the bottom part show the difference between measurements and simulations.

Figures to the left correspond to the case of greedy control, in which all turbines point into the wind. Figures to the right correspond to the case where the two upwind machines have been optimally yawed out of the wind to deflect their wakes and reduce the shading of the downstream turbines. For both the greedy and the optimal yaw cases, the figures show a good qualitative accordance between experiments and simulations. A significant wind farm power increase can be achieved by yaw control in this particular turbine layout and operating conditions. In fact, compared with the baseline greedy case, the optimally-yawed turbine cluster produces 17.6% more power.

On-going Research / Outlook

Our group is actively researching new and efficient methods for wind farm control. For this to be successful, a thorough understating of the behavior of wakes is indispensable. CFD, and in particular the LES framework described herein, is providing a wealth of information that is enabling and accelerating wind farm control research.

We plan to perform extensive studies using the framework in the coming months. CoolMUC-2 offers great support to our current research efforts, since it provides abundant computational resources and offers reliable service support for code development and maintenance. We look forward to using CoolMUC-2 in the future as a fast and reliable HPC cluster for wind farm control research.

References and Links

[1] http://www.wind.mw.tum.de/index.php?id=67&L=1
[2] Jiangang Wang, Dan McLean, Filippo Campagnolo, Tong Yu, Carlo Luigi Bottasso. 2017. Large-Eddy Simulation of Waked Turbines in a Scaled Wind Farm Facility. IOP publishing 854, 1.
[3] Jiangang Wang, Spencer Foley, Emmanouil Nanos, Tong Yu, Filippo Campagnolo, Carlo Luigi Bottasso, Alex Zanotti, Alessandro Croce. 2017. Numerical and Experimental Study of Wake Redirection Techniques in a Boundary Layer Wind Tunnel. IOP publishing 854, 1.
[4] Chengyu Wang, Jiangang Wang, et al. 2018. Validation of large-eddy simulation of scaled waked wind turbines in different yaw misalignment conditions. IOP publishing preprint.
[5] Churchfield Matthew, Sang Lee. 2012. NWTC design codes-SOWFA. URL: wind.nrel.gov/designcodes/simulators/SOWFA

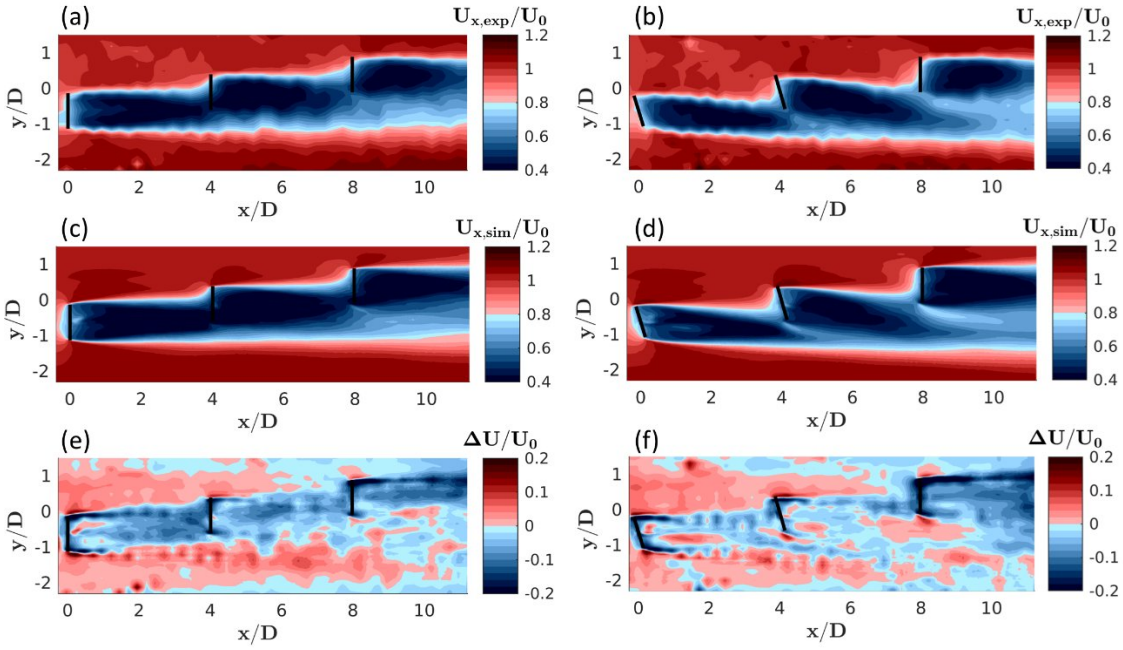

Figure 4: Stream-wise velocity field 0.09D above hub height.

CFD-Simulation of Oil Flow and No-load Gear Power Loss in Gearboxes

Research Institution
Institute of Machine Elements (Gear Research Centre)

Principal Investigator
K. Stahl

Researchers
H. Liu

Linux Cluster Project ID: pr89ca

Introduction

Most transmissions use gears and gear trains to convert speed and torque. Current developments on geared transmissions focus on three main concerns: load carrying capacity, noise-vibration-harshness (NVH) behavior and efficiency. Increasing the efficiency of modern gearboxes contributes significantly to the reduction of energy consumption and saving of resources. In order to guarantee operational reliability, gearboxes are often designed conservatively with an oversupply of oil. An oversupply of oil results in an unnecessary high amount of oil kept in motion and therefore in high no-load losses. Detailed information on the oil distribution in the early design stages helps to optimize the lubrication and to increase the efficiency.

Due to the increasing computational power, the CFD (Computational Fluid Dynamics) has become a new alternative for the approximation of oil flow and power loss behavior in geared transmissions. First results have shown that it is a very promising approach, as it is able to calculate the no-load gear power losses with high accuracy. Moreover, it offers a very flexible way to gain a deeper insight onto the oil distribution inside gearboxes with almost no restrictions on the geometry and operating conditions [1–3], which cannot be done by other methods.

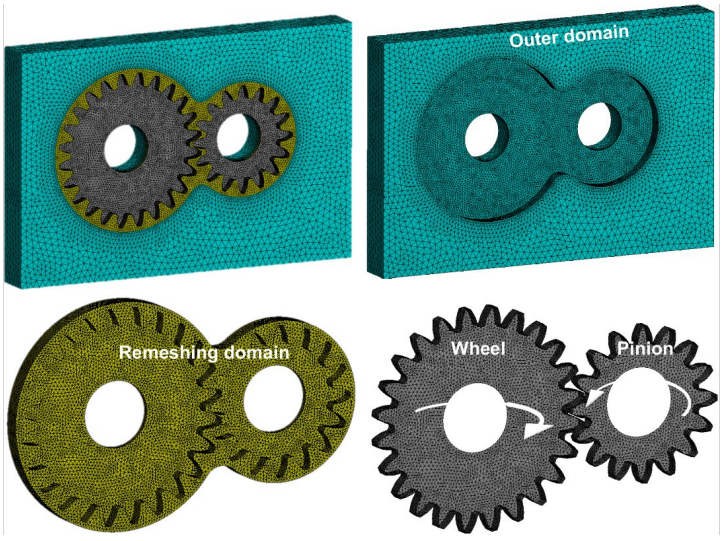

Figure 1: Mesh model of the considered test gearbox [3].

Within this project, the oil flow behavior and the no-load power losses of a single stage test gearbox are studied at various operating points with regard to the gear geometry, oil properties as well as the gear kinematics. The long-term goal of this project is to derive a best practice guideline for CFD-users from industry to simplify the application for gearbox simulation.

In addition to that, on the basis of the new findings, existing empirical equations can be optimized.

Results and Methods

During a CFD analysis, conservation equations with regard to mass and momentum in discrete form are solved iteratively in control volumes. Thus, the fluid domain has to be discretized in a first step.

The object of investigation is a single stage gearbox of the FZG no-load power loss test rig with test gears of type C. The mesh model represents the negative of the test gearbox and can be divided into four domains: the pinion and wheel domain, the outer domain and the dynamic zone, i.e. the remeshing domain. During the simulation, the pinion and wheel domain, which are discretized by prism elements, rotate inside the outer domain at predefined circumferential speeds. The outer domain is a stationary body meshed with tetrahedral elements. The remeshing domain fills the cavity between the gearbox domain and the pinion and wheel domain. During operation, the meshing zone of the pinion and wheel is a transient area that changes at every gear meshing position. Therefore, the remeshing domain consists of a deformable meshing structure that changes with every time step of the rotating pinion and wheel domain. The domain of the remeshing domain is discretized with deformable tetrahedral elements that follow every rigid movement. The entire mesh model is shown in Figure 1.

Based on this simulation model, the influence of the oil viscosity of different mineral oils on the oil flow was studied. Figure 2 shows an exemplary result of three different mineral oils, which oil viscosity was varied from 32 cSt (FVA2) to 460 cSt (FVA4) [3].

The simulation was performed with the commercial

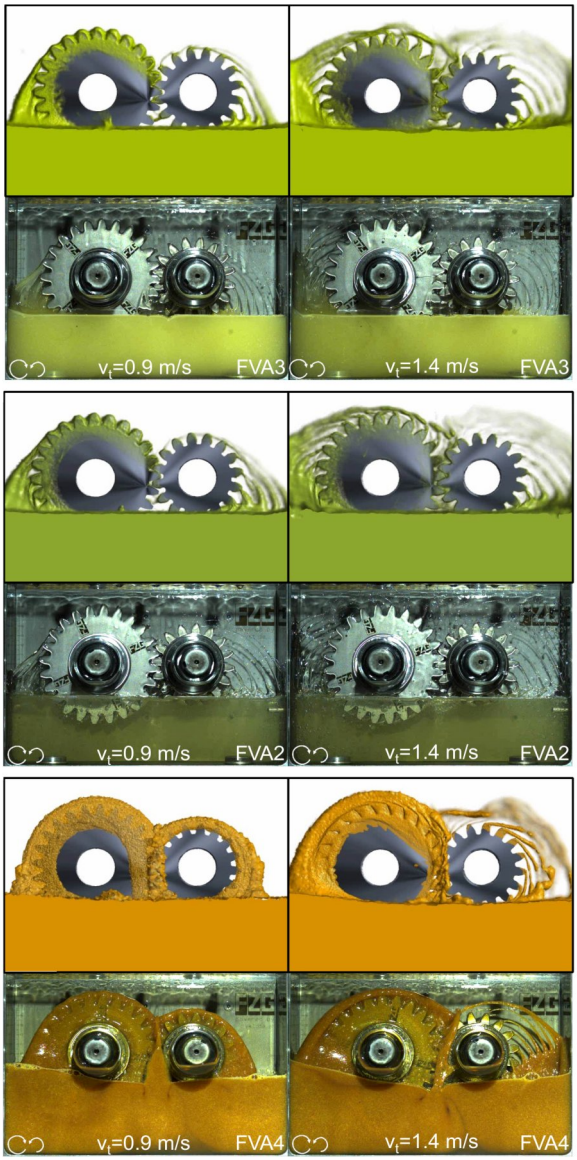

Figure 2: Simulated oil distribution in comparison with high-speed camera recordings with mineral oils FVA3, FVA2, FVA4 (ϑ_{oil}=40°C) at v_t = {0.9; 1.4} m/s [3].

software ANSYS Fluent. The licenses were provided by CoolMUC-2 (LRZ). The transient simulation of one operating point acquires several gear rotations until a quasi-stationary condition in terms of oil flow behavior is established. In general, the simulation is usually performed with 40–80 cores, so that one operating point acquires 10,000–15,000 CPU hours. In the framework of this project, a total amount of around 200 operating points including geometrical, oil specific as well as kinematic influencing parameters is required. Therefore, a total number of 3.32 mio. CPU hours is needed. For this project, 100 GB storage is provided in the local register.

On-going Research / Outlook

In addition to the running DFG project STA 1198/14-1, different gear and transmission types will be studied. The research contents include injection lubricated spur gears, crone gears, hypoid gears, planetary gears as well as transmissions for electric mobility applications.

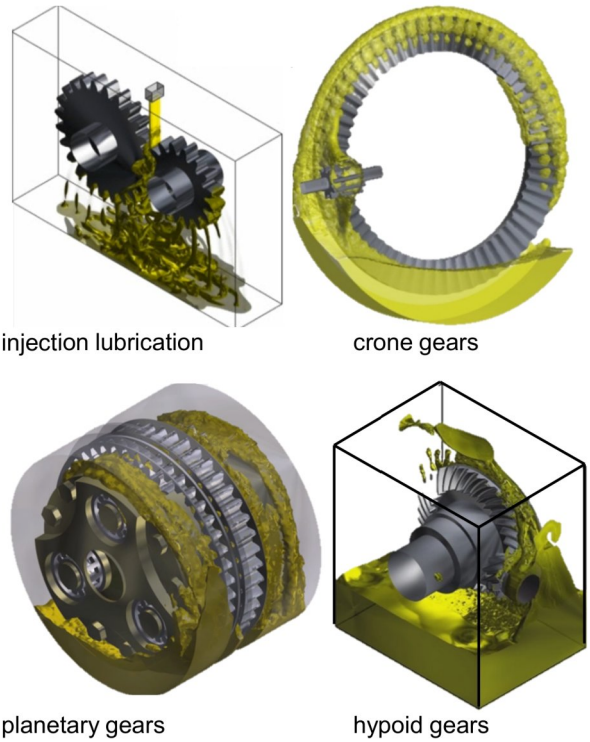

Figure 3: Forseen research on CFD gearbox simulation at the Gear Research Centre.

Figure 3 gives an overview of forseen research on CFD gearbox simulation at the FZG.

Due to the high demand of computational power, the solution process of all simulations has to be accomplished at the CoolMUC-2 and the Supermuc at LRZ. As the number of software licenses is limited and the utilization rate at LRZ is considerable high, the progress of the research highly depends on the occupancy of software licenses at CoolMUC-2. Because of the high demand, a higher number of software licenses would contribute to an even faster progress of the project.

In 2018, a new project aimed at CFD simulation of a hypoid geared rear axle transmission is planned. In this project, different CFD methods including the Smoothed Particle Hydrodynamics and the Finite Volume Method will be applied. The computational power will also be provided by LRZ.

Acknowledgement

The authors would like to thank the DFG (STA 1198| 14-1) and LRZ (CoolMUC-2) for their sponsorship of this research.

References and Links

[1] Liu, H., Arfaoui, G., Stanic, M., Montigny, L., Jurkschat, T., Lohner, T., Stahl, K. Numerical Modelling of Oil Distribution and Churning Gear Power Losses of Gearboxes by Smoothed Particle Hydrodynamics. Journal of Engineering Tribology. doi: https://doi.org/10.1016/j.triboint.2016.12.042. (2017)

[2] Liu, H., Jurkschat, T., Lohner, T., Stahl, K. Determination of oil distribution and churning power loss of gearboxes by finite volume CFD method. Tribology International, 346–354. doi: https://doi.org/10.1177/1350650118760626. (2017)

[3] Liu, H., Jurkschat, T., Lohner, T., Stahl, K. Numerical modeling and validation of oil distribution and churning losses in gearboxes. 6th World Tribology Congress 2017, Beijing. (2017)

Thermoacoustic Instabilities and Combustion Noise

Research Institution
Professur für Thermofluiddynamik, TU Munich

Principal Investigator
W. Polifke

Researchers
A. Albayrak, A. Avdonin, A. Ghani, S. Guo, M. Häringer, M. McCartney, M. Meindl, M. Merk, D. Rouwenhorst, F. Schily, C. Silva, T. Steinbacher, S. van Buren

Project Partners
École Centrale Paris, GE, IMFT Toulouse, SIEMENS, U. Cambridge

Linux Cluster Project ID: pr94ho

Research Focus

In recent years, the research efforts of the thermo-fluiddynamics (TFD) group have focused almost exclusively on thermoacoustic combustion instabilities. This type of self-excited instability results from a feedback between fluctuations of heat release rate and acoustic perturbations of velocity and pressure, and may occur in combustion applications as diverse as domestic heaters, gas turbines or rocket engines. Possible consequences are increased emissions of noise or pollutants, limited range of operability or severe mechanical damage to a combustor. Thermoacoustic instabilities have hindered the development of low-emission, reliable and flexible combustion systems for power generation and propulsion. Due to their multi-scale and multi-physics nature, the prediction and control of such instabilities is a very challenging problem with manifold exciting research opportunities. In the following, recent achievements of the TFD group are summarized.

Linearized (Reactive) Flow Solvers

Analysis of thermoacoustic combustion instabilities is typically based on linearized perturbation equations for compressible reactive flow, with important effects of convection by mean flow. A discontinuous Galerkin finite element method with superior accuracy and stability for this type of equation has been developed in the TFD group [1]. Combined with the state-space framework of the in-house taX software, this method makes possible the computation of transfer functions and thermoacoustic eigenmodes with unprecedented speed and flexibility.

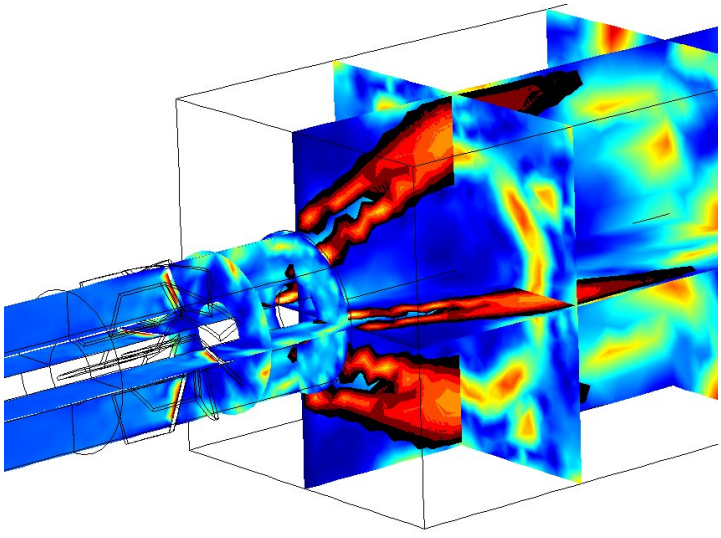

Figure 1: Axial velocity of the unstable, intrinsic thermoacoustic eigenmode of a swirl burner [1].

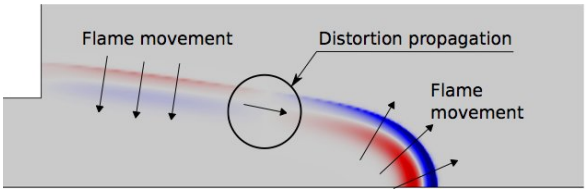

Figure 2: Distribution of heat release rate fluctuations of the intrinsic thermoacoustic eigenmode of a laminar flame [2].

Inclusion of a linearized source term for species production and heat release allows the explicit inclusion of flow-flame-acoustic coupling in the computation of thermoacoustic eigenmodes [2], which has hitherto not been possible.

Inertial waves as well as entropy waves can also be described in this framework. First results on the propagation speed of inertial waves, the effect of inertial waves on flame dynamics, and the source term of entropy waves have been achieved and published [3]. Such fundamental investigations of flow-flame-acoustic interactions provide important guidance for the proper formulation of analysis and design tools for thermoacoustic stability.

Uncertainty Quantification

Thermoacoustic instabilities are highly unpredictable, because they respond in a very sensitive manner to slight changes in operating or boundary conditions. As a result instabilities are detected often only at the later stages of development in full combustor tests, resulting in significant overruns of development cost or time. It is essential to deploy robust and reliable simulation methodologies that include strategies to quantify the uncertainty of model predictions and their

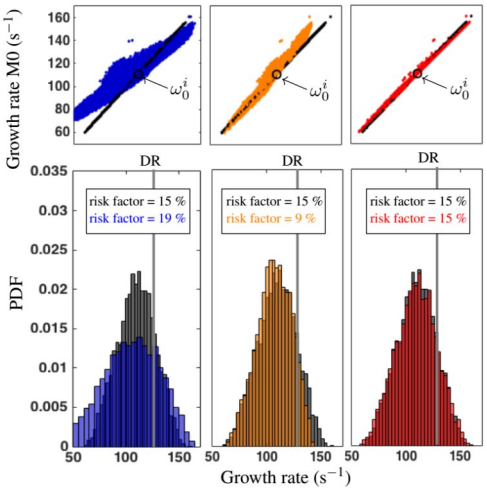

Figure 3: Uncertainty of growth rates and risk factor of thermoacoustic instability, predicted with adjoint-based surrogate models of increasing order [6].

sensitivity to parameter changes. The TFD group has developed and applied successfully a variety of strategies for uncertainty quantification in thermoacoustics, such as non-intrusive Polynomial Chaos Expansion [4], or Active Subspace [5]. The development of surrogate models by analytical means, or by exploiting adjoint numerical solutions [6], has played an important role in these efforts.

Combustion Noise

In the past year, the TFD group has developed characteristic-based, state-space boundary conditions, which allow for imposing non-trivial acoustic impedances at the computational domain boundaries in a robust and flexible manner. Furthermore, advanced techniques for system identification were introduced, which estimate noise models as well as

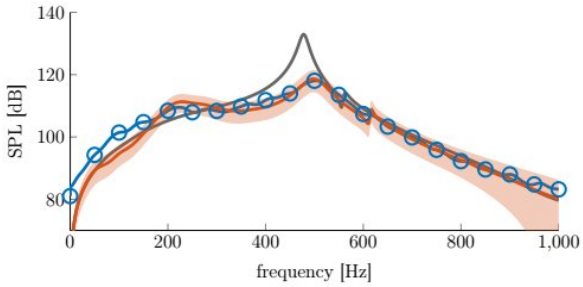

Figure 4: Power spectral distribution of pressure fluctuations generated by an enclosed turbulent swirl burner. Measurements (o) vs. modeling with one-way (—) and two-way coupling (—). Shading indicates the 95 % confidence interval of results [7].

confidence intervals from time series data generated by high-fidelity simulations [7].

Combining these techniques with Large Eddy Simulation of turbulent combustion makes possible the accurate and efficient prediction of combustion noise. Furthermore, eigenmode analysis of the spectral distribution of pressure fluctuations elucidates the interplay between combustion noise generation, flame dynamics, and thermoacoustic resonances. The results emphasize the necessity of including full two-way coupling in simulations of flow-flame-acoustic interactions.

On-going Research / Outlook

The research of the TFD group strongly relies on adequate computational resources. The majority of the compute-intensive numerical simulations were performed on CoolMUC-2.

In further investigations, we will extend the applicability of the linearized reactive solver and the uncertainty quantification techniques to more realistic problems, including turbulent flow.

Links and References

Link to the research institution: www.tfd.mw.tum.de

[1] M. Meindl, A. Albayrak, W. Polifke, submitted to Journal of Computational Physics (2018).
[2] A. Avdonin, M. Meindl, W. Polifke, 37th Int'l Symposium on Combustion (2018).

Evaluating the efficiency of parallelization in CFD-Applications

2

Research Institution
Chair I of Technical Chemistry

Principal Investigator
O. Hinrichsen

Researchers
D. Hirche

Linux Cluster Project ID: pr95xu

Introduction

With the increasing performance and cores of computers CFD applications became more and more popular in engineering sciences. CFD simulations can resolve a fluid flow geometry by any range of detail imaginable, but therefore the total number of equations which have to be solved increases with the degree of detail. Many CFD software packages allow parallelization of simulations to decrease the simulation time. The geometry is split up in parts and every part is calculated by an individual core of the computer. But with increasing parallelization, i.e. more cores for calculations, the number of non-calculating-tasks, e.g. information passing between cores, increases as well. According to Amdahl's law [1] the theoretical speed up due to parallelization is linear with the number of cores used, but limited by the factor of parallelization and serial share of computational time.

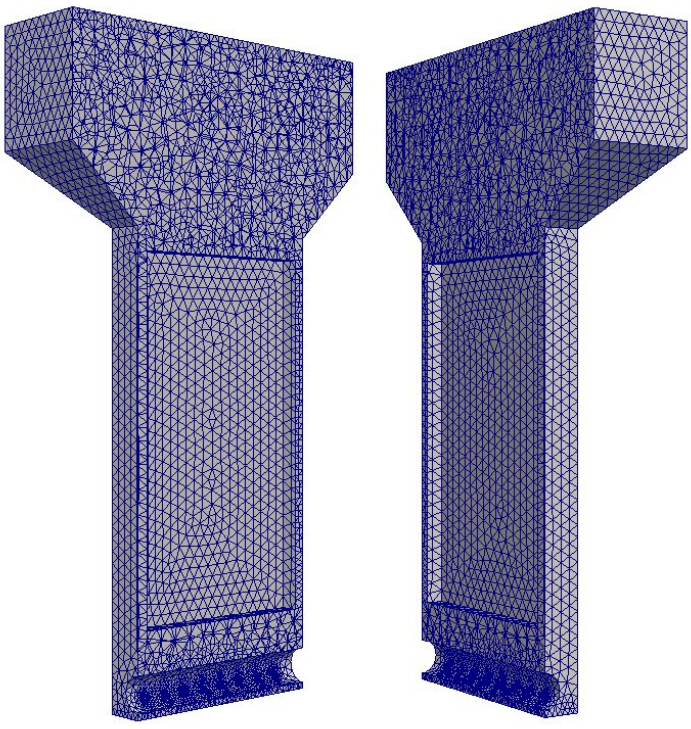

Figure 1: Exemplary illustration of simulated mesh geometry of case medium (128,696 cells).

Name of System	CPU	# cores per node	# nodes
CoolMUC-1	AMD Opteron 6128 HE	16	172
CoolMUC-2	Intel Xeon E5-2697 v3	28	384
Dell Precision Rack 7910	Intel Xeon E5-2687W v3	20	1

Table 1: Overview of hardware used for parallelization testing.

In the following, the degree of parallelization of an anaerobic fluidized membrane bioreactor (AnFMBR) [2] will be investigated by analyzing the required simulation times depending on the total number of cores used for the simulation. The open-source C++ based CFD package OpenFOAM [3] was used for the simulations.

Results and Methods

The degree of parallelization is investigated for two different HPC systems (Linux-Cluster CoolMUC-1 and CoolMUC-2) and one workstation (Dell Precision Rack 7910). Table 1 states the processor name, number of cores per node and the total number of nodes available for simulations.

The effect of parallelization is also dependent on the size of the problem, i.e. the mesh size. Five different

Simulation Name	# mesh cells	# total cores used
very coarse (VC)	28,045	50
coarse (C)	63,053	50
medium (M)	128,696	150
fine (F)	228,105	250
very fine (VF)	478,088	400

Table 2: Definition of cases tested for parallelization study.

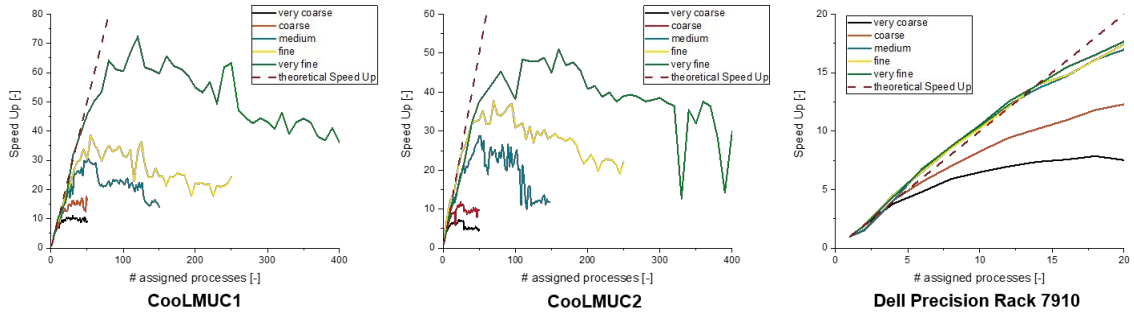

Figure 2: Comparison of speed ups for different hardware systems depending on the number of assigned processes.

mesh sizes of the AnFMBR are tested. The mesh sizes and the number of cores used for the parallelization testing are given in Table 2 and an exemplary figure of the medium mesh is illustrated in Figure 1.

Figure 2 shows the speed up for the finalized parallelization testing. For a lower number of assigned processes the total speed up of all meshes is close to the theoretical speed up. With more assigned cores the increase in achieved speed up is not correlating with the number of cores anymore, begins to stagnate at first. A further increase in assigned cores leads to a speed up decrease for all mesh sizes. Figure 2 also shows, that the efficiency of parallelization is highly dependent on the mesh size as well. Smaller mesh sizes can utilize a higher number of assigned cores, because the number of calculations for each core are too small. It can be concluded that the efficiency of the parallelization, i.e. achieved speed up closest to theoretical speed up, in this specific CFD setup is highest for a lower number of assigned cores. The highest speed up can be reached by further increasing the number of assigned cores. Depending on the mesh size an upper boundary for the speed up exists at which the achieved speed up decreases with increasing the number of assigned cores.

Depending on the importance of efficiency or highest achievable speed up, the selection of the assigned cores can be chosen accordingly.

Figure 3 shows an exemplary illustration for the application of an AnFMBR, where the particles are fluidized to lessen the fouling at the membrane. The simulation time was optimized by the acquired knowledge in this project.

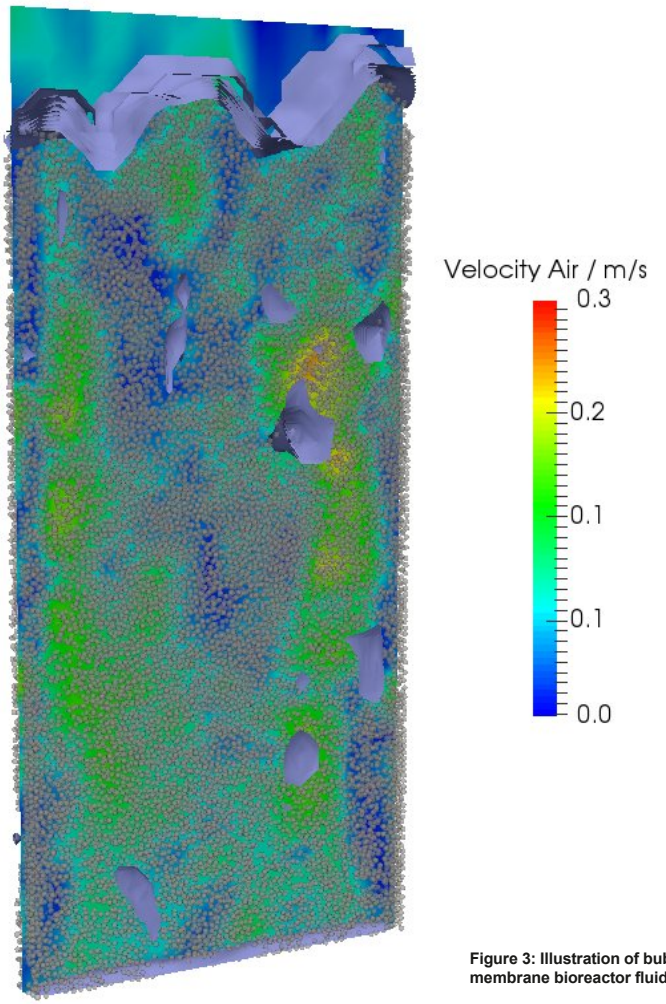

Figure 3: Illustration of bubble behavior in an anaerobic fluidized bed membrane bioreactor fluidized with GAC-particles for waste-water treatment.

On-going Research / Outlook

We gratefully acknowledge the computational resources provided by Leibniz-Rechenzentrum München. Still, the parallelization of CFD applications has many questions left to be answered. In further work, the effect of renumbering the mesh cells after the decomposition can be analyzed. Also the importance of the message passing algorithm, e.g. MPI and OpenMPI, has not been investigated yet as a part of this project as well as the parallelization efficiency of matrix solvers.

References and Links

[1] G. Amdahl. 1967. Validity of the Single Processor Approach to Achieving Large-Scale Computing Capabilities, AFIPS Conference Proceedings, 30 (1967), 483–485.
[2] J. Wang, F. Zamani, A. Cahyadi, J.Y. Toh, S. Yang, B. Wu, Y. Liu, A.G. Fane and J.W. Chew. 2016. Correlating the hydrodynamics of fluidized granular activated carbon (GAC) with membrane fouling mitigation, J. Membr. Sci. 510 (2016), 38–49.
[3] H. G. Weller, G. Tabor, H. Jasak and C. Fureby, A tensorial approach to computational continuum mechanics using object-oriented techniques, Comp. Phys., 12 (1998), 620-631.

Numerical Simulations of Boundary-Layer Instabilities on a Generic Capsule Geometry with Rough Surface

Research Institution
Chair of Aerodynamics and Fluid Mechanics, Technical University of Munich

Principal Investigator
Christian Stemmer

Researchers
Antonio Di Giovanni

Project Partners
DLR Göttingen, TU Braunschweig, RWTH Aachen

Linux Cluster Project ID: t7841

Introduction

Laminar-turbulent transition on spherical forebodies is a topic in hypersonic transition which still lacks full understanding. Stability analyses of the flow for the smooth-wall configurations showed that the boundary layer is stable against modal, crossflow as well as Görtlex-vortex instabilities. Therefore, it is believed that the boundary-layer transition, which is observed both in wind-tunnel and free flights experiments, is mainly influenced by the presence of surface roughness. In hypersonic blunt bodies, such as re-entry capsules, surface roughness can originate due to ablation of the Thermal Protection System (TPS) or it is already present in the original configuration because of TPS joints and gaps between heat-shield tiles.

Compared to experiments and numerical methods based on linear stability theory, Direct Numerical Simulations (DNS) of the unsteady boundary layer in presence of roughness provide a deeper insight of the transition process and allow for a comprehensive characterization of the instability growth in the roughness wake both in the linear and non-linear range. The generation of secondary instabilities and the mechanisms that lead to laminar-turbulent breakdown can be investigated as well.

Our LRZ project is used to study the growth of unstable modes, in both linear and non-linear stage, developing in the boundary layer of a capsule-like hemispherical geometry with a rough wall. The growth of unsteady disturbances forced in the flow is analyzed and quantified. Freestream conditions have been chosen to match the wind-tunnel conditions at $M=5.9$ and $R_e=18x10^6\ m^{-1}$ in the Hypersonic Ludwieg Tube of the Technical University of Braunschweig (HLB).

Methods

The considered geometry is a segment of hemisphere with a radius of $R = 203\ mm$ which ends with a shoulder resembling the shoulder of an Apollo capsule. The shoulder acts as a natural sponge region at the outflow.

In order to ease the computational efforts, simulations of the three-dimensional boundary layer in the presence of roughness are conducted on a restricted domain. The restricted domain is found close to the shoulder in the region of the sonic line, where the boundary layer is subsonic to transonic, and does not include the shock ahead of the capsule geometry. A body-fitting grid consisting of about 40 million points is used.

The patch of distributed roughness is obtained by shaping the wall with a sinusoidal function (see Fig. 1). The roughness height is $k=100\ \mu m$ and it corresponds to 0.35 boundary-layer thicknesses. The roughness Reynolds number, defined with the values of the flow for the smooth configuration at roughness height, is $R_{ekk}=406$.

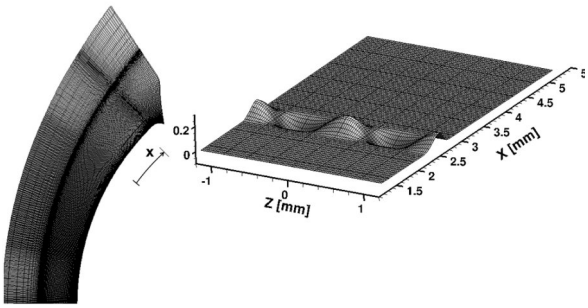

Figure 1: Computational grid of the full hemisphere geometry and close-up of the rough wall.

For the unsteady simulations, pressure disturbances are introduced at the inflow boundary. The perturbation frequency is 250 kHz. This value has been suggested by previous analyses based on two-dimensional Linear Stability Theory.

Parallel DNS are performed with the Navier-Stokes Multi Block (NSMB) solver. NSMB is an MPI-parallelized, Fortran-based code with a large variety of numerical schemes. To guarantee sufficient accuracy of the solution, a 4th-order central space discretization scheme and a 4th-order Runge-Kutta time integration

scheme are used.

Simulations of the steady base flow are typically performed on about 50 cores with a total computing time of about 1,000 CPU-hrs. Unsteady simulations are performed on up to 500 cores with a total computing time of about 50,000 CPU-hrs.

Results

At the roughness element, a couple of counter-rotating vortices generate and induce an helicoidal motion of the fluid downstream of the roughness (see Fig. 2). The presence of these vortices is associated with the presence of high-shear layers, which result to be very unstable for the unsteady disturbances forced at the inflow.

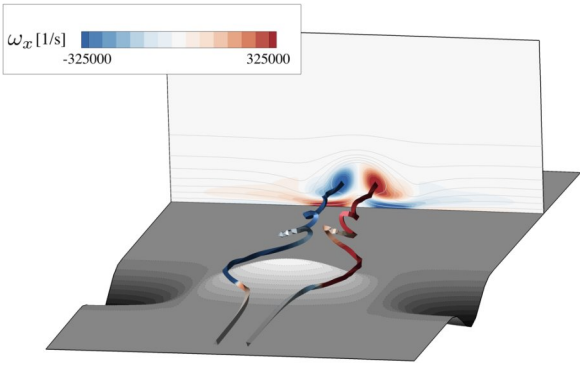

Figure 2: Slice downstream of the roughness and sample streamlines colored by streamwise vorticity.

The evolution of the unsteady disturbances forced are analyzed with a two-dimensional Fourier analysis. Two main unstable modes are investigated. These modes resemble the symmetric and antisymmetric modes already known from the investigation of isolated roughness elements on flat plate and are represented in Fig. 3 (two-dimensional) and Fig. 4 (three-dimensional).

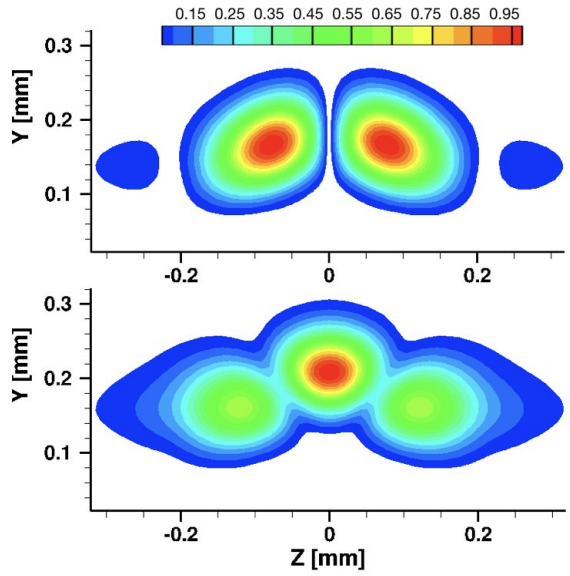

Figure 3: Shape and amplitude of the velocity modes for antisymmetric (top) and symmetric (bottom) mode.

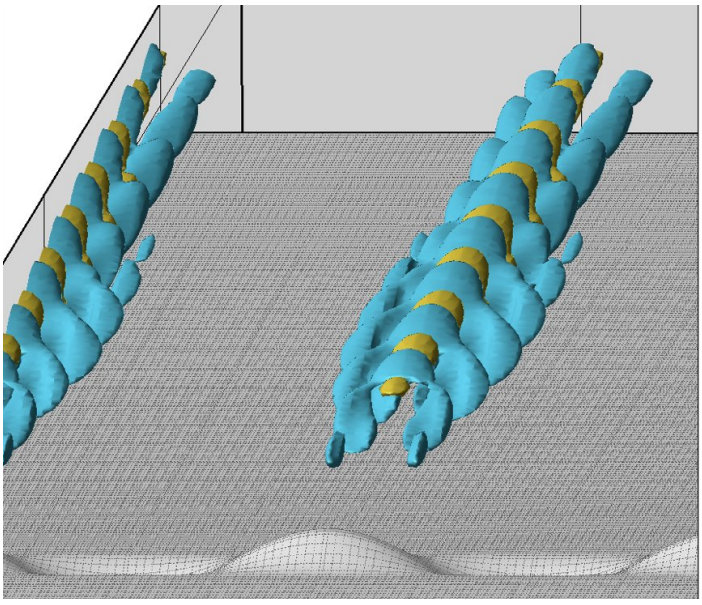

Figure 4: Three-dimensional representation of the symmetric mode obtained with isosurfaces of the instantaneous disturbance velocity.

Investigation of the unstable modes showed that, for the case analyzed here, both symmetric and antisymmetric modes undergo a strong amplification downstream of the roughness. In particular, the maximum amplitude observed for the symmetric mode is more than 10^4 times larger than its amplitude at the inflow (*N*-factor = 9.6), whereas for the antisymmetric mode a total amplification of about 10^3 (*N*-factor = 7.4) is observed.

Ongoing Research / Outlook

As shown by the present analysis, Direct Numerical Simulations are a useful tool to shed light on the instability mechanisms which lead to laminar-turbulent transition on blunt-body configurations in presence of roughness. As further step, the amplitude of the disturbances forced at the inflow will be increased and the growth of the unstable modes in the non-linear range will be investigated. Eventually, laminar-turbulent breakdown is expected to occur. In addition, the disturbance evolution in the wake of the roughness might strongly depend on the considered roughness geometry. Hence, further simulations for different roughness shapes and sizes are planned for future work.

References and Links

[1] www.aer.mw.tum.de
[2] Di Giovanni, A.; Stemmer, C.: Numerical Simulations of the High-Enthalpy Boundary Layer on a Generic Capsule Geometry with Roughness. New Results in Numerical and Experimental Fluid Mechanics XI (Notes on Numerical Fluid Mechanics and Multidisciplinary Design 136), 2017, Contributions to the 20th STAB/DGLR Symposium Braunschweig, Germany, 2016, pp. 189-199
[3] Hein, S.J.; Theiss, A.; Di Giovanni, A.; Stemmer, C.; Schilden, T.; Schroeder, W.; Paredes, P. Choudhari, M.; Li, F.; Reshotko, E.: Numerical Investigation of Roughness Effects on Transition on Spherical Capsules. AIAA Aerospace Sciences Meeting, AIAA SciTech Forum Kissimmee Florida, AIAA Paper 2018-0058.

Linearized CFD and Reduced-Order Models for Unsteady Aerodynamics

Research Institution
Chair of Aerodynamics and Fluid Mechanics, Technical University of Munich

Principal Investigator
Christian Breitsamter

Researchers
Vladyslav Rozov, Maximilian Winter

Linux Cluster Project ID: t784a

Introduction

The next generation of aircraft will be characterized by the application of flexible wing technology, which enables weight reduction without restricting the flight envelope. The increased flexibility of the wing structures also entails challenges. The fluid-structure interaction becomes more prominent. Thus, special attention must be paid to the resulting aeroelastic instabilities (instabilities involving aerodynamic, inertial, and structural forces).

The activities of the Chair for Aerodynamics and Fluid Mechanics are focused on the identification of unsteady aerodynamic forces by means of Computational Fluid Dynamics (CFD) as well as reduced-order models (ROMs).

The scope of the ongoing research within the DFG Project "Development of ROMs for Buffeting and Buzz" is the development and refinement of ROMs for highly nonlinear behavior of aerodynamic systems on the one hand [1, 2]. The refinement and application of linearized CFD methods for aeroelastic analysis is conducted within the EU-project "Flutter Free FLight Envelope eXpansion for ecOnomical Performance improvement" (FLEXOP) on the other hand [3, 4]. Linearized CFD methods are used to identify accurately the unsteady aerodynamic response aroused by modal deflections of an aircraft. This information can be subsequently employed to identify flutter critical flight regime.

Results and Methods

A novel sequential nonlinear identification process based on artificial neural networks has been developed. It is able to reproduce accurately essential linear and nonlinear characteristics of unsteady aerodynamics. Moreover, by examining the results in

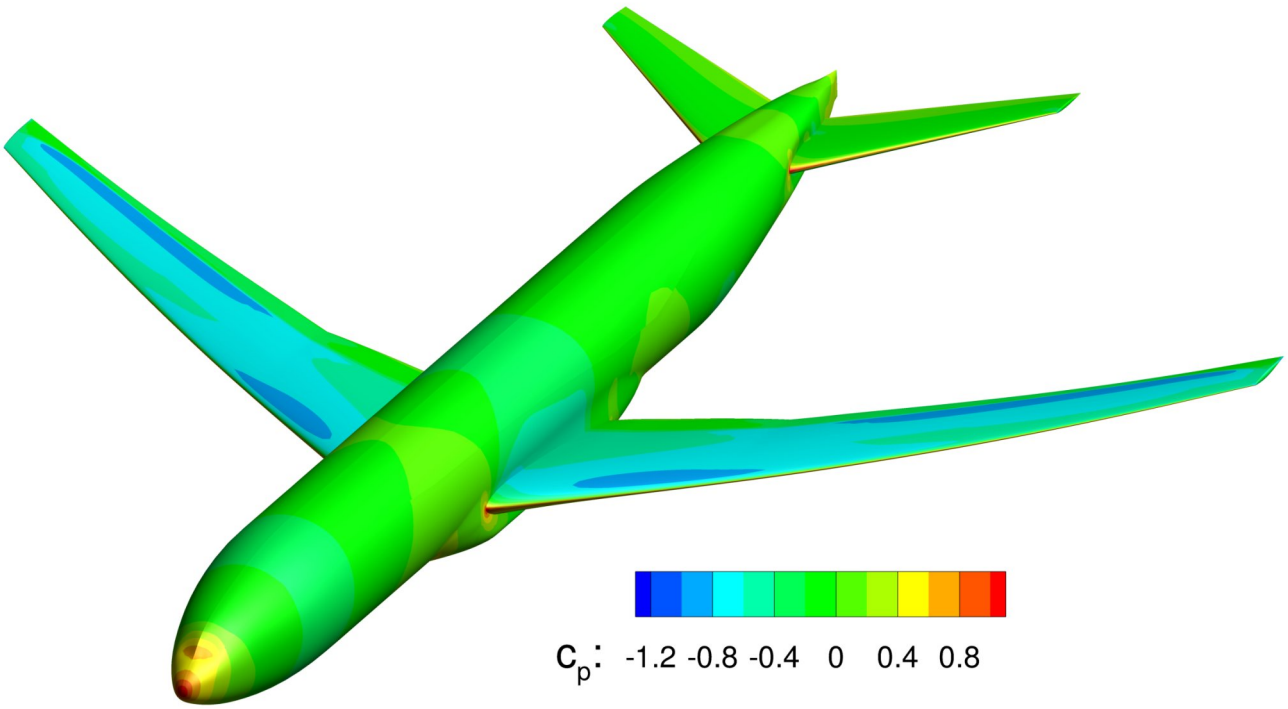

Figure 1: Pressure coefficient distribution over the NASA Common Research Model. The generic airliner model is used as a validation case for specific applications of computational aerodynamics.

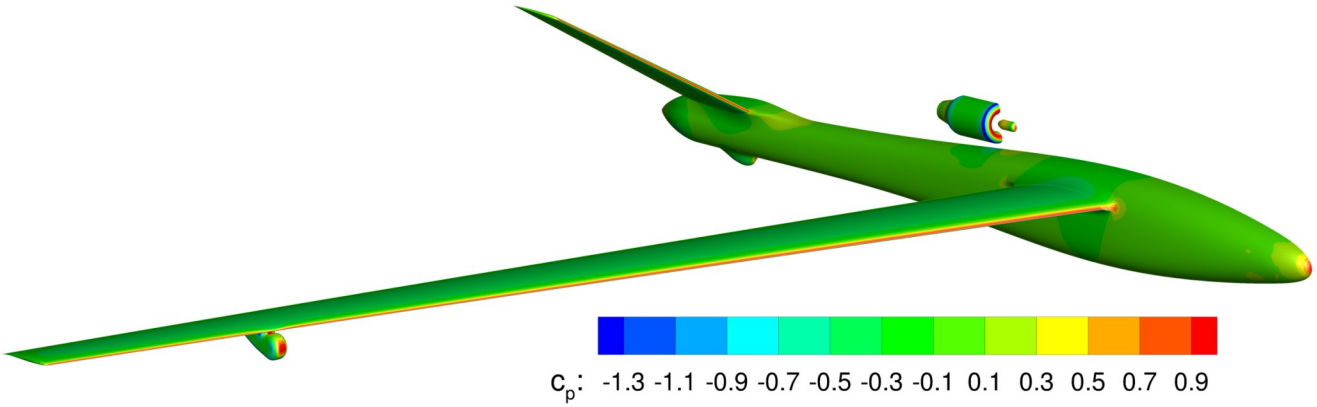

Figure 2: Pressure coefficient distribution over the half-model of the FLEXOP demonstrator UAV.

comparison to established ROM methods it is shown that the novel neural network technique leads to an enhanced prediction performance [2]. A great number of unsteady CFD simulations are necessary to generate data sets for training of the neural network as well as for the assessment of its prediction quality. The simulations have been conducted by means of the in-house CFD-solver AER-Eu/NS on CoolMUC-2. AER-Eu/NS is implemented in FORTRAN 90 and solves Euler or Navier-Stokes equations that are discretized with the Finite-Volume method. The code supports shared memory multiprocessing enabled by the OpenMP technology.

Another research activity, which benefited from CoolMUC-2 resources, is the development of a novel boundary condition for linearized CFD. It allows to exploit the properties of antisymmetry in the case of antisymmetric deflections of an aircraft. Thus, merely a half-model of an aircraft is necessary to compute the pertinent data for the prediction of the flutter boundary. This approach reduces the requirements of both memory and computational effort by a factor of two.

Linearized CFD is being applied to identify the flutter boundary of the demonstrator UAV within the project FLEXOP. Therefore, several configurations of the UAV are investigated to examine the impact of distinct components on the unsteady aerodynamics. Several simulations are needed to sufficiently resolve the aerodynamic behavior of the aircraft. One simulation for each structural mode and frequency of interest has to be conducted.

The linearized-CFD-solver AER-SDEu/NS is algorithmically based on the CFD-solver AER-Eu/NS. Due to the shared memory parallelization approach, a simulation can only be executed on a single node. However, a vast amount of simulations has to be performed to generate the essential data for an aeroelastic analysis. Therefore, the job farming strategy is pursued to optimally exploit the computational resources of a node, i.e. several simulations are conducted in parallel on the same node within a job.

The largest files that arise in the context of each distinct simulation are the restart file, several computational grids and time step data in the case of the time accurate CFD. Each simulation accesses several computational grids to compute relevant data. Files consisting computational grids that are common for several simulations, are distributed among the simulations as links. In this way, storage needed in SCRATCH is saved.

Roughly 150,000 Core-hours have been used in our projects.

On-going Research / Outlook

CoolMUC-2 provides essential computational resources to conduct research relevant to the computational aerodynamics. The research activities include parameter studies, generation of data sets for system identification and training of artificial neural networks.

All aforementioned topics are parts of the on-going research.

Since the computational models are typically very large, the number of simulations to be run simultaneously on a node is restricted solely by the available RAM per node.

References and Links:

[1] M. Winter, C. Breitsamter, Application of Unsteady Aerodynamic Reduced-Order-Modeling Techniques to a Complex Configuration, in: 17th International Forum on Aeroelasticity and Structural Dynamics, Como, Italy, 2017
[2] https://doi.org/10.1016/j.ast.2018.03.034
[3] https://www.flexop.eu/
[4] V. Rozov, A. Hermanutz, C. Breitsamter, M. Hornung, Aeroelastic Analysis of a Flutter Demonstrator with a Very Flexible High-Aspect-Ratio Swept Wing, in: 17th International Forum on Aeroelasticity and Structural Dynamics, Como, Italy, 2017

Computational Wind Engineering

RESEARCH INSTITUTION
Chair of Structural Analysis
PRINCIPAL INVESTIGATOR
KAI-UWE BLETZINGER
RESEARCHERS
PHILIPP BUCHER, ADITYA GHANTASALA, MICHAEL ANDRE, MÁTÉ PÉNTEK

Linux Cluster Project ID: t5112

Introduction

In recent years, computational wind engineering has emerged as a valuable tool for the assessment of wind effects on structures. The current trend of building larger and more flexible structures creates additional challenges for structural engineers. Recent developments in numerical methods combined with greater access to HPC resources permit state of the art simulations for the investigation of wind effects on structures while avoiding scaling issues and problems with model construction and instrumentation.

For some applications the mutual fluid-structure interaction (FSI) plays an important role and the coupled problem must be solved using FSI simulation. This results in a high computational effort when the interaction is strong, i.e. the effects of one domain on the other are very significant.

Using the computing resources of CoolMUC-2, researchers at the Chair of Structural Analysis have analyzed several wind sensitive structures by performing time-resolved FSI simulations of complete structural models in the atmospheric boundary layer to obtain additional insight into the structural response.

As the fluid and the structure simulations are performed on separate grids, an exchange of data (data mapping) is required on the interface. Methods for mapping in a distributed environment were developed in order to achieve an efficient and robust exchange of data.

Results and Methods

Research is conducted on the CoolMUC-2 using Kratos Multiphysics [1], which is developed in collaboration by partners at the International Center for Numerical Methods in Engineering, Barcelona, andTechnicalUniversity of Munich. Kratos Multiphysics is based on the finite element method and is used both for the fluid and the structural analysis as well as for distributedmapping.

Parabolic Trough Solar Collectors

Parabolic trough solar collector technology, a form of concentrated solarpower,is among the most proven large-scale solar power technologies currently in use around the world. The installed cost of such large-scale plants depends strongly on the design of the solar collector assemblies in the solar field. In order to minimize these costs while ensuring plant performance and reliability, it is important to accurately estimate wind effects on the solar modules. In this project,an

experimental validation of the numerical algorithms and subsequent aeroelastic study were performed in order to improve understanding of the aeroelastic stability of a collector module in natural wind.

Olympic Roof Simulation

This case simulates wind flow over the olympic roof in Munich and the interaction with it. A mesh with 15M elements for the fluid and 60k elements for the structure was used in this simulation. Due to the strong interaction between fluid and structure, several measures had to be used in order to ensure the numerical stability and thus the convergence of the simulation. One focus of this problem was to test the mapping in a very complex and challenging example for its stability and robustness. Additional scaling tests were also performed for the distributedmapper.

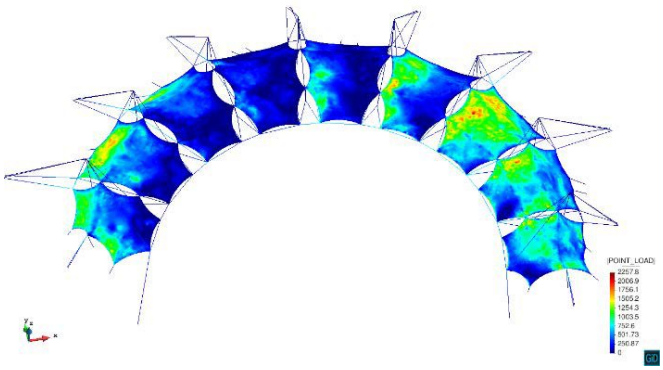

Figure 1: Fluid-structure interaction simulation of theolympic roof [2].

High-rise Buildings and Large-span Bridges

FSI simulations have been performed on a generic

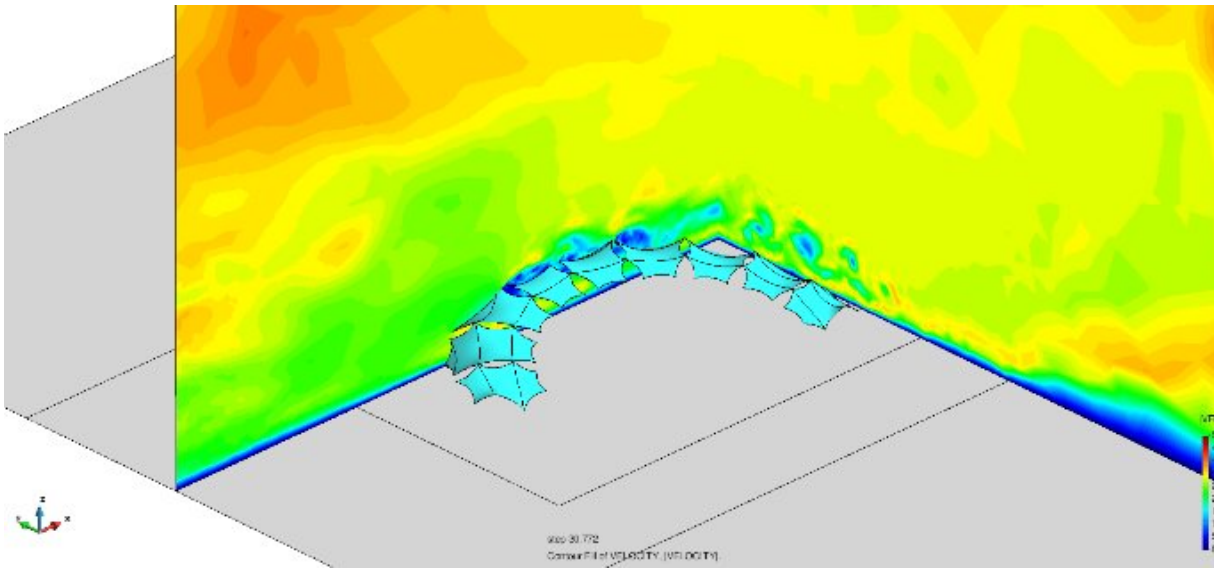

Figure 2: Wind simulation of the olympic roof [2].

high- rise building as well as two selected bridge decks to investigate possibilities of feedback between wind and structure. The fluid domain, which spans over 100m in each direction is discretized with approximately 14M degrees of freedom while the structure is discretized with 70k degrees of freedom. In a later stage the effect of an additional tuned-mass damper on high-rise buildings and bridges is investigated. Various wind-flow scenarios are considered.

CoolMUC-2 Resources

The resources used for these studies are summarized in table 1.

Example	Solar Collector	Scaling Mapping	High-rise & Long-span
Cores/job	56	Up to 1680	56
Jobs	280	30	125
CPU-hours	380k	6k	300k

Table 1: Simulation resources used on CoolMUC-2.

On-going Research / Outlook

The resources provided by CoolMUC-2 have enabled the use of state of the art, high-fidelity numerical methods. Such studies would not have been realized without access to the modern HPC systems administered by the LRZ.

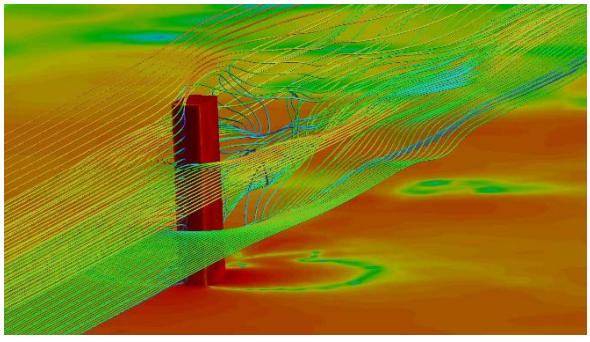

Figure 3: Flow field and streamlines around a generichigh-rise.

Current projects include the simulation of wind in an urban environment, which will require large grids with as many as 1k cores, large-scale wind turbine simulations and shape optimization in a distributedenvironment.

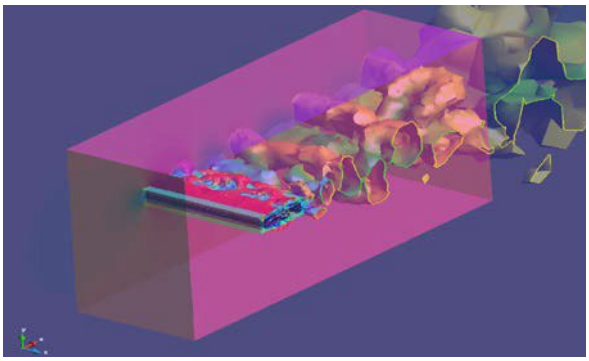

Figure 4: Vortex structures around a generic bridge deck.

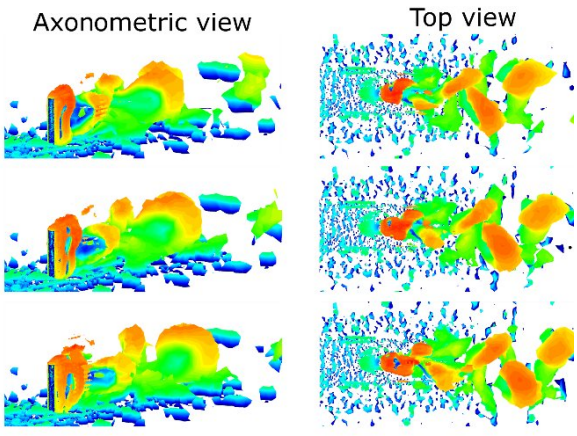

Figure 5: Evolution of vortex shedding around thebuilding.

References and Links

[1] https://github.com/KratosMultiphysics/Kratos.
[2] J. Cotela-Dalmau,P.Bucher, A. Ghantasala, M.Andre, A. Winterstein, R. Rossi and R. Wüchner, Implementation of mapping strategies on a distributed memory environment, Coupled Problems, Rhodes, 2017.

Development of high-performance interactive urban flooding simulator

2

Research Institution
Chair of Hydromechanics, Technical University of Munich

Principal Investigator
Michael Manhart

Researchers
Hao Zeng

Project Partners
Chair for Computation in Engineering

Linux Cluster Project ID: t5112

Introduction

This report aims to outline the high-performance interactive flooding simulator development project iFlood [1], and document the preliminary results of our simulations performed on LRZ CoolMUC-2 cluster with the corresponding usage statistics of the HPC system.

Flood events have increased both in terms of magnitude and frequency due to a combination of natural and man-made factors. As a consequence, a sustainable urban flood risk assessment tool could be of great value for city managers. The main purpose of this research project is to develop, implement, and validate a prototype for real-time and interactive urban flood simulators based on multi-scale 2D-3D fluid flow solvers, in order to evaluate possible impacts on building infrastructures. The 2D–3D coupling approach is essential to combine the capability of simulating geographic-scale flow phenomena in 2D domain far from cities, whereas capturing the complex 3D flow dynamics inside densely-populated areas with many buildings.

To accomplish the project objectives, 3 research groups closely collaborate and split the tasks as follows: Chair for Computation in Engineering is responsible for integrating Geographic Information System (GIS) and Building Information Modelling (BIM) data into an interactive computing environment that supports real-time exploration on modern visualization installations; Chair of Hydromechanics will focus on coupling 2D–3D flow models, the validation and integration in the environment provided by the Chair for Computation in Engineering, and the School of Engineering and Computing Science provides support for improving the use and efficiency of the developed software on modern high-performance computing architectures (see Figure 1).

In this report, we exclusively discuss about the development of the 2D–3D coupling solver performed at Chair of Hydromechanics.

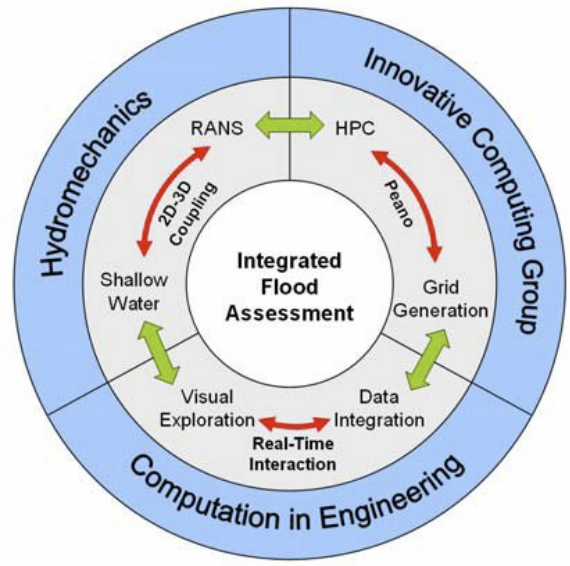

Figure 1: Schematic of project task distribution among 3 research groups.

Methods and Validations

Development of shallowInterFoam
The development of the 2D–3D coupling strategy is done under the framework of OpenFOAM: An open-source CFD software package which is written in C++ and parallelized by MPI. We combine our in-house 2D shallow -water solver shallowFoam and the

OpenFOAM's standard 3D solver interFoam, hence the new solver's name shallowInterFoam. The coupling strategy is realized by coupling the two solvers via interfaces between 2D and 3D computational domains, where shallowFoam and interFoam perform respective computations. The coupling solver framework translates physical quantities travelling from one kind of grid to the other, such as water-level elevation in the 2D domains to the volume-of-fluid indicator value in the 3D domains. A special care must be taken when flow in question exhibit sub-/supercritical transition, constituting as hydraulic jumps, which may travel across the 2D–3D interface in both directions. Depending on the direction

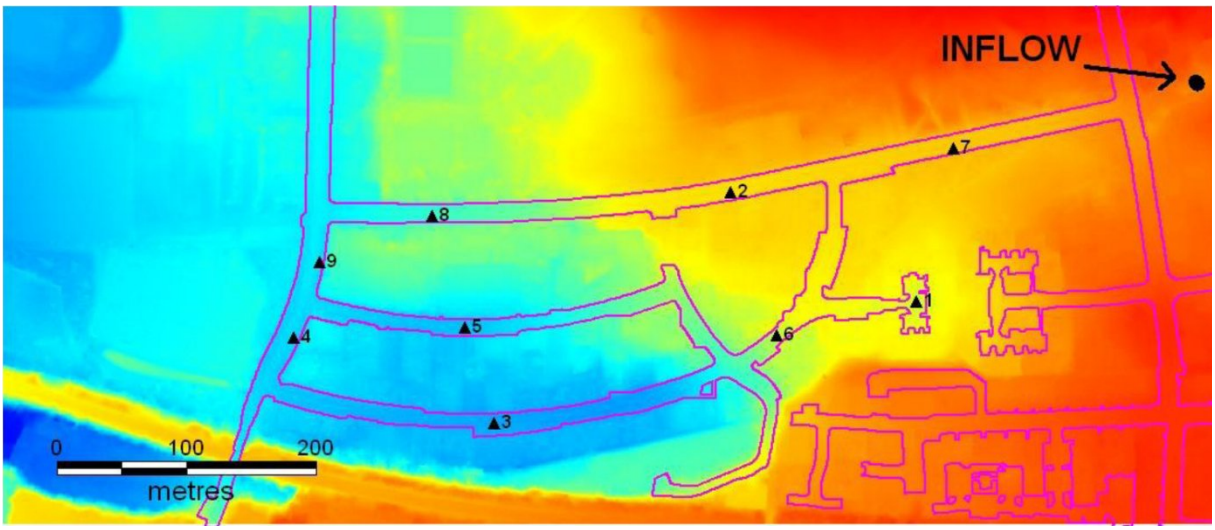

Figure 2: Visualization of benchmark flooding scenario simulated by shallowFoam. The color indicates instantaneous water-level distribution: red, high; blue, low.

of the transition (e.g. super-critical to sub-critical across an interface), different combinations of boundary conditions have to be prescribed. So far, we developed a version of the coupling solver which is capable of handling fixed combinations of boundary conditions, therefore apriori knowledge of flow situation is still necessary. We are currently working on an extension of the solver which detects the type of the transition and automatically selects the appropriate combinations of boundary conditions.

In the following, we validate the accuracy of our 2D shallow-water solver with a standard large-scale benchmark case as first step, which will be followed by the corresponding usage statistics of the CoolMUC-2 system.

Validation of shallowFoam
We employ the large-scale flooding benchmark case, which was originally published and utilized by Environment Agency to compare various popular 2D solvers in the market. In this scenario, a flood is assumed to arise from two sources: a uniformly distributed rainfall event with an intensity of 400mm/h applied to the entire domain, and a point source (see **INFLOW** on Figure 2) over a time period of 15 minutes, with a peak flow rate at 5m³/s starting 35 minutes after the rainfall event.

The red line on Figure 3 shows the time evolution of the point-wise water-level at Point 1 simulated by

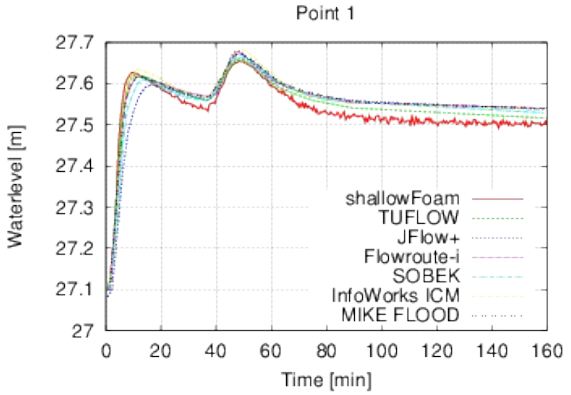

Figure 3: Time evolution of water-level observed at the location marked as Point 1 on Figure 2.

shallowFoam, being compared with the results from the other established 2D solvers. It is readily visible that the shallowFoam solver is capable of capturing the time-dependent 2D flow dynamics accurately.

Resource usage for performed simulations
So far, we performed 5 large-scale 2D simulations consisting of 1.9 million cells and computed by 448 parallel processes, which generated approximately 500GB of data. Due to the time-dependent nature of the flow problem, the intermediate results need to be written out at a relatively high frequency of approximately 10–30 seconds in walltime. The typical duration of the above simulations ranged between 9,000-18,000 seconds.

More recently, we often employ 2 Haswell nodes (56 cores) for much shorter walltime for the development of the coupling solver. Once the current development will be completed, we plan to run large-scale 2D–3D simulations which will be in the scale of O(108) cells.

On-going Research / Outlook

CoolMUC-2 system
We are truly grateful for the HPC resources and technical supports provided by LRZ. Without such support, it would have been impossible to run the simulations at the scale necessary to represent real-world flooding phenomena. However, our recent experience with long queuing time (order of days) on CoolMUC-2, even with the size of less than 100 cores, became a main challenge for our development and production work.

Outlook

We plan to improve our coupling solver further to incorporate more treatments on the 2D–3D interfaces to complete the requirements (cf. Section: Methods and Validations), then to carry out performance tuning together with our collaborators. In the meantime, we will post-process the results form the current production simulations and publish accordingly.

References and Links

[1] https://www.cie.bv.tum.de/en/research/projekte/efficient-algorithms/17-forschung/projekte/282-iflood
[2] Néelz and Pender, Benchmarking the latest generation of 2D hydraulic modelling packages, Environmental Agency (2009)

DNS of transient flow through close-packed porous media

Research Institution
Chair of Hydromechanics, Technical University of Munich

Principal Investigator
Michael Manhart

Researchers
Yoshiyuki Sakai

Linux Cluster Project ID: t5112

Introduction

This report aims to outline the transient porous media flow research project founded by DFG [1], and document the preliminary results of our simulations performed on the LRZ CoolMUC-2 cluster with the corresponding usage statistics of the HPC system.

Porous media flow can be found in many environmental and industrial systems, and is often transient, referring to the fact that is not statistically steady. Examples of such flow are: an atmospheric boundary layer interacting with forest canopies, a wave-induced ocean current through coral colonies, and a stream of air in human lungs. Better understanding of such flow phenomena, especially from the viewpoint of mass and energy transport, is therefore of fundamental importance.

In this project, we investigate the transient porous media flow by means of a series of direct numerical simulations of flow through a pack of uniform spheres, which are arranged in the close-packed hexagonal configuration.

Numerical methods and simulation set-up

MGLET
In the current contribution, we employ our in-house flow solver MGLET, which discretises flow variables in the incompressible Navier-Stokes equations by 2nd-order finite volume method in space, and a 3rd-order explicit low-storage Runge-Kutta scheme in time. A Cartesian grid with staggered arrangement of the variables is adopted, which enables an efficient and accurate formulation of the spatial approximations. Geometrically complex surfaces, arbitrarily curved, can be represented by an immersed boundary method [2]. The local grid refinement is implemented by adding refined grids in a hierarchical, overlapping manner which leads in total to a multi-block grid design.

The code is parallelised by a domain decomposition method using Message Passing Interface (MPI). Recently, the code has been optimized for massively-parallel computing architectures within two successive KONWIHR projects with their outcomes being published in [3,4]. At the time of writing, an excellent efficient parallel scaling performance has been confirmed up to ~33,000 MPI processes.

Simulation set-up
We performed 14 independent direct numerical simulations of the transient porous media flow with the flow Reynolds number (based on the sphere diameter and the steady-sate superficial velocity) ranging between 10–6 and 302, which covers the linear (Darcy), inertial and chaotic flow regimes.

To study the transient effect, the flow is accelerated from rest at a constant pressure gradient.

For the flow with Re < 58, a spatial resolution of approximately 160 grid cells per diameter was chosen, and utilising 1 Haswell node (i.e. 28 cores) on the CoolMUC-2 system to simulate. A typical simulation run lasts for 10 days of walltime, generating approximately 10GB/case of data to record the time-dependent flow phenomena.

For the higher Reynolds number flow cases, we employed approximately 320 grid cells per diameter to resolve the finer flow structures that appear in the flow cases, resulting 8 times more grid cells in comparison to the lower Reynolds number simulations. Simulating such high-resolution cases required 32 Haswell nodes (896 cores) for 2 days of walltime, generating approximately 30-40GB/case of data depending on the time required to reach to the statistically steady flow condition.

Results

We observed that the accelerating flow at Re > 1 exhibits a 4-vortex cross-flow pattern inside the pores as the bulk flow velocity reached its peak (see Figure 1(a) for an example), which is similar to the 8-vortex flow pattern that was previously reported for the steady-state flow through a square sphere pack.

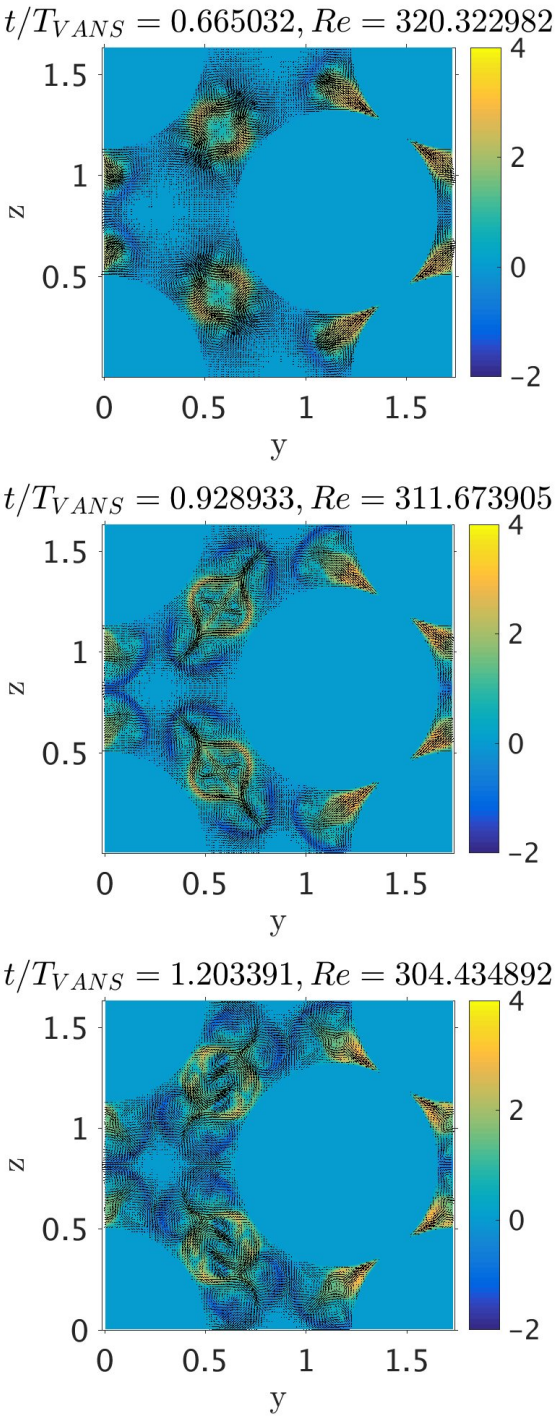

Figure 1: Instantaneous streamwise (colour) and cross-flow velocity (vectors) of flow through close-packed spheres at the steady-state Reynolds number 302, sampled from an arbitrary streamwise location. The bulk flow direction is into the page. Notice the (a) 4-, (b) 8-, (c) 5-vortex patterns in the pore regions respectively. Instantaneous time-stamp and Reynolds number are indicated on top.

Subsequently, the cross-flow structures of different Re cases underwent consistent topological evolution up to certain point, whereas the time-scale related to such flow structure formation was determined to be inviscid-scaling.

On-going Research / Outlook

CoolMUC-2 system

We are truly grateful for the HPC resources and technical supports provided by LRZ. Without such support, it would have been impossible to run the simulations at the resolution necessary to resolve all the relevant scales of the complex flow phenomena. However, our recent experience with long queuing time (order of days) on CoolMUC-2, even with the size of less than 100 cores, became a main challenge for our development and production work.

Outlook

We plan to simulate the flow through hexagonal sphere pack at even higher Reynolds numbers, namely up to 400. Furthermore, we will simulate the flow through randomly-arranged spheres over the same range of Reynolds number. For that purpose of performing large-scale simulations, we plan to apply for a project for the LRZ SuperMUC supercomputer.

References and Links

[1] http://gepris.dfg.de/gepris/projekt/276859331
[2] N. Peller et al. 2006. High-order stable interpolations for immersed boundary methods. Int. J. Numer. Methods Fluids, 52, 1175-1193.
[3] H. Strandenes et al. 2016. Improving scalability for the CFD software package MGLET. InSiDE – Innovatives Supercomputing in Deutschland (2), 2016, 48 – 50.
[4] Y. Sakai et al. 2017. Performance evaluation of a Parallel HDF5 Implementation to Improve the Scalability of the CFD Software Package MGLET. InSiDE – Innovatives Supercomputing in Deutschland (2), 2017, 82 – 85.

Numerical Investigations on Unsteady Flow Phenomena in Turbomachinery with Tandem Blades

Research Institution
Chair of Turbomachinery and Flight Propulsion

Principal Investigator
Volker Gümmer

Researchers
Michael Hopfinger, Mattia Straccia, Jannik Eckel

Linux Cluster Project ID: t7132

Introduction

The Chair of Turbomachinery and Flight Propulsion (LTF) [1] conducts experimental and numerical investigations that cover a wide range of turbo-machinery applications. The main research activities comprise the following topics:

- turbomachinery aerodynamics
- propulsor technologies
- design and make concepts and
- systems and components

Hereby, the flight propulsion technologies are combined with energy system purposes. Currently, the LTF counts 30 research associates (including the space propulsion department) of which more or less the half of them work numerically and, subsequently, require computational power provided by the various LRZ capabilities. Therefore, the linux cluster environment is used for a variety of different research projects, this report sets focus only on one particular research topic: the numerical investigations on unsteady flow phenomena in tandem blades configurations.

The reduction of engine weight and cost as well as the increase of engine life and performance are a main design and operating goal. Based on these requirements the power density has to increase. That means that the capability of modern compressors to do work on the fluid has to rise. One way to reach this aim is an increase of flow turning. The following stator has to work on flow conditions with a high circum-ferential velocity component and the flow tends, depending on the turning, to separate. One concept to sustain such high loading and turning are tandem arrangements, see Fig. 1. A tandem design means that two separate airfoil rows are positioned close together with a short axial distance. Therefore, the loading is split to both airfoils [2].

Because of a newly formed boundary layer on the second airfoil and the interference effect between both blades a tandem concept allows higher pressure gradients to be resisted without incurring higher losses compared to an identically loaded single airfoil [3]. A practical application are high-lift profils on commercial airplanes that supply additional lift force during the take-off and landing phases.

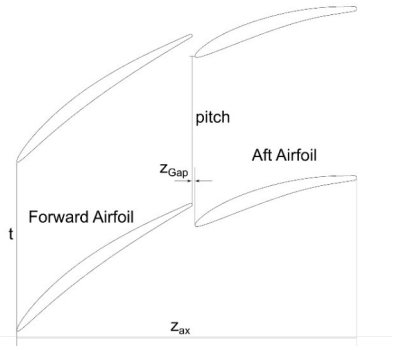

Figure 2: Hybrid Tandem Blade.

The project was proposed to both the FVV (Forschungsvereinigung für Verbrennungs-kraftmaschinen e.V.) and the DFG (Deutsche Forschungsgemeinschaft) that assumingly support the investigations financially. Besides the numerical research, a low-speed compressor test rig will be established at the LTF to investigate the flow behavior experimentally. In a first step, an industrial partner that is part of the accompanying FVV group provided an initial geometry which already has been investigated thoroughly. Next, the reference geometry needs to be scaled and adjusted to the new LTF test facility geometry. Until this point, most effort has been made to re-calculate the reference geometry with a different, commercial solver, compare results and draw conclusions on the flow behavior of the reference geometry. Currently, the geometry scaling and adapting process is under process. Once the final geometry of the stage is derived, the unsteady, time and computational cost consuming calculations are conducted.

Results and Methods

The LTF and, in particular, this project uses the CoolMUC-2 data mainly to run computational fluid dynamics (cfd) calculations with the commercial flow solver ANSYS CFX or FLUENT. The blading, meshing, pre-processing is done on local machines at the institute. Since the local machines work mainly on Windows the complete set-up is then uploaded via a cross-platform FTP application to the linux cluster. The

calculation is then submitted by a batch file that defines the calculation process.

A standard calculation uses Intel MPI on 56 cores for 3–4 h. It must be addressed that these values outline a steady-state, 1.5-stage (inlet guide vane, rotor, tandem domain) calculation with approximately 8e6 cells. Once the model increases in complexity or the calculations respect the time dependency, computational cost will rise significantly.

The cluster assigns the job to a certain job-ID so the current processing status of the queuing system can be checked. The submitter gets informed automatically once the job starts to run and finishes due to reaching the set computational time or due an occurrence of an error. The pending time depends on the capacity of the cluster and the requested calculation time. The respective pending times have not been tracked but in overall they are deemed acceptable by the LTF research assistants. In case of error the automatic generated BASH output helps tracing back the error source.

The CoolMUC-2 provides the necessary computational environment for the majority of the LTF numerical work. Therefore, the CoolMUC-2 delivered approximately 800,000 core-hours for the project t7132. At this point, the project storage of the home directory is 30 GB, work directory 800 GB. Unfortunately, the scratch storage where most of the results is stored could not have been read.

The institute uses the SuperMUC mostly for particular calculations, e.g. combustion processes in space propulsion applications that require great amounts of computational power and are well suited for high parallelization. The new CoolMUC-3 will get integrated more and more in future numerical work by the institute.

On-going Research / Outlook

Based on the unsteady flow phenomena two follow-up research projects will be set up in the future. Since both projects are currently in the conceptual phase, precise predictions regarding the computational request can not be made at this point. This report is outlining the basic ideas

Hybrid Tandem Blade
Design and numerical investigations of hybrid compressor blades based on an existing tandem-stator and single-rotor of a modern compressor stage. The hybrid blade is using a tandem profiling in the middle section of blade passage and single profiling near hub and shroud. Due to the removal of the second stagnation point at the leading edge of the rear tandem vane near the end walls, the hybrid blade will be able to reduce secondary flow effects compared to a classical tandem design. Because of this the hub corner separation, which is one of the major limiting factors of modern compressor tandem blades, will be lowered. However new vortex structures will be created by the transition area between the single and tandem profiling that have to investigated. Future CFD

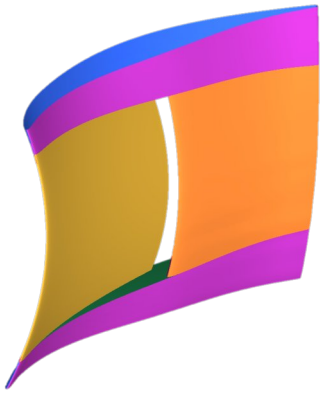

Figure 2: Hybrid Tandem Blade.

investigations will lead to a better understanding of the flow physics inside the whole blade passage to find an optimum geometrical solution of the hybrid blade. The goals of the work are to find completely new design rules, which will be used to even further increase the working range of the existing compressor stage and efficiently raise the pressure ratio at the same time.

Control Flow Systems: Contouring and Recirculation
For the LTF project related to development of hub/case contouring with addition of a recirculating system, the usage of the LRZ CoolMUC-2 cluster is indispensable, due to the heavy computational load required. The project focus on the implementation of an optimization loop process of a single compressor stage in tandem configuration, modifying the contour of the hub and case of the stage during an unsteady simulation in order to achieve an optimum configuration. Until today, the usage of the CoolMUC-2 has been relegated to mapping the compressor stage, as starting point of the research. The next step is to implement the optimization process in order to make it work on the cluster. This optimization process will utilize several commercial software used in batch mode by executables, which will run sequentially until an optimum contour configuration of the hub is achieved/created. In particular, compilers for Fortran 90 and Python codes are required to run and create those batch files.

Estimated starting point of the test campaign is November 2018–January 2019. A first rough estimation of the computational time required for this process is about 48–96 hours. The most part of the computational time is occupied by CFD Unsteady (URANS) simulations in CFX, about 50% of the entire estimated time. The post processing part covers another 30~35% of the computational time. The rest is dedicated to the logical process of simulation updating, geometry creation, results evaluation to define the evolution path of the entire process.

References and Links

[1] http://www.lfa.mw.tum.de/index.php?id=5
[2] Tesch, A., Ortmanns, J., Gümmer, V., 2014, “An Experimental Investigation of a Tandem Stator Flow Characteristic in a Low Speed Axial Research Compressor”, Proceedings of ASME Turbo Expo 2014: Turbine Technical Conference and Exposition, Düsseldorf.
[3] Smith, A. M. O., 1975, “High-Lift Aerodynamics”, AIAA, Journal of Aircraft, Vol. 12 (1975), No. 6.

Numerical investigation of cavitating two-phase flows and cavitation-induced erosion

Research Institution
TUM - Chair of Aerodynamics and Fluid Mechanics

Principal Investigator
Steffen J. Schmidt, Nikolaus A. Adams

Researchers
Theresa Trummler, Daria Ogloblina, Polina Gorkh, Christian Lang, Bruno Beban

Linux Cluster Project ID: t7171

Introduction

The formation of vapor bubbles in a liquid due to pressure reduction is called “cavitation” [1]. Flows involving cavitation feature a series of unique physical properties [2] such as discontinuous jumps in the speed of sound from *O(1000) m/s* to *O(1) m/s*, a jump in density of up to 4 orders in magnitude, and intense compressibility effects, such as the formation of intense shock-waves with post-shock pressures of more than 1GPa. Flows involving cavitation occur in a wide range of technical systems. In particular, injection systems for combustion engines, high pressure hydraulics, naval propellers and biomedical applications are prone to cavitation and cavitation-induced material erosion.

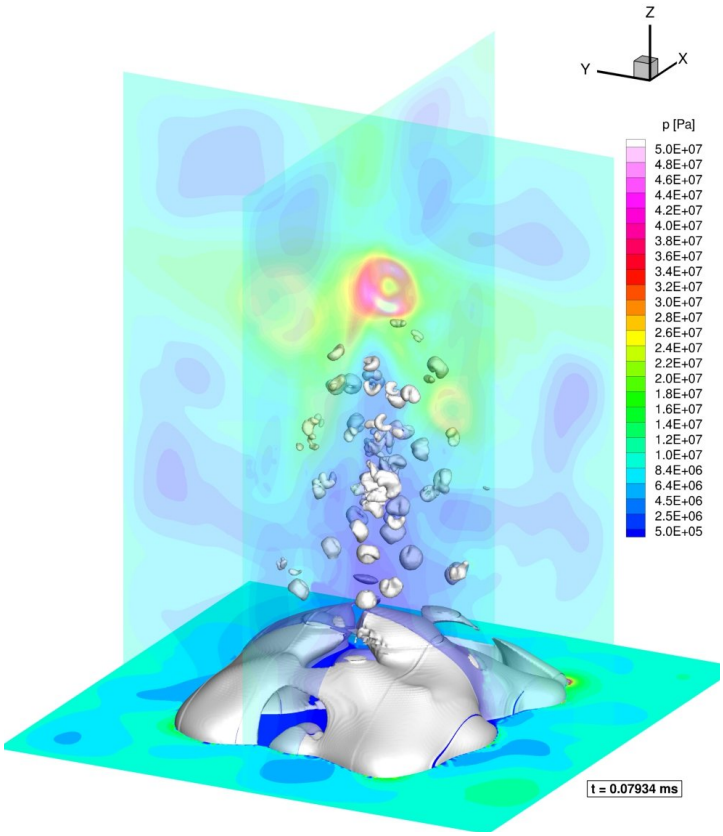

Figure 1: Collapse and rebound of a cluster of 125 vapor bubbles in a liquid ambient. Shock focusing, bubble indentation and vapor rebound are observed. High surface loads of > 10,000 bar may lead to material damage - called cavitation erosion.

Our objective is to develop efficient and accurate simulation approaches for predicting all dominating phenomena in cavitating flows including shock-wave formation and propagation, with the goal to provide the groundwork for the design optimization of future technical devices [2].

Results and Methods

A series of numerical approaches, including state-of-the art Large-Eddy Simulation (LES) schemes [3] enable high performance computing with linear scaling on HPC systems, such as CoolMUC-2 and SuperMUC. Our approaches are “monolithic” in a sense that all involved fluid components (liquid, vapor, inert gases) are handled in a consistent way. Shock wave formation due to collapsing vapor patterns is resolved by application of time-steps smaller than one nanosecond. The resulting loads on material surfaces – and thus the potential of material erosion -are obtained without the need for additional models. Fundamental research is funded by the European Union (Project “CaFE”), while applied research is performed in collaboration with several automotive suppliers, the U.S. Office of Naval Research and with the European Space Agency.

Selected Test-Cases

Our research field involves all types of cavitating flows, ranging from fundamental test-cases to industrial applications. In the following, three selected simulations are briefly described.

Simulation 1: A cluster of 125 liquid-embedded vapor bubbles collapses under high ambient pressure (Figure 1). The cluster is located in the vicinity of a solid surface resembling a teal part of a hydraulic device. Shock focusing towards the center of the cluster leads to indentation of individual bubbles, followed by an intense shock wave with post-shock pressure of > 10,000 bar. Subsequent re-evaporation due to wave interaction and liquid inertia forms a second vapor pattern at the surface (depicted in Figure 1). The secondary collapse of the rebound vapor structure results in extremely high surface loads and thus to material damage.

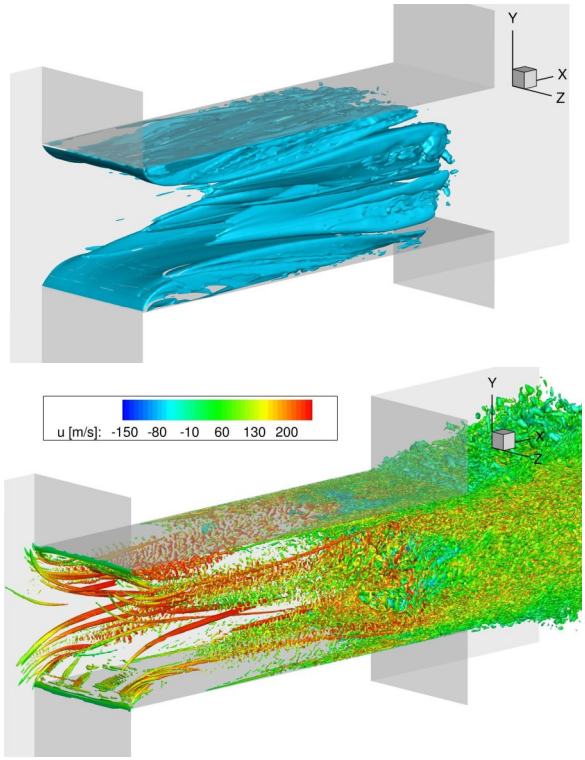

Figure 2: Iso-surfaces of a vapor volume fraction of 10% (top) and vortical structures colored by axial velocity (bottom) of the cavitating flow in a generic injector throttle. Stable sheet cavities, cavitating corner vortices and transition to turbulent flow can be predicted in agreement with experimental findings.

Simulation 2: The cavitating flow through a generic throttle is investigated. Liquid water with a stagnation pressure of 300 bar enters the numerical domain from left and starts to evaporate at the inlet of the throttle when the pressure decreases to vapor-pressure level. At the exit of the domain, a static pressure of 125 bar is prescribed. The preformed LES required about 300h*280CPU=84,000 CPUh on CoolMUC-2. A flow visualization is shown in Figure 2.

Simulation 3: An experimental test-rig of a cavitating jet is simulated numerically. The upstream pressure is ~200 bar and the pressure in the material test-section is ~5bar. A target plate, located about 10 mm downstream of the exit of the nozzle, forces the vapor pockets within the liquid jet to collapse (Figure 3 - top). The resulting shock waves impinge on the target and produce strong loads with durations of ~100 nanoseconds. The “foot-prints” of high pressure impacts at the surface of the target are collected by several algorithms (Figure 3 - bottom). Pressure level, duration and diameter of the impacts are used to estimate the energy transferred into the target material. The comparison of numerically predicted footprints to experimental pits (material damage) leads to in-depth understanding of flow mechanisms the cause cavitation erosion. Excellent agreement with experimental findings was achieved.

On-going Research / Outlook

We will continue our numerical simulations of cavitating flows and cavitation erosion using HPC

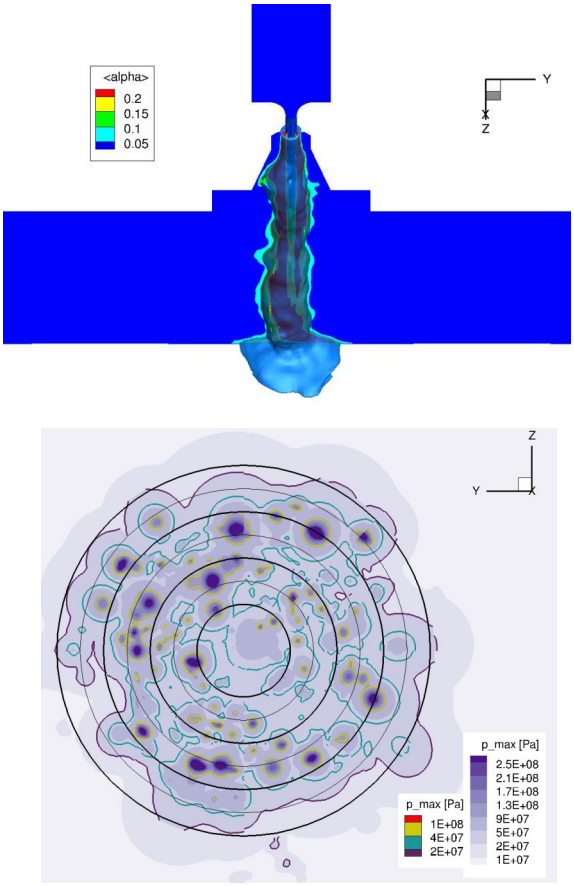

Figure 3: Perspective view of cavitating jet visualized by iso-surfaces of the vapor volume alpha (top) and shock impacts (=pressure foot-prints) of collapsing vapor structures at the target surface (bottom).

systems such as CoolMUC-2 and SuperMUC. Upcoming projects involve life-science processes such as high pressure homogenization of food products, where cavitation is utilized to maximize the homogenization procedure. Additional to the need of state-of-the-art HPC systems, HP visualization tools are required to handle the enormous amount of collected data. Especially, fast 3-D rendering soft- and hardware would be helpful to analyze complicated flow fields.

References and Links

[1] https://www.aer.mw.tum.de/abteilungen/gasdynamik/
[2] Budich, B.; Schmidt, S.J.; Adams, N.A.: Numerical Simulation and Analysis of Condensation Shocks in Cavitating Flow. To appear in Journal of Fluid Mechanics (accepted 2017)
[3] Egerer, C.P.; Schmidt, S.J.; Hickel, S.; Adams, N.A.: Efficient implicit LES method for the simulation of turbulent cavitating flows. Journal of Computational Physics, Volume 316, 2016, Pages 453-469.
[4] Örley, F.; Hickel, S.; Schmidt, S.J.; Adams, N.A.: Large-Eddy Simulation of turbulent, cavitating fuel flow inside a 9-hole Diesel injector including needle movement. International Journal of Engine Research, 2016, Pages 1-17.

Analysis of Deflagration to Detonation Transition of Hydrogen-Carbon Monoxide-Air Mixtures in various applications

Research Institution
Lehrstuhl für Thermodynamik, Technische Universität München

Principal Investigator
Thomas Sattelmayer

Researchers
Christoph Barfuß, Christoph Wieland

Project Partners
GRS, BASF

Linux Cluster Project ID: t7811

Introduction

The increased environmental awareness of the society lead to high investment in renewable energies. But due to the intermittent nature of most renewable energy sources, conventional power generation applications will remain its important role in the future as a reliable energy supply. In a global scope, nuclear power plants (NPPs) remain a major contributor to the energy supplying network. When operating NPPs, the possibility of severe accidents cannot be neglected as Fukushima has shown.

In a severe accident scenario, such as a 'loss of coolant accident' (LOCA), hydrogen is formed by the oxidation of the fuel rod cladding. In addition to the hydrogen formation, carbon monoxide will be produced by the molten core concrete interaction (MCCI), if a core meltdown occurs.

As the final events in the Fukushima accident have proved, ignition of the combustible mixture hydrogen-carbon monoxide-air, or syngas-air, cannot be fully omitted. The resulting flame can accelerate from a slow to a fast flame due to self excitation and even transition to a detonation.

Detonations are connected to strong dynamic pressure loads on structures. In order to prevent detonations, the phenomena flame acceleration (FA) and deflagration-to-detonation-transition (DDT) are investigated at the chair of thermodynamics at the Technical University of Munich with the means of computational fluid dynamics (CFD) [1]. The application of syngas in various industries such as the technical chemistry, e.g. BASF, further motivates the investigation of syngas DDT.

The phenomenon of flame acceleration (FA) is driven by heat and mass transfer across the flame front and the detonation maintains stable due to self ignition and gas dynamic effects. The self ignition is a result of the preconditioning of the fresh gas by shock waves. Thus, a weak and a strong detonation exist. The first is described as flame acceleration by self induced turbulence enhancement followed by a DDT and the second is a result of shock focusing on obstacles or walls.

Results and Methods

A CFD solver has been developed at the chair of thermodynamics in the open source C++ library OpenFOAM (Version 2.1.0). Since the solver application is focused on technical facilities such as reactor buildings, an under resolved simulation approach is pursued. Subsequently, the computational grid's base cell size is comparably large varying from 8 mm to 40 cm. On these scales, most physical phenomena have to be modelled on a sub-grid level. The correct prediction of the global flame propagation as well as the pressure loads are the major aspects of interest in the under resolved CFD approach.

The solver has an explicit density based architecture solving for the unsteady compressible Navier-Stokes equation. Turbulence modeling is achieved by the k-ω SST turbulence model. In order to preserve computational resources an adjustable time step size with an Courant number of 0.3 is used as well as adaptive mesh

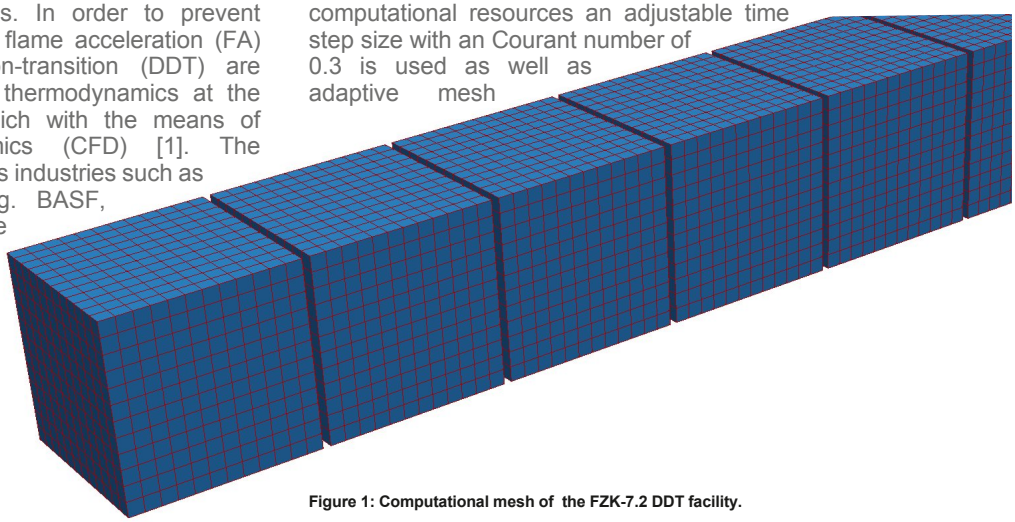

Figure 1: Computational mesh of the FZK-7.2 DDT facility.

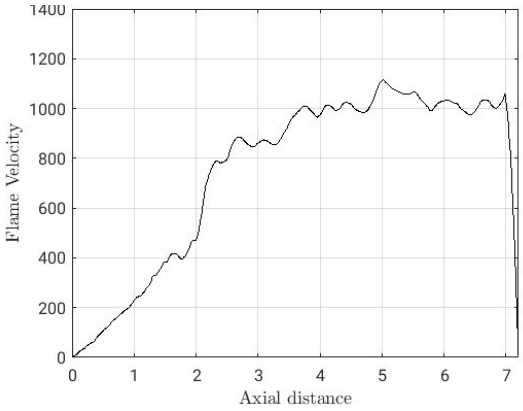

Figure 2: Simulated velocity profile of the flame of a 75/25 H_2/CO fuel mixture at stoichiometric conditions.

refinement (AMR) is applied.

Due to their importance, shock waves have to be captured and preserved as discontinuities. This is done by the density based architecture in combination with an approximated Riemann solver, namely the Harten-Lax-van Leer contact scheme (HLLC). The flame propagation is modeled with a geometrical 'Volume of Fluid' (VoF) method. The transport equation of the VoF method is closed with a deflagration source term similar to the turbulent flame speed closure and a detonation source term. Hence, a prediction of the onset of DDT can be achieved for the weak as well as the strong detonation.

The solver allows simulations on small geometrical scales as well as on large scales. Because of the tube-like geometries like the small scale FZK DDT facility and the smooth pipe of BASF in combination with AMR and the VoF-method, the effectiveness of massive parallelisation is decreased.

The FZK facility is 7.2 m long and has a side length of 0.095 m in the quadratic cross section. In order to accelerate the flame, turbulence inducing obstacles are installed. They block 30 % of the passage way and are placed repeatedly every 100 mm. The computational mesh is shown in Figure 1.

An onset of DDT can be simulated in the FZK 7.2 geometry for stoichiometric mixtures with 75% hydrogen fuel content, as the velocity profile in Figure 2 indicates. DDT occurs shortly after 2 metre of steady flame acceleration.

The simulation is carried out on 56 cores of the CoolMUC-2 in an execution time of about 2 days. In this case, the high frequency of CoolMUC-2's processors saves computational time compared to a higher degree of parallelisation.

While the onset of DDT can be predicted well when distinct obstacles are present, which create large turbulent wake flows behind them, the DDT prediction in smooth pipes is more difficult. Without distinct obstacles the wall boundary layer is the major source of turbulence. The under resolved approach has to

Figure 3: Fast flame in a smooth pipe filled with a stoichiometric homogeneous H_2-air mixture.

rely only on wall functions of the turbulence model as turbulence source in the smooth pipe case.

Simulations in a smooth pipe case with a length of 9.39 m and a diameter of 0.043 m. The cases are computed on the CoolMUC-2 with 28 cores. Figure 3 shows the contour of the flame during flame acceleration. Typically for fast flames in pipes, the flame close to the wall is behind the flame tip in the core region.

When a critical flame velocity is surpassed, the flame close to the wall will catch up and the entire turbulent flame brush will couple with the incident shock resulting in a DDT. Figure 4 shows a typical detonation front.

Figure 4: Detonation front in a smooth pipe filled with a stoichiometric homogeneous H_2-air mixture.

OpenFoam typically generates a huge number of files and directories in the working folder, which hindered us from running many cases on the scratch folder. But the CoolMUC-2 helped us to obtain these CFD results due to availability of more than 16 cores per node.

On-going Research / Outlook

In the ongoing work a porosity distributed resistance model is going to be implemented in the solver in order to account for hardware installations, which are cannot be depicted in the coarse mesh. Furthermore, a load balancing approach for the VoF-method shall be introduced. This would allow for a better effectiveness of the massive parallelisation and, hence, make better use of the CoolMUC-2 multicore capabilities.

Acknowledgement

The presented work is funded by the German Federal Ministry of Economic Affairs and Energy (BMWi) on the basis of a decision by the German Bundestag (project no 1501545A) which is gratefully acknowledged.

References

[1] http://www.td.mw.tum.de/forschung/forschungsbereiche/projektbeschreibungen/development-of-combustion-models-and-detonation-criteria-for-stratified-hydrogen-carbon-monoxide-air-mixtures-with-partial-containment

[2] Hasslberger J. (2017). Numerical Simulation of Deflagration-to-Detonation Transition on Industry Scale. Technische Universität München, Garching, Germany.

Large Eddy Simulation of Confined Boundary Layer Flashback

Research Institution
Lehrstuhl für Thermodynamik, Technische Universität München

Principal Investigator
Thomas Sattelmayer

Researchers
Aaron Endres

Linux Cluster Project ID: t7811

Introduction

One possible method to decrease CO_2 and NO_x emissions in gas turbines is the combustion of premixed hydrogen rich fuels. One problem of premixed combustion in gas turbines is the existence of flammable gas mixtures upstream of the stable flame position, possibly leading to upstream flame propagation. Hydrogen flames exhibit high burning velocities and a high reactivity in proximity to walls. Upstream flame propagation in the wall boundary layer of the approaching flow is thus particularly likely to occur in hydrogen combustion. This phenomenon is also called boundary layer flashback. [1]

It is essential to predict and prevent the occurrence of boundary layer flashback as it may lead to engine shutdown and structural damage of the gas turbine. One possible method to predict flashback limits is by conducting numerical simulations. So far, the flashback limits of turbulent hydrogen-air flames could however not be reproduced by numerical simulations. One promising method to predict the onset of the highly transient boundary layer flashback process is to perform large eddy simulations (LES). This approach and the corresponding results will be briefly presented in the following.

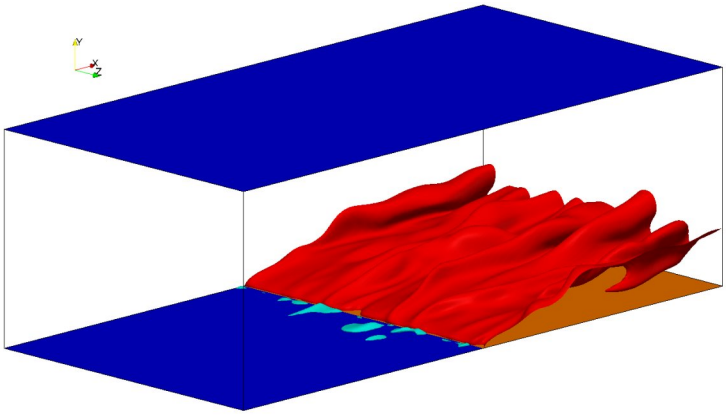

Figure 1: Stable flame front (red isosurface) and flow separation zones (turquoise isosurface) at 10 m/s and Φ=0.33.

Results and Methods

Numerical Setup
LES of the confined case of turbulent turbulent boundary layer flashback of hydrogen-air flames were conducted with the open source library OpenFOAM in order to numerically obtain boundary layer flashback limits. These numerical flashback limits are compared to experimental results of Eichler [2]. In these experiments, the flame is stabilized inside a rectangular channel by a hot ceramic tile. When increasing the equivalence ratio, that is the fuel content of the fresh gases, the flame speed increases and the flame starts to propagate on the cold steel walls of the mixing channel. These thermal boundary conditions are modelled in the simulations as an adiabatic and an isothermal wall, respectively. The configuration can be seen in Figure 1. Herein, the stable flame is depicted by the red 1,000 K isosurface. The isothermal walls are colored in blue, while the adiabatic wall is orange. At the inlet at the left of the domain, a time dependent fully developed velocity profile sampled from inert LES is prescribed.

The inert LES were performed with the Smagorinsky turbulence model and the standard OpenFOAM Smagorinsky constants. The inert computational domain consists of a rectangular channel with the channel half height δ, a channel length of 6δ and a channel width of 3δ. All boundary conditions besides the walls are cyclic boundary conditions. The channel bulk velocity is controlled by automatically setting an according pressure gradient in the domain. The inert mesh for a bulk velocity of 10 m/s consisted of 0.7 million cells, while the inert mesh for a bulk velocity of 20 m/s consisted of 3.9 million cells.

In order to model the physical combustion phenomena, the Navier-Stokes equations are solved together with the transport equations for each species mass fraction involved in the chemical processes. The chemical source term is modelled with a finite rate model of Arrhenius type without accounting for turbulence-chemistry interaction in the subgrid scales. The chosen detailed chemical reaction mechanism for hydrogen combustion contains 9 species and 23 reactions. Differential diffusion effects and thus thermodiffusive instabilities are accounted for by

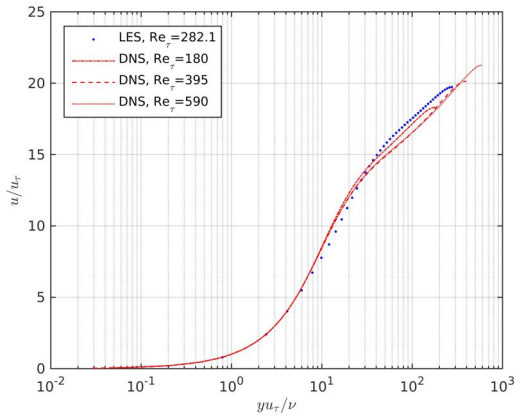

Figure 2: Average velocity profile for 10m/s from LES [4] compared to DNS results [3].

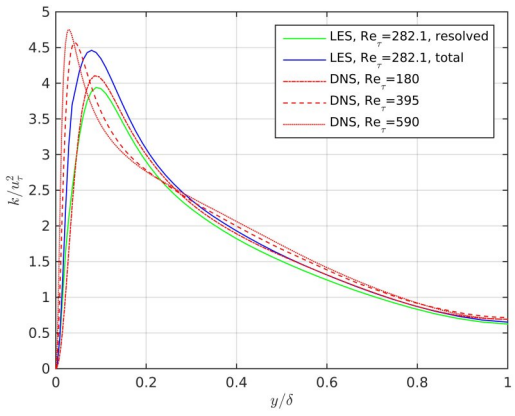

Figure 3: Average turbulent kinetic energy profile for 10m/s from LES [4] compared to DNS results [3].

modelling the species diffusion coefficients including Soret diffusion according to the kinetic gas theory.

Bulk velocities of 10 m/s and 20 m/s at equivalence ratios between 0.33 and 0.55 are investigated. The mesh of the inert calculation was refined for the combustion calculations. In the 10 m/s case the mesh consisted of approximately 4 million cells, while the mesh of the 20 m/s case consisted of approximately 20 million cells. The calculations were performed on 4 to 10 CoolMUC-2 nodes, resulting in 112 up to 280 parallel processors and a total calculation time of approximately 1 million CPU hours, including all failed runs and test runs. The overall storage needed for all relevant cases is approximately 220 GB.

Results

In Figure 2, the inert average velocity profile for a bulk velocity of 10m/s is compared to DNS data of Moser et al. [3]. It can be seen that the profile of the mean velocity u fits the DNS data very well [4]. The same holds for the profile of the turbulent kinetic energy *k*, which can be seen in Figure 3. All inert data is non-normalized by the molecular viscosity v, the channel half height δ and the shear-stress velocity u_τ, which is calculated from the velocity gradient of the first cell adjacent to the wall.

With this inert velocity profile, the flashback limits were obtained and compared to experimental flashback limits. The flashback limit is defined by the last stable equivalence ratio, where no flame propagation takes place and the first unstable equivalence ratio, where the flame starts to propagate on the isothermal wall. For 10m/s, the flame was stable up to Φ=0.33 and started propagation at Φ=0.38. In experiments, flashback was observed at approximately Φ=0.34 [2]. It can be seen that for this specific bulk velocity, the flashback limit is reproduced very well. For higher equivalence ratios and bulk velocities, the flashback tendency was slightly overpredicted. However, the overall trend of the experimental data is captured by the reactive LES [4].

The stable flame fronts and the flow separation regions for the 10 m/s case can be seen in Figure 1 and Figure 4, respectively. It is clear, that also before the onset of flashback at an equivalence ration of 0.33 flow separation locally occurs, as assumed by Eichler [2]. However, due to flame quenching at the isothermal walls, the separation zones appears not to be large enough for the flame to propagate inside the separation zones. The sole occurrence of boundary layer separation is thus not a sufficient criterion to predict boundary layer flashback. When the equivalence ratio is increased to 0.38, the size of the flow separation zones increases and propagating flame tongues are formed from the flame bulges, which can be seen in Figure 4.

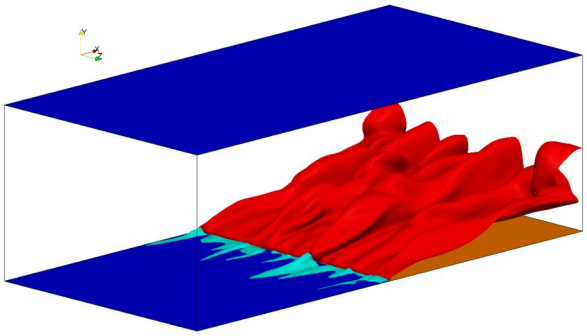

Figure 4: Flame front (red isosurface) and flow separation zones (turquoise isosurface) at flashback at 10 m/s and Φ=0.38.

On-going Research / Outlook

Currently the confined flashback simulations are extended to higher velocities. Furthermore, the unconfined configuration will be analyzed, where the flame is not stabilized inside the channel but at the transition from the channel outlet to the burning chamber. This will include calculations with even higher cell counts and computation time and due to the high workload of CoolMUC-2 also to long queuing times. However, the presented results promise accurate predictions for higher velocities and equivalence ratios as well. Furthermore, the computational times can be reduced by switching to a newer OpenFOAM version which provides the in-situ adaptive tabulation functionality for chemistry.

References and Links

[1] http://gepris.dfg.de/gepris/projekt/272154358
[2] Eichler, C. T. (2011): Flame Flashback in Wall Boundary Layers of Premixed Combustion Systems: Verlag Dr. Hut.
[3] Moser, R. D.; Kim, J.; Mansour, N. N. (1999): Direct numerical simulation of turbulent channel flow up to Reτ=590. In: Physics of Fluids 11 (4), S. 943–945.
[4] A. Endres, T. Sattelmayer (2017): Large Eddy Simulation of Confined Turbulent Boundary Layer Flashback: Poster presented at the 2nd International Workshop on Near-Wall Reactive Flows, Darmstadt, Germany.

Numerical Simulation of a Pilot Ignited Natural Gas Jet using Detailed Chemistry Calculation

Research Institution
Lehrstuhl für Thermodynamik, Technische Universität München

Principal Investigator

Thomas Sattelmayer

Researchers
Michael Jud

Project Partners
MTU-Friedrichshafen

Linux Cluster Project ID: t7811

Introduction

The use of natural gas as a main fuel in heavy-duty internal combustion engines is motivated by the high availability and the emission reduction potential. Due to the low C/H-ratio of methane, a significant reduction of CO_2 can be achieved. The use of natural gas in classical spark ignition gas engines or dual-fuel engines with homogeneous gas-air mixture, leads to significant emissions of unburned hydrocarbons due to flame quenching at the wall and valve overlap. High pressure direct injection of natural gas can create a spatially limited mixing zone and thus avoid fuel slip. Since typical natural gas self-ignition temperatures of 1100–1200 K [1] are not reached at top dead center, a small amount of Diesel is needed for ignition. In contrast to homogeneous charge dual-fuel engines, this technology provides maximum flexibility regarding to natural gas and Diesel injection timings.

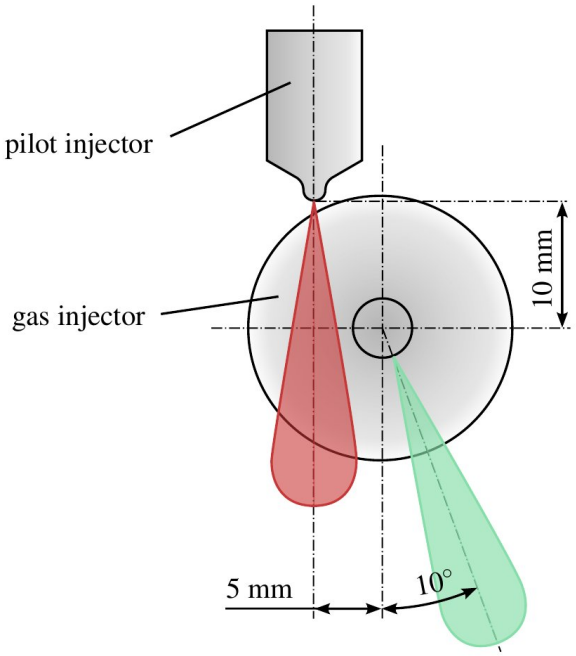

Figure 1: Arrangement of Diesel and gas injector.

At the chair of thermodynamics this new combustion strategy is investigated using a simple experimental setup in combination with 3D RCFD simulation. The experimental results are mainly used to validate the developed numerical model. The modeling strategy of 3D RCFD simulations is based on detailed chemical calculations in each computational cell. Thus, the computational effort is large even for small domains . It exceeds the computing capacity of a normal desktop PC and workstations.

Detailed information about the project and the institute of thermodynamics can be found in [2].

Results and Methods

The physical setup can shortly be described using Figure 1. First, a natural gas jet (green jet) is injected in a high temperature and high pressure environment. Then a Diesel jet (red jet) is injected and ignites itself. Consequently the gas jet is ignited by interacting with the hot Diesel products. This process is followed by a mainly diffusive combustion of the natural gas jet.
Figure 2 shows a qualitative comparison of shadowgraphs obtained from the experiment and the density field from the numerical simulation. Sharp gradients within the jets indicate the position of the flame front. With the chosen simulation method, the simple experiment can be predicted well. A more detailed description of the setup and detailed description and interpretation of numerical results can be found in [3].

The 3D RCFD simulations based on detailed chemistry calculations in each computational cell are conducted with the Converge software package. The solver is written in C programming language and uses the MPI libraries version 1.2 to enable simulations to be run in parallel on shared memory machines or across distributed memory machines [4]. Until now, most of the calculations using CoolMUC-2 were conducted using one computation node. The limit for the maximum number of nodes and cores is given by the number of computational cells (about 500,000) and the random access memory (RAM) limit of the cluster nodes.

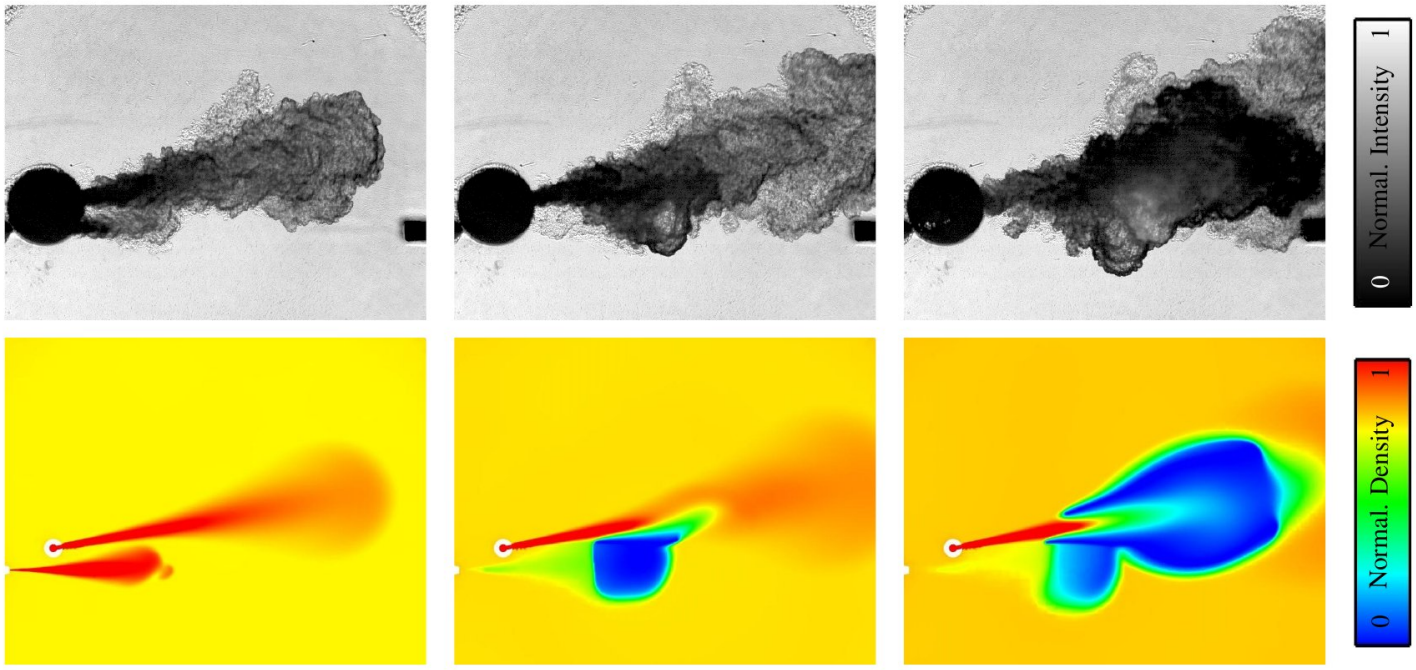

(a) 1.4 ms before TDC (b) 0.7 ms before TDC (c) 0.1 ms before TDC

Figure 2: Qualitative comparison of shadowgraphs and the density field in the plan of jet interaction for different times before top dead center of an internal combustion engine.

On-going Research / Outlook

During the first part of the project, the focus was on model testing and validation. Now, in the second part of the project the focus is on the calculation of different geometrical arrangements and variants. This involves the transfer of knowledge from the simple two-jet case, shown in Figure 2, to a full engine simulation with nine gas and nine Diesel jets. The computational time needed for the simple two-jet case was between 3–5 days depending on initial and boundary conditions. CoolMUC-2 provides the ideal cluster setup for these calculations. The number of cores per node was ideal for calculating a variation. To avoid much longer computational times for the full engine case, multiple computation nodes will be used.

When performing the calculations, the following challenges arise:

- High computational effort per cell
- Small cell number limits maximum core number
- Flops/s per core limits the calculation time
- Memory (RAM) limit per node
- 3 days wallclock limit

References and Links

[1] Huang, J., Hill, P. G., Bushe, W. K., and Munshi, S. R.,2004. “Shock-Tube Study of Methane Ignition Under Engine-Relevant Conditions: Experiments and modeling”. Combustion and Flame, 136(1-2), pp. 25–42.
[2] Institute of Thermodynamikcs. 2018. Available at: http://www.td.mw.tum.de/en/home/.
[3] Jud, M., Fink, G., and Sattelmayer, T. 2017, “Predicting Ignition and Combustion of a Pilot Ignited Natural Gas Jet Using Numerical Simulation Based on Detailed Chemistry”. In ASME 2017 Internal Combustion Engine Division Fall Technical Conference.
[4] Richards, K. J., Senecal, P. K., and Pomraning, E., 2016. CONVERGE (v2.3) Manual.

Computer Science and Mathematics

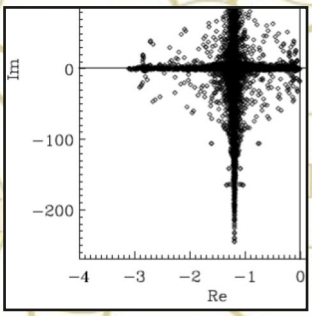

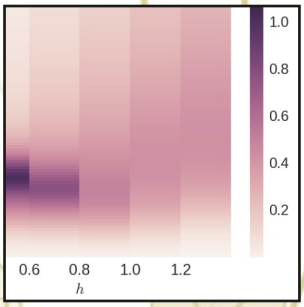

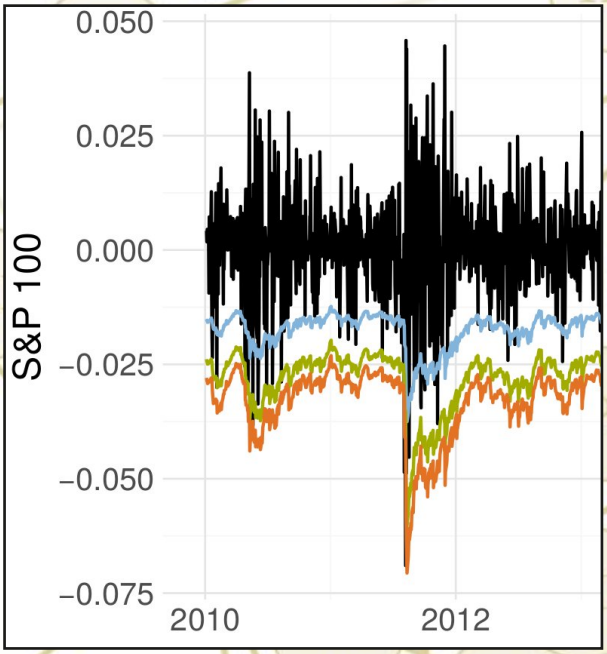

Dependence Modelling in Ultra High Dimensions with Vine Copulas

Research Institution
Department of Mathematics, TUM

Principal Investigator
Claudia Czado

Researchers
Dominik Müller, Thomas Nagler

Linux Cluster Project ID: pr23fo

Introduction

Vine copulas [1] are highly versatile statistical models for the dependence between several quantities. They express how multiple variables are related to each other, for example: stocks in a stock market, weather stations covering a country, or gene expressions in a genetic dataset.

In general, describing the joint behavior of variables in arbitrary dimensions is a highly complicated task. Vine copula models tackle this problem by decomposing the dependence structure into several two-dimensional building blocks. This leads to a graphical model consisting of several nested trees, where the first tree encodes unconditional pairwise dependencies, and subsequent trees encode conditional pairwise dependencies. An example on four variables is shown in Figure 1. Yet, this reformulation of the problem comes with a price tag: the number of (conditional) pairs in the model grows quadratically in the number of variables.

In high dimensional applications (e.g. 1,000 variables), the model needs to be simplified to keep it computationally tractable. In the end, only the important dependences should be included to obtain a sparse model. The main difficulty is to find the right tradeoff between model fit and complexity. Additionally, an efficient implementation of the model is essential.

Results and Methods

Advances in statistical methodology
The established standard for fitting vine copula models is the algorithm of Dißmann et al. [2], a greedy algorithm that aims to capture most of the dependence in the first couple of trees. In high dimensions, the resulting models become overly complex and computationally infeasible. A popular trick to obtain sparser model is truncation, i.e., only modeling dependencies in the first few trees, while assuming conditional independence for the remainder. But even truncated models can be unnecessarily complex when there are many independent pairs in the data.

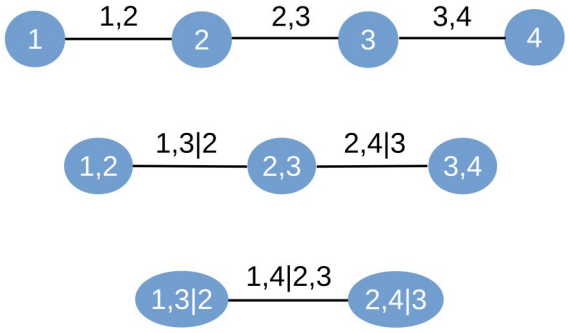

Figure 1: Illustration of a vine on four variables.

Our research group developed several techniques to exploit sparsity patterns in the data. Müller [3] builds on techniques from sparse graphical models to first obtain a simple proxy model, which is then translated into a vine copula. A more aggressive approach proposed by Müller [3] allows to cluster the variables first and then estimate isolated models on each cluster, which heavily reduces the computational burden. An alternative route was taken by Nagler et al. [4], who developed a method that only includes dependencies whose strength passes a certain threshold. The optimal threshold can be selected automatically with almost no computational overhead.

Advances in computation
The standard implementation of vine copula models, the R package VineCopula, has been actively developed and maintained from our group. However, it was initially designed for problems of small or moderate dimensions and has severe limitations in high dimensional applications. One issue is that the R interpreter is single-threaded by design and multiple instances have to be run for concurrent computations. Hence, the R implementation cannot fully exploit the fact that fitting a vine copula is a sequence of embarrassingly parallel tasks. Another issue is that the standard algorithms for vine copula models are of quadratic complexity in both memory and time.

To empower applications in high dimensions, we developed a pure C++ implementation, vinecopulib [5], that has interfaces to both R and Python. It implements optimized data structures and algorithms

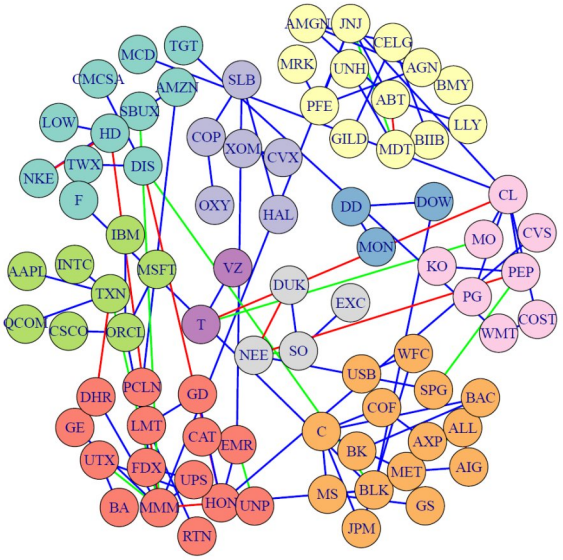

Figure 2: A high dimensional network of the stocks which are comprised in the S&P100 index. The picture shows how the algorithms of [2] detect connections between stocks of similar industry sectors, which are encoded by the colors. Picture taken from [2].

that remove many redundancies and scale linearly with the dimension if the model is truncated.

Numerical evaluation on simulated data
All newly developed methods were benchmarked extensively against the standard method of Dißmann et al. [2] via simulations. To assess their performance, we fitted baseline models on several data sets from various disciplines and used it as ground truth. One example we used are 85 stocks of the S&P100 stocks index, see Figure 2. We then simulated from the baseline model and fitted all competitor models to the synthetic data. The new methods were found to fit almost equally well to the data while at the same time being of much lower complexity.

All this, however, requires extensible computation time. For all implementations, the statistical software R and several individually developed libraries were used. Most of the algorithms and simulation run in parallel, typically using 28–32 cores per job. For the simulations we carried out in 85 dimensions, the standard fitting routine took about 5 hours. With the newly developed methods, the fitting time was reduced to approximately 30 minutes. Other benchmarks went over 2,000 dimensions and took almost two days for a single fit of a sparse model. Fitting the standard method was only feasible until around 400 dimensions, i.e., 400 stocks or similar.

Application to financial risk management
Several of the new methods were successfully applied to risk management problems in financial markets. We fitted models to portfolios of hundreds of stocks and evaluated how well the one-day ahead risk is predicted. This procedure is repeated for every trading day over several years, thus requiring many computing hours. Figure 3 shows the realized returns of a portfolio of S&P 100 stocks along with predicted levels of the risk.

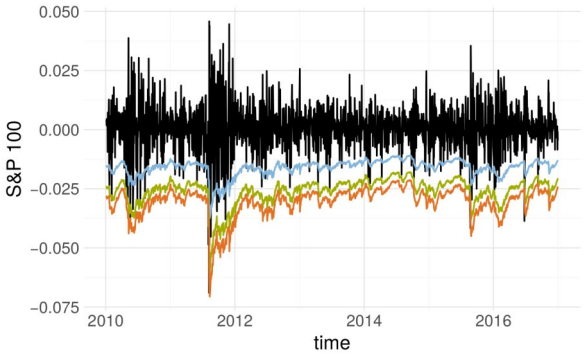

Figure 3: Time series of returns of a portfolio of stocks from the S&P 100 index (black) along with one-day-ahead predictions of the Value-at-Risk for different risk levels (colors).

Summary

This research project developed, evaluated, and applied statistical dependence models for hundreds or thousands of variables. It used approximately 340,000 CPU hours and generated thousands of files totaling almost 500 GB of data. Without the CoolMUC-2, exploration, development and validation of the new methods would not have been possible.

On-going Research / Outlook

The project required extensive computational capabilities for running simulations, fitting the models, as well as storing the models and data sets. The algorithms we use run many tasks in parallel so that computation time is inverse proportional to the number of threads. One node of the CoolMUC-2 allows for only 28 threads. Hence, an implementation that runs on multiple nodes will be necessary to scale the models up to problems of higher magnitudes.

References and Links

[1] http://www.vine-copula.org/
[2] Jeffrey Dißmann, Eike C. Brechmann, Claudia Czado, Dorota Kurowicka. 2013. Selecting and estimating regular vine copulae and application to financial returns. COMPUT STAT DATA AN 59 (March 2013), 52-69. DOI: https://doi.org/10.1016/j.csda.2012.08.010
[3] Dominik T. Müller. 2017. Selection of Sparse Vine Copulas in Ultra High Dimensions. PhD Dissertation. Technical University of Munich. http://mediatum.ub.tum.de/node?id=1382835
[4] Thomas Nagler, Christian Bumann, and Claudia Czado. 2018. Model selection in sparse high-dimensional vine copula models with application to portfolio risk. arXiv:1801.09739. Retrieved from https://arxiv.org/abs/1801.09739
[5] http://www.vinecopulib.org/

Machine Learning: Benchmarking, Optimization and Automation

Research Institution
Computation Statistics, Department of Statistics, LMU

Principal Investigator
Bernd Bischl

Researchers
Janek Thomas, Giuseppe Casalicchio, Xudong Sun, Quay Au, Christoph Molnar, Florian Pfisterer

Linux Cluster Project ID: pr74ze

Introduction

Machine learning has achieved considerable successes in recent years and an ever-growing number of scientific disciplines rely on it. However, this success crucially relies on human machine learning experts, who select appropriate features, workflows, machine learning algorithms, and their hyper-parameters. Even for expert researchers it is challenging to find the best approach: the relation between a data set and the performance of a particular machine learning approach on it cannot be predicted in a straightforward manner. The rapid growth of machine learning applications in both science and industry has created a demand for off-the-shelf machine learning methods that can be used easily and without expert knowledge.

The collection of machine learning experiment data and optimization of machine learning algorithms are crucial steps to automate this process further.

Results and Methods

The working group Computational Statistics of the LMU realized multiple research goals using the CoolMUC-2 system at the LRZ. An overview of current research that utilized the LRZ computing resources can be found at [1].

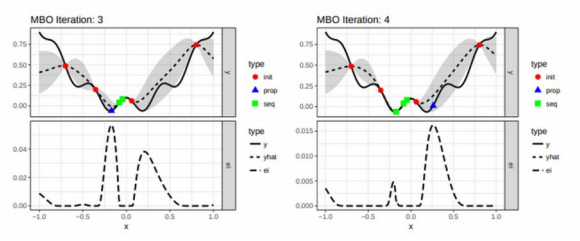

Research was done especially in the area of Bayesian optimization. mlrMBO [2] was evaluated and optimized on the LRZ. mlrMBO is a flexible and comprehensive R toolbox for model-based optimization (MBO), also known as Bayesian optimization, which addresses the problem of expensive black-box optimization by approximating the given objective function through a surrogate regression model. It is designed for both single- and multi-objective optimization with mixed continuous, categorical and conditional parameters. Additional features include multi-point batch proposal, parallelization, visualization, logging and error-handling. mlrMBO is implemented in a modular fashion, such that single components can be easily replaced or adapted by the user for specific use cases, e.g., any regression learner from the mlr toolbox for machine learning can be used, and infill criteria and infill optimizers are easily exchangeable.

We empirically demonstrated that mlrMBO provides state-of-the-art performance by comparing it on different benchmark scenarios against a wide range of other optimizers, including DiceOptim, rBayesian-Optimization, SPOT, SMAC, Spearmint, and Hyperopt.

Further work was done on parallel execution of bayesian optimization. As it is often indispensable to apply parallelization to speed up the computation. This is usually achieved by evaluating as many points per iteration as there are workers available. However, if runtimes of the objective function are heterogeneous, resources might be wasted by idle workers. We compared different established parallelization strategies on a set of continuous functions with heterogeneous runtimes. Our benchmark covered comparisons of synchronous and asynchronous model-based approaches and investigates the scalability.

Research was also conducted in the area of machine learning benchmarking where a large datasets of machine learning experiments [3] was created with the help of the CoolMUC-2 system. The dataset contains the performance results (AUC, accuracy and Brier score) of six different machine learning algorithms, the used hyperparameters that were set by a random search, runtimes and meta-data for each dataset. These data helps to understand the influence of hyperparameters on the performance of a machine learning algorithms which is an important part of finding a well performing and adequately tuned algorithm for a given dataset. As to date no dataset exists to support this required understanding for state of the art algorithms like gradient boosting or random

forest, The data can be used for meta-learning, finding good defaults, measuring the tunability of algorithms and hyperparameters, benchmarking of algorithms and other tasks mainly related to hyperparameters.

All of the above work leveraged the OpenML platform [4]. This platform allows researchers to upload new datasets in a way that allows the machine learning community to instantly evaluate algorithms on them. Moreover, it makes sure that all machine learning models are evaluated consistently so that they can be directly compared to each other, and that all results are reproducible for easy verification and reuse. It offers APIs so that researchers can easily run large-scale evaluations of many different algorithms and configurations, from any computational infrastructure. These APIs will be leveraged to build the proposed platform.

OpenML unites a growing community of about 30 researchers that aim to develop and compare high-quality open source machine learning tools. It includes developers for popular libraries such as scikit-learn and mlr, working at major universities in New York, Paris, Munich, Vancouver, Eindhoven, Leiden, Freiburg, London, Manchester, Sheffield, Porto and many more. OpenML has about 900 registered users and many more daily visitors. OpenML is led by Joaquin Vanschoren, who also collaborates with domain scientists to include recent and relevant scientific datasets.

On-going Research / Outlook

Without the CoolMUC-2 system all of the above introduced research would not have been possible, as massive computation power is required for the evaluation of the bayesian optimizer and the generation of a large amount of machine learning meta data.

Future plans are to scale the benchmarking further up and generate metadata in a smarter way.

Additional research in the area of automatic machine learning is also planned. Especially the optimization of more complex and dependent parameter spaces, e.g., kernel choice in SVMs (compare the figure above) or the optimization over multiple models at the same time is planned.

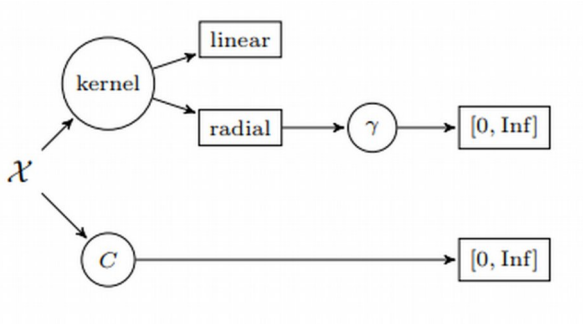

References and Links

[1] www.compstat.statistik.uni-muenchen.de/publications/
[2] https://github.com/mlr-org/mlrMBO
[3] figshare.com/articles/OpenML_R_Bot_Benchmark_Data_final_subset_/5882230
[4] https://www.openml.org/

Activities at the Chair of Scientific Computing in Computer

Science: Research and Teaching on CoolMUC-2

Research Institution
[1]TUM, Dept. of Informatics, Chair of Scientific Computing in Computer Science (SCCS)

Principal Investigator
Hans-Joachim Bungartz[1], Thomas Huckle[1], Michael Bader[1]

Researchers
Ionut-Gabriel Farcas2, Tobias Goerler2, Tobias Neckel2, Moritz August3, Mari Carmen Banuls3

Project Partners
2Max Planck Institute for Plasma Physics, Tokamak Theory Division (Farcas et al.)
[3]Max Planck Institute for Quantum Optics, Theory Group (August et al.)

Linux Cluster Project ID: pr63so

The Chair of Scientific Computing in Computer Science (SCCS) [1] at TUM's Department of Informatics focuses on various fields of computational science and engineering including numerical algorithms, parallel and distributed computing as well as the development of simulation applications for various application areas (e.g., fluid dynamics, traffic or quantum chemistry). In order to support both research and teaching in these interdisciplinary fields, CoolMUC-2's resources have been intensively exploited within the pr63so project for a variety of teaching activities as well as third-party funded research projects.

With respect to teaching, CoolMUC-2 has regularly been used by students within the practical courses offered by SCCS. For instance, students are taught how to develop parallel numerical software in the practical course on "Molecular Dynamics", where a simple parallel application for simulating molecular interactions is developed. Key educational objectives are both shared and distributed memory parallelization as well as scalability. In this regard, CoolMUC-2 provided a platform for performance engineering and parallel application development. A similar course that made use of CoolMUC-2 is the Bachelor's practical course on Tsunami simulation.

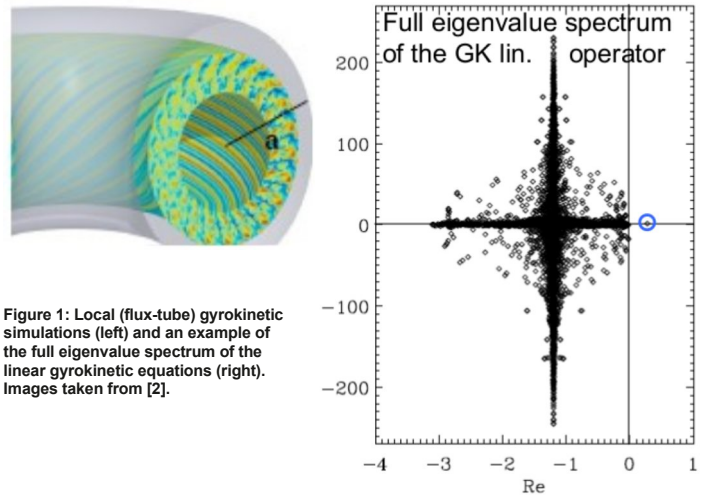

Figure 1: Local (flux-tube) gyrokinetic simulations (left) and an example of the full eigenvalue spectrum of the linear gyrokinetic equations (right). Images taken from [2].

Besides teaching, CoolMUC-2's compute nodes were also extensively used for research activities within several projects both by SCCS's PhD candidates as well as students working on their Bachelor's or Master's theses. For instance, several researchers have used CoolMUC-2's resources for improving the performance of the molecular dynamics software ls1-mardyn: optimization techniques include vectorization and one-sided MPI communication. In other cases, CoolMUC-2 was used for numerical tests and development (e.g., for the ELPA eigenvalue solver library and the preCICE coupling library). In the following, two of these subprojects will be described in more detail:

- Sensitivity-driven Dimension-adaptive Sparse Approximations in Gyrokinetic Simulations
- Fighting the Curse of Dimensionality in Quantum Physics

Sensitivity-driven Dimension-adaptive Sparse Approximations in Gyrokinetic Simulations (Farcas et al.)

Introduction
The simulation of micro-turbulence in plasma fusion is paramount for understanding the confinement properties of fusion plasmas with magnetic fields. The micro-instability is driven by the free energy provided by the unavoidably steep plasma temperature and density gradients. Unfortunately, the measurement of the latter – as well as further decisive physics parameters affecting the underlying micro-instabilities – are subject to uncertainties, which requires an uncertainty quantification framework. Here, we employ the established plasma micro-turbulence simulation code GENE [1] and restrict ourselves to the linear gyrokinetic problems in 5D phase space, taking into account electrons and deuterium ions. In addition, in our simulations we also consider collisions between the constituent particles.

GENE is a Eulerian code written in Fortran which self-consistently solves the gyrokinetic Vlasov-Maxwell system of integralo-differential equations. Further-

more, it allows for arbitrarily long simulation times, exhibits very good convergence properties and is highly parallelizable. As stated above, we use GENE in linear mode and we calculate the growth rate of the micro-instabilities driving the turbulence. To compute the growth rate, we solve the linearized equations either as initial value problems, using fourth-order Runge-Kutta time stepping, or as eigenvalue problems, using solvers from the PETSc/SLEPc package.

Uncertainty propagation in model-based physical phenomena is a three-step process. Initially, the uncertain parameters are modeled in a probabilistic framework, afterward, they are propagated through the underlying model and, finally, outputs such as expectation, standard deviation are collected. Computationally, this is realized in an outer-loop fashion, meaning that the underlying model is queried many times and the corresponding results are collected for post-processing. We note that we are interested in deterministic, non-intrusive approaches, i.e.. approaches in which the GENE code as a black-box. However, when the number of uncertain parameters, i.e. the stochastic dimensionality, is large, standard collocation-based methods are not suitable for uncertainty propagation, because of the “curse of dimensionality”: the exponential growth of the necessary number of model evaluations with the stochastic dimensionality.

To this end, for the propagation of uncertainty we employ sparse grid-based methodologies. In a nutshell, sparse grids [3] aim at delaying the curse of dimensionality by neglecting grid points whose contribution to the overall solution is negligible. Variants include sparse grid quadrature, sparse interpolation or sparse pseudo-spectral projection. In this work, to have a better overview of such methodologies in linear gyrokinetic problems, we consider both sparse grid interpolation – constructed using a Lagrange basis and Leja points – and sparse pseudo-spectral projection, constructed using Legendre polynomials and Leja points. The standard formulation of sparse grid approaches is based on a priori, theoretical knowledge about the problem at hand Since, on the one hand, we do not always have the theoretical analysis required by standard sparse grids, and, on the other hand, we aim to construct methodologies that take advantage of the structure of the problem at hand, such as anisotropy, we employ here so-called dimension-adaptive sparse grids. Dimension-adaptivity means that we do not choose the sparse grid a priori, but, using suitable metrics, we construct it while we perform our simulations. The standard dimension-adaptive algorithm [4] uses local error indicators, i.e. heuristics that mimic the approximation error, to drive the adaptive process. Although this algorithm works very well for deterministic problems, stochastic problems such as the ones considered in this work might have a richer structure, of which we aim to take advantage.

Results and Methods

Our contribution is in formulating enhanced dimension-adaptive sparse approximations that employ stochastic information to further tune the adaptive process. To this end, on top of the standard dimension-adaptive algorithm, we additionally employ sensitivity information to prevent the algorithm to refine in directions that are rendered unimportant. Even more, in the standard dimension-adaptive part of our method, we use a quasi-variance gradient as local error indicator. In other words, if, e.g., the underlying problem has three stochastic parameters, but just one contributes significantly to the resulted variance, our algorithm will preferentially refine more in the first direction that in the other two. This formulation is very natural when employing spectral projection based on Legendre polynomial, as these polynomials are orthogonal in the projection space. On the other hand, to obtain the needed sensitivity information when using interpolation, we use the fact that the sparse grid approximation is an inclusion-exclusion of full grid approximations and that on each of these grids, interpolation and spectral projection are equivalent [5].

In the following, we present results in a test case having three uncertain inputs. The physical quantity for which we perform the quantification of uncertainty is the growth rate (the real part) of the dominant eigenvalue, which we compute using the iterative solver. Further, we perform the quantification of uncertainty using a deterministic design-parameter, the normalized poloidal wavenumber.

We performed all individual GENE simulations using 32 cores. With this setup, a single run takes between a few minutes to a few hours, depending on the number of iterations. To further speed up the computations, we take advantage of the non-intrusiveness of our approach and perform the quantification of uncertainty using up to three layers of parallelism: all single runs are performed in parallel on 32 cores, multiple runs corresponding to the same wavenumber are performed in parallel to each other and simulations associated with different wavenumbers are performed in parallel as well. With the aforementioned setup, we typically used up to few tens of compute nodes, depending on the availability of the cluster.

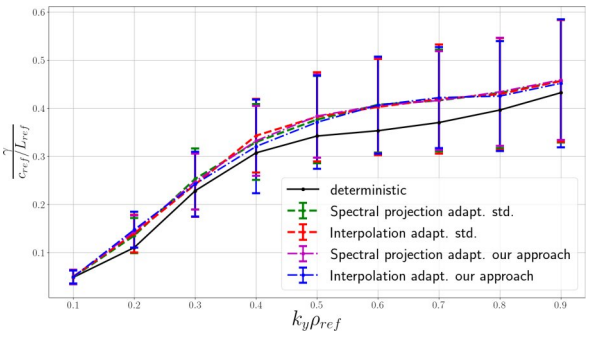

Figure 2: Expectation and standard deviation for all wave numbers, using dimension-adaptive (standard and our version) interpolation and spectral projection.

In Figure 2, we depict the deterministic results and the expectation and standard deviation for each wavenumber, obtained using both the standard and our version of dimension-adaptive interpolation and spectral projection. We see that all results are very

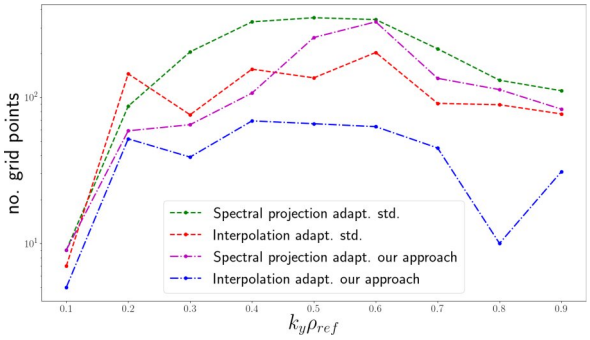

Figure 3: Number of grid points (model evaluations) for all wave numbers, using the standard and our version of dimension-adaptive s interpolation and spectral projection.

similar. Regarding their associated computational cost, in Figure 3, we depict the number of grid points for each approach and we see that the interpolation approach based on our enhanced version of dimension-adaptivity is clearly superior to all other versions. These results are very promising and they show that using sensitivity information in dimension-adaptive sparse approximations is a suitable approach to overcome the challenges posed by the quantification of uncertainty in complex scientific computing problems.

On-going Research / Outlook

Our on-going research concentrates on improving sensitivity-exploiting sparse grid approaches. Moreover, we will test our approaches in higher-dimensional, computationally more expensive test cases. In the near future, we plan to extend the current methodology to a multi-fidelity approach, in which we employ GENE as the "high-fidelity" model together with several "lower-fidelity" models, such as simplified physics models or our current sparse approximations, in a unified framework so that all components contribute to the uncertainty quantification computations. As a long term goal, we want to use our methodologies in fully nonlinear GENE simulations (one such run can take several tens of thousand of CPU hours) and with this, to better connect uncertainty quantification and high-performance computing.

References and Links

[1] http://genecode.org/
[2] T. Goerler, Multiscale effects in plasma microturbulence, Dissertation, Universität Ulm, 2009
[3] H.-J. Bungartz and M. Griebel, Sparse grids, Acta Numerica, vol. 13, pp. 147–269, 5 2004.
[4] T. Gerstner and M. Griebel, Dimension–adaptive tensor–product quadrature, Computing, vol. 71, no. 1, pp. 65–87, 2003
[5] https://www5.in.tum.de/pub/farcas_siam_uq_18.pdf

Fighting the Curse of Dimensionality in Quantum Physics (August et al.)

Introduction

Of all branches of science, quantum physics can safely be regarded as one of the most puzzling. While its predictions have been confirmed with in many cases unprecedented accuracy, these predictions at the same time appear utterly strange to us humans who evolved to understand Newtonian dynamics. The challenges of quantum mechanics however reach beyond the conceptual level as it also poses a major challenge to computational scientists. This is due to the fact that the complex Hilbert space in which quantum systems are formally expressed as normalized vectors and matrices, grows exponentially in dimension with the number of particles in the system. For instance, a system of 100 spin-1/2 particles resides in a Hilbert space of dimension 2^{100}. This illustrates that the exact description of even medium-sized quantum systems is out of reach for classical computers. To tackle this quantum incarnation of the curse of dimensionality, numerical physicists and numerical computer scientists and mathematicians have developed a formalism to decompose and approximate the Hilbert space and the objects it contains into smaller tensors. These approaches are consequentially called tensor networks (TN) and today constitute the most successful approach to simulating quantum physical systems.

Results and Methods

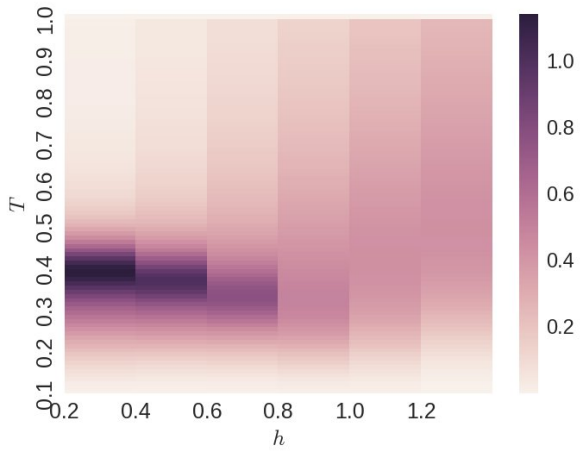

Figure 4: A diagram depicting the heat capacity of a Gibbs state with 80 particles in the space of temperature (*T*) and a magnetic field strength parameter of the Hamiltonian. Signals of a thermal phase transition are clearly visible for *h*=0.2,0.4 and 0.6.

In this project we have dealt with the question of how to approximate functions of Hermitian complex matrices *A* in the exponential Hilbert space of the form trace *f(A)*. This type of function is of particular importance in quantum physics as many quantities of interest, such as the entropy, heat capacity, thermal fidelity or the trace-norm can be expressed in this way. Additionally, expectation values of operators with respect to mixed quantum states take a respective form.

Computing these quantities is not possible with existing TN methods as they rely on a local description of the individual particles a given system consists of and thus are in general not able to approximate global properties taking into account the entire spectrum. By leveraging the connection of Lanzcos-type algorithms with Gauss quadrature and combining it with the TN framework, we were able to develop the first algorithm [7] able to approximate such functions to a good degree.

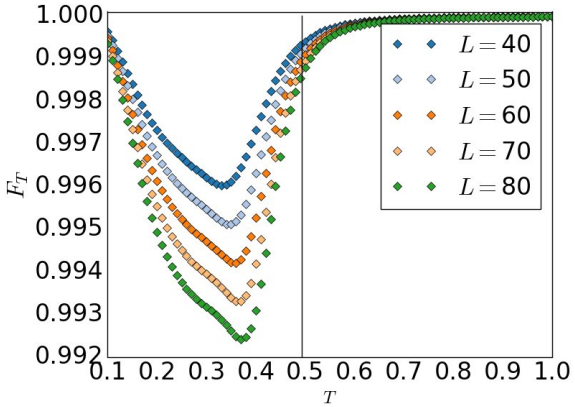

Figure 5: A diagram showing the thermal fidelity (F_T) of a Gibbs state over the temperature (T) for various numbers of particles L and a magnetic field strength h=0.2. The plots illustrate the more pronounced signal of the thermal phase transition for larger system sizes.

We have subsequently demonstrated how our algorithm can be used to approximate properties of mixed quantum states in thermal equilibrium which signal a thermal phase transition [8]. Example plots of the obtained results for two particular such quantities of interest are provided in Figures 4 and 5. All of the results in Refs. [7] and [8] have thereby be obtained on the CoolMUC-2-cluster in a total of several weeks of production runs. As Lanczos-type algorithms are inherently of sequential nature, a single run made use of one node but used parallelized implementations of core linear algebra routines such as matrix-matrix and matrix-vector products as well as the singular value decomposition.

On-going Research / Outlook

Having introduced, analyzed and successfully demonstrated our algorithm for a relevant problem in quantum physics, two main branches of future research exist. Firstly, it would naturally be interesting to identify further applications in quantum mechanics and help to solve these with our method. Secondly, more can still be done in terms of analyzing the properties of the algorithm and possibly combining it with other methods to approximate extremal eigenvalues.

References and Links

[6] http://www.exqm.de
[7] M. August and MC. Banuls and T. Huckle, On the approximation of functionals of very large Hermitian matrices represented as matrix product operators, Electronic Transactions on Numerical Analysis, vol. 45, pp. 215-232, 2017 http://etna.mcs.kent.edu/volumes/2011-2020/vol46/abstract.php?vol=46&pages=215-232
[8] M. August and MC Banuls, Efficient approximation for global functions of matrix product operators, http://www.arxiv.org/abs/1804.03613

Forecasting realized volatilities with regular vines

3

Research Institution
University of Augsburg

Principal Investigator
Eugen Ivanov

Researchers
Yarema Okhrin

Project Partners
Claudia Czado, Chair of Mathematical Statistics, Technical University of Munich

Linux Cluster Project ID: b5101

Introduction

The concept of using realized volatility (*RV*) and its multivariate counterpart, realized covariances (*RCOV*), has largely spread since the availability and improved accessibility of high-frequency data in finance. First models have arisen in the continuous time framework, leading to fundamental results and methods. However, practical issues, like microstructure noise, asynchronicity of data, stress on short and long term forecasting, etc. lead to a shift from stochastic to statistical modeling of realized volatilities. Given the very general assumptions of a multivariate diffusion process underlying the various estimation methods for *RV* and *RCOV*, the key advantage of realized covariances is that they are observable time-series. In most applied empirical work, the main task lies in modeling and forecasting realized variances. The problem of standard models is the imposed linearity, i.e. the current level of the (log-)*RV* is modeled as a linear function of its past (log-)values. In our research project we consider an alternative approach which helps us to incorporate non-linear causal dependence into the predictive models for realized volatilities. We consider a regression based on conditional copulas, where the regression equation is derived as conditional expectation computed from the joint multivariate distribution of dependent and explanatory variables. We model this joint distribution with vine copulas [1], since they offer a flexible modelling framework which precisely reflects the inherited dependence in our data. The multivariate copula is constructed through bivariate (conditional) copulas. The Figure illustrates a popular vine construction, where the edges together with their titles present the modeled dependencies, the numbers of variables.

Results and Methods

The estimation procedure is based on a matrix representation of the vine structure. Due to conditioning, new “pseudo” copula data for each tree in a vine must be computed sequentially in order to calculate the log likelihood. Hence the estimation procedure is mildly memory and CPU savvy. Due to the sequential nature of the procedure the use of parallelisation is constrained. The project realies crucially on the R-Package “VineCopula”, where the estimation procedures are implemented. Since the models were re-estimated daily for 10 years and different indices, the maximum available amount of cores per user was used, with one core estimating about 20 days.

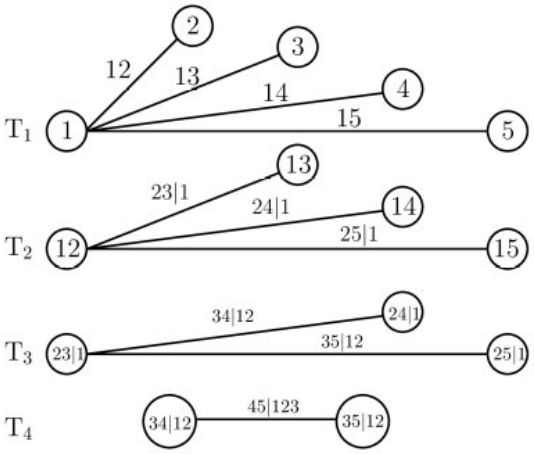

Figure 1: C-vine in 5 dimensions.

Results show that vine based regression delivers statistically better forecasts than widely used linear models.

On-going Research / Outlook

CoolMUC-2 enabled us to estimate models over a long period of time for different indices and assess the consistency of performance. The only limitation faced in the project was the starkly fluctuating wait time.

For further project we consider forecasting multivariate realized covariances.

References and Links

[1] Aas, K., Czado, C., Frigessi, A., and Bakken, H. (2009). Pair-copula constructions of multiple dependence. Insurance: Mathematics and Economics, 44(2):182–198.

Earth, Climate, and Environmental Sciences

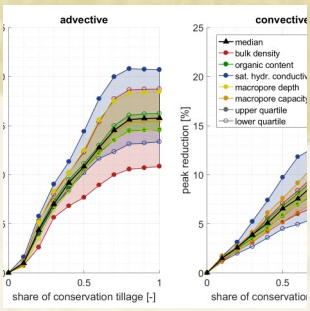

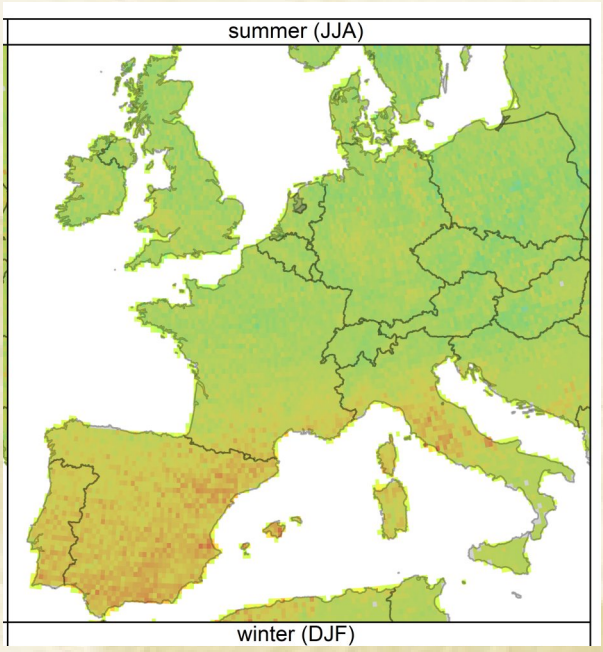

Structure-property relations for resistivity in Fe-alloys at conditions of the Earth's core from first principles simulations

Research Institution
Bayerisches Geoinstitut, Universität Bayreuth, 95440 Bayreuth

Principal Investigator
Gerd Steinle-Neumann

Researchers
Fabian Wagle, Esther Posner

4

Linux Cluster Project ID: b1301

Introduction

Electrical resistivity and thermal conductivity are key to understanding the stability of the geodynamo that generates Earth's magnetic field [1] and the thermal evolution of our planet. These properties are currently challenging to determine experimentally under the relevant conditions of high pressure and temperature. In previous work on the subject, we have computed them for pure liquid iron, the dominant elements in planetary cores, by means of electronic structure simulations [2]. However, iron must be alloyed by light elements in the Earth's core, with silicon, oxygen [2] and sulfur [3] the most probable candidates. The presence of light elements strongly influences the electronic transport properties.

Results and Methods

We perform density functional theory based molecular dynamics (MD) simulations using the VASP code for Fe alloys with Fe_7X and Fe_3X (X=S, O, Si) composition and at unit cell volumes and temperatures covering the conditions of the Earth's core. For uncorrelated snapshots from the MD trajectories we compute electronic wavefunctions, their energy eigenvalues, and the gradients of the Hamiltonian which provide access to electronic transport properties through the Kubo-Greenwood formalism. These linear response calculations are performed with the electronic structure package Abinit.

The resulting electrical resistivity changes due to light element incorporation (impurity resistivity) differ significantly between the light elements (Figure 1). While the influence of O is negligible and resistivity increases with temperature, a high concentration of S or Si (i.e., for the Fe_3X compositions) leads to a saturation in resistivity. Specifically, resistivity appears to saturate at values near 100 μΩcm for conditions of the Earth's core, and further increasing temperature does not result in changing resistivity. For Fe_3S, we even observe a negative temperature coefficient of resistivity.

By fitting the frequency-dependent electrical (optical) conductivity results with a Drude model, we also have access to the electron mean free path and can

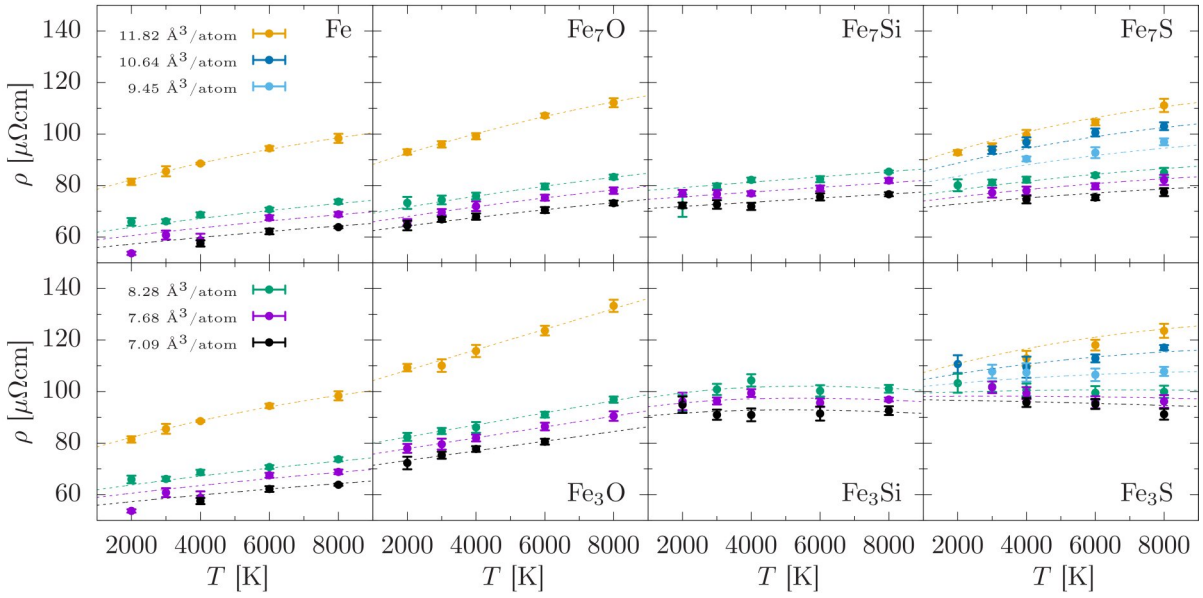

Figure 1: Electrical resistivity of liquid iron and various binary Fe-alloys as a function of temperature for different cell volumes (isochore) at conditions up to those of the Earth's core. The T-dependence of resistivity diminishes for high concentrations of Si and reverses sign for sulfur. Dashed lines show the fit of an analytical model to the simulation results.

correlate it with the interatomic distance in the liquid metals (Figure 2). We find that for Fe_3Si and Fe_3S the electron mean free path becomes smaller than interatomic distance at densities of the Earth's core which accounts for the saturation in resistivity, as formulated by the Ioffe-Regel condition.

The value of resistivity of 100 μΩcm near saturation can be viewed as an upper limit for the Earth's core which is smaller by at least a factor of two than long accepted values in the geodynamics literature. As electrical resistivity directly enters the dissipation term of the geodynamo creating Earth's magnetic field, a smaller resistivity value has two implications: (i) the dynamo is expected to be more stable in a given polarity, and (ii) the magnetic field can be generated by smaller fluid velocities in the Earth's outer core.

For the presented project, we have performed the following simulations on the CoolMUC-2 cluster:

For conditions not yet explored by previous studies [2], we performed MD simulations of liquid Fe-X alloys using VASP. Jobs with 128 atoms were distributed over four nodes (112 cores) for various cell volumes and temperatures (a total of 80 ensembles) and divided into runs with 12h wall time. This task consumed 1.6M core hours and ~800 GB of disk space.

Independent configurations along the MD trajectories were used to calculate electrical and thermal conductivity with the Abinit software package. This includes one electronic relaxation and three linear response calculations within the DFT framework per snapshot, which consumed ~1M core hours in total. Wall times did not exceed 12h using four nodes (112 cores). The task required ~2TB of disk space, mainly due to large files containing charge densities and wave functions.

In complementary VASP-MD runs, we studied diffusivity of Fe and light elements in liquid iron [4,5] (see below). For this project, a total of 140 ensembles were investigated with similar parameters as outlined in the previous paragraph. These MD simulations required 2.8M core hours and 1.4 TB of disk space.

On-going Research / Outlook

Similar to the structure-property relations outlined above for electrical resistivity, other transport properties of light elements in iron melt are determined by the melt structure. Another important example for that is chemical diffusion of light elements in Fe liquid that partly determines the initial budget of these elements in the core and the thickness of a possible stagnant layer at the top of the outer core. We have computed chemical diffusion of Si [4] and O [5] in iron, and found good agreement with experiments at similar P-T conditions, also performed by ourselves [4].

We are now in the process of looking into the incorporation mechanism of other light element candidates for the Earth's core into liquid iron, their diffusivities and the relation between them. Such

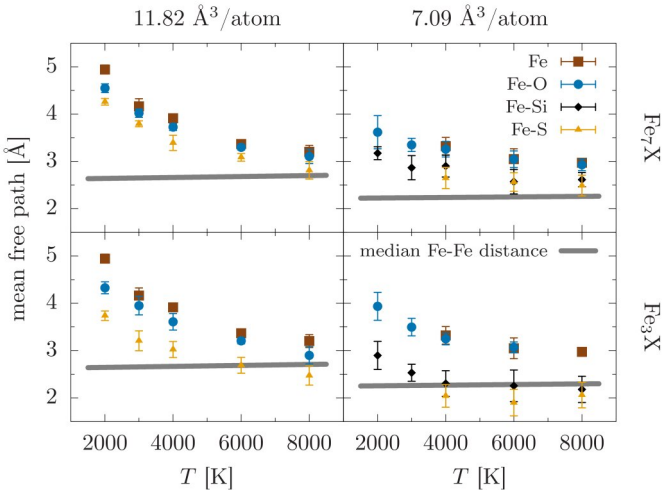

Figure 2: Electron mean free path for liquid iron alloys with 12.5 at% (Fe7X) and 25 at% (Fe3X) light element content for two cell volumes, near ambient pressure (left) and at conditions of the Earth's core (right), obtained by a Drude fit to optical conductivity. The mean free path approaches the Fe-Fe interatomic distance in the alloys (grey thick line) with increasing temperature, compression and impurity concentration. For Fe3Si and Fe3S at the smallest cell volume, the Ioffe-Regel condition is satisfied.

results provide an important benchmark for geodynamic and geochemical studies as experiments for both liquid structure and diffusivity are technologically challenging and still out-of-reach at pressures of the Earth's core.

References and Links

[1] https://en.wikipedia.org/wiki/Dynamo_theory
[2] Nico de Koker, Gerd Steinle-Neumann, and Vojtěch Vlček. 2012. Electrical resistivity and thermal conductivity of liquid Fe alloys at high P and T, and heat flux in Earth's core, Proc. Natl. Acad. Sci. USA 109, 4070-4073. DOI: 10.1073/pnas.1111841109
[3] Fabian Wagle, Gerd Steinle-Neumann, and Nico de Koker. 2018. Saturation and negative temperature coefficient of electrical resistivity in liquid iron-sulfur alloys at high densities from first-principles calculations, Phys. Rev. B. 97, 094307. DOI: 10.1103/PhysRevB.97.094307
[4] Esther Posner, David C. Rubie, Daniel J. Frost, Vojtěch Vlček, and Gerd Steinle-Neumann. 2017. High P-T experiments and first principles calculations of the diffusion of Si and Cr in liquid iron, Geochim. Cosmochim. Acta 203, 323-342. DOI: 10.1016/j.gca.2017.01.024
[5] Esther Posner, Gerd Steinle-Neumann, Vojtěch Vlček and David C. Rubie. 2017. Structural changes and anomalous self-diffusion of oxygen in liquid iron at high pressure, Geophys. Res. Lett. 44, 3562-3534. DOI: 10.1002/2017GL072926

Investigation of the regional CO_2 budget based on atmospheric meas-urement series

Research Institution
Chair of Physical Geography and Quantitative Methods, Institute of Geography at the University of Augsburg

Principal Investigator
Jucundus Jacobeit

Researchers
Esther Giemsa

Project Partners
Umweltbundesamt, Dessau-Roßlau

Linux Cluster Project ID: b5101

Introduction

The primary aim of the project [1] is to give detailed insights into the measurement time series underlying emission structures by means of origin-related examinations of the Alpine carbon dioxide (CO_2) budget. For not only climate gases time series themselves which document the unbroken increase in the atmospheric concentrations of greenhouse gases regarding their pre-industrial level (CO_2 by 40% IPCC 2013) but more particularly their interpretation with a special attention on the regional emission budget within the catchment area of a measurement station are of high scientific as well as socio-political interest. Only the knowledge about regional emission structures provides a sound understanding of the regional climate gas budget and with that the estimate of varying contributions in the catchment area of the measurement site.

The derivation of such variables of a climate political dimension from the high-precision measurement time series of the climate gases on whose basis efficient emission reduction actions can be verified and adapted if necessary is anything but trivial and requires the differentiated breakdown of the measurements by their origin. The interaction of man and biosphere as emitters or absorbers in connection with the long atmospheric lifetime – especially of CO_2 – is decisive for the complexity of this task. The long lifetime of climate gases emitted once together with the interference of the anthropogenic emissions – here the burning of fossil fuels as well as land-use changes have primarily to be mentioned – and the seasonal carbon cycle of the biosphere just like natural biogeochemical cycles prevent atmospheric measurement time series of the climate gas from immediately providing information about changes of the regional emission situation (Keeling 1993).

Results and Methods

The present project gives detailed insights into the measurement time series underlying emission structures by means of origin-related examinations of the Alpine CO_2 budget. The time series of this prominent climate gas from the atmospheric measurements carried out at the four high-alpine observatories Schneefernerhaus, Jungfraujoch, Sonnblick and Plateau Rosa form the basis for the characterisation of regional CO_2 budget of the Alpine region as the focus area of the Central European study region. For the investigation area so outlined, the project identifies the source and sink regions with influence on the Alpine climate gas measurement as well as their temporal variations.

The therefore required combination of the measurements with the synoptic situation prevailing at the respective measuring time that gives the information about the origin of the analysed air masses is derived by means of a trajectory based receptor model (Carslaw & Ropkins 2012). Trajectories calculated from a measurement site backward in time give information about the transport pathways and potential source regions of the detected air masses. Backward trajectories from the dispersion and transport modelling are therefore a widespread tool for the source determination of measured trace.

The Lagrangian particle dispersion model FLEXPART developed at the Norwegian meteorological service simulates the atmospheric transport of small air volumes on the meso and large scale under consideration of diffusion, convection, turbulence as well as dry and damp deposition (Stohl et al. 2005). For dispersion modelling of pollutants, FLEXPART is operated originating from the known source forward in time. In its backward mode, however, it serves the allocation of source regions for a certain receptor. The meteorological driving fields of a numerical weather prediction model form the basis of the particle dispersion simulations and thus also its centroid tracks. Since the model of the European Centre of Medium-Range Weather Forecasts (ECMWF) has established itself as the most exact input base in the dispersion modelling for European study areas, FLEXPART is operated with the meteorological fields of the ECMWF weather prediction model. Based on these meteorological fields, ten thou-sand air volumes with the specific tracer characteristics of carbon dioxide released every two hours at the respective

receptor observatory are tracked back more than ten days. The over 17,500 ten-day particle dispersion calculations for every year of the investigation period form the basis for the source contribution studies of the climate-relevant gas together with the CO_2 concentrations measured at the respective release time. Hereto over 150,000 backward particle dispersion simulations with the Lagrangian model FLEXPART based on the ECMWF reanalysis fields are carried out at the LRZ CoolMUC-2 cluster system (> 500,000 CPU hours).

To take the restricted reliability of the dispersion modelling into account due to intrinsic model uncertainties, such as the restricted resolution of the meteorological fields and the parametrisations of the particle dispersion model itself, and to reduce these, the backward simulations of the particle dispersions are aggregated in a first step to their centroid tracks. On the assumption that the uncertainties are equally distributed, the coordinates of the centroid pathways represent the middle and thus the least erroneous transport positions of the particle tracking.

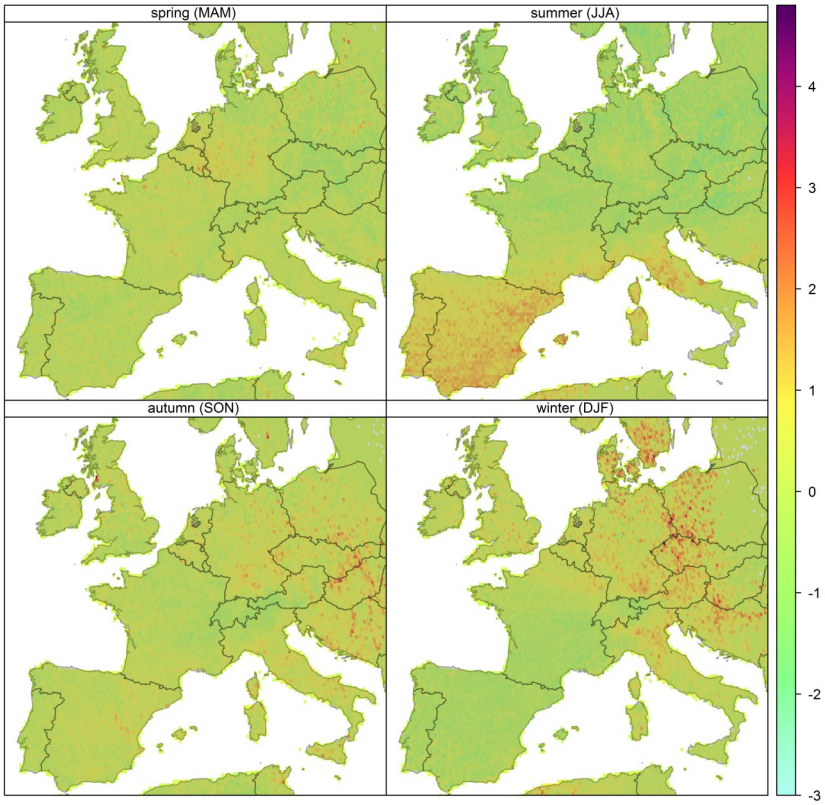

Figure 1: Concentration Weighted Trajectory fields quantifying the seasonally influence of source and sink areas to the deseasonalised and detrended CO2 concentrations (in ppm) at the high-alpine receptor sites Jungfraujoch (JFJ), Plateau Rosa (PRO), Sonnblick (SON) and Schneefernerhaus (UFS) over the entire study period 2011–2015.

The result of the cumulative consideration of the CO_2 concentrations and particle dispersion simulations of all four high-alpine observatories in the form of the concentration weighted trajectory fields locates CO_2 emitting regions all around the Central Alps with the exception of France in the west which has got out of the coal mining since the beginning of the 2000s and uses the very much CO_2-poorer nuclear power as main source of energy today. Furthermore, particularly the area around the Alpine main ridge appears as the most important large-scale CO_2 sink of Central Europe averaged over the years. Air masses originating from this central region in the midst of the study area caused a significant reduction of the CO_2 concentration levels in the measurements of the years 2011–2015 by their recording at the receptor sites.

The seasonally differentiated maps of the CO_2 contributions from the grid cells of the accumulated catchment area record a higher reliability compared to the pendant of a single receptor site and identify single emission hotspots particularly in winter reliably (see Fig. 1). In winter these are located primarily north and east of the Alps and suggest CO_2 emissions by the wood and coal firing, whereas during summer CO_2 measurements increased by two ppm on average occur mainly at air mass advection from the Mediterranean area southwest of the Alps as well as from Central Italy. The positive effect on the Alpine concentrations of carbon dioxide from the emissions of burning fossil fuels which amounts to values of up to four ppm in winter, is already ascertainable in fall —though less strong—and stems to this season from eastern European regions located further inland. Spring, however, shows hardly any strong CO_2 emission hotspots and instead displays the seasonally most homogeneous map of potential source and sink regions. Commonly to all seasons, the central study area around the Alpine main ridge is classified as a significant carbon dioxide sink whereupon the Alpine core region shows the largest negative influence on the CO_2 concentrations of Central Europe over all seasons.

The reliable project results achieved with this approach emphasise in connection with the positive results of the model-internal uncertainty assessments and external plausibility checks the validity of the model and underline in particular the strength of the model to illustrate dependably spatial-temporal variations of the relevant emitters and absorbers of CO_2 in high spatial resolution.

References and Links

[1] https://www.geo.uni-augsburg.de/lehrstuhl_professur/phygeo/projekte/klima/CO2_haushalt/
[2] Intergovernmental Panel on Climate Change (IPCC) (2013): Climate Change 2013 – The Physical Science Basis. Working Group I Contribution to the Fifth Assessment Report of the Intergovernmental Panel on Climate Change. Cambridge University Press, New York, 1552 S.
[3] Keeling C. D. (1993): Global observations of atmospheric CO_2. In: Heimann, M. (Hrg): The Global Carbon Cycle, Springer-Verlag, 1-29.
[4] Stohl A., Forster C., Frank A., Seibert P., Wotawa G. (2005): Technical note: The Lagrangian particle dispersion model FLEXPART version 6.2. Atmos. Chem. Phys., 5, 2461-2474.
[5] Carslaw D. C., Ropkins K. (2012): openair – An R package for air quality data analy-sis. Environ. Model. Softw., 27-28, 52-61.

Process-based hydrological modelling of flood events in Bavarian catchments

Research Institution
Chair of Hydrology and River Basin Management, TU Munich

Principal Investigator
Markus Disse

Researchers
Sonja Teschemacher, Matthias Kopp

Project Partners
Bayerisches Landesamt für Umwelt

Linux Cluster Project ID: pr74zo

Introduction

Hydrological models can be differentiated in conceptual models and process-based models depending on the physical basis of the implemented equations. Process-based distributed hydrological models integrate physical approximations of the hydrological processes and therefore allow a detailed spatial analysis of the related catchment response. However, the increasing number of model parameters, which can only be measured at some locations and thus have to be calibrated, lead to a large parameter uncertainty varying among the catchments.

The aim of the project *ProNaHo* is to investigate the effect of decentralized and natural flood mitigation measures on different flood events in multiple catchments [1]. The measures include small decentralized retention basins as well as land use change and soil management practices. The analyses are performed for five flood events in eight (sub)catchments of different scales, resulting in a large number of simulation runs and requiring a high degree of automation and parallelization. The focus of the project *ProMoS* is on the simulation of snow hydrologic processes in pre-alpine catchments, that often lead to large problems in runoff simulation during spring [2]. In consequence, different methods for the simulation of snow accumulation and ablation are applied in two small catchments and are evaluated in terms of performance in the spatial and temporal snow distribution. The main goal is the development of a methodology to include vegetation influences in the simulation of snow processes.

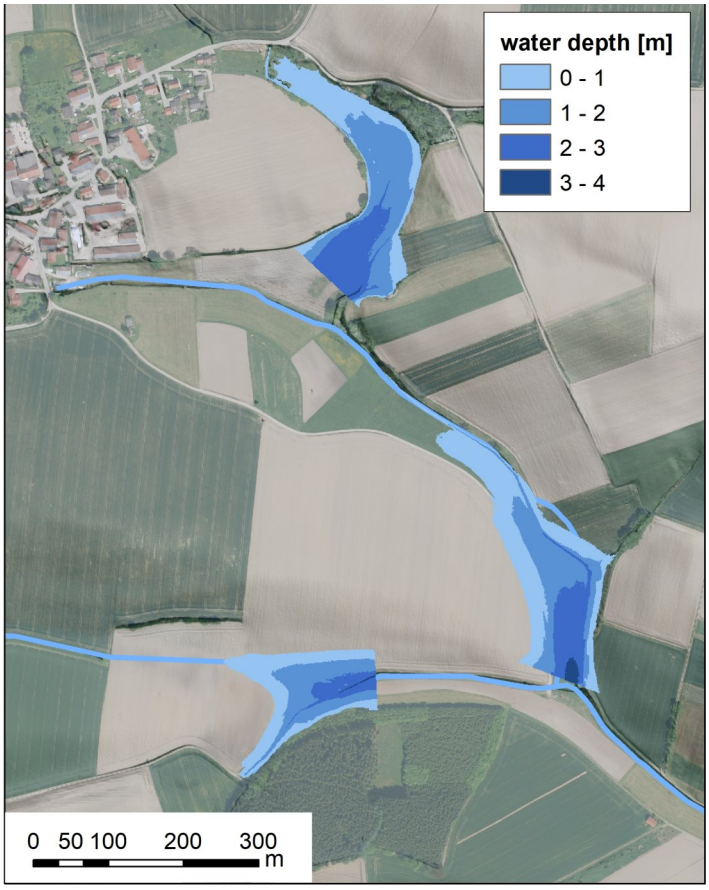

Figure 1: Location of three exemplary potential decen-tralized retention basins. The basins are situated on the brook and are dammed up by notional dams.

The simulations in both projects are performed with the physically-based and distributed hydrological water balance model *WaSiM* [3]. It was chosen due to its modular structure in which the level of detail of the single processes can be chosen depending on the catchment characteristics and the specific objective.

Results and Methods

The required resources for the jobs, which were run on CoolMUC-2, were largely dependent on the modeling purpose, the catchment, the selected spatial and temporal resolution of the model and the duration of the simulation period, i.e. single events or several model years.

After setting up the *WaSiM* models for all catchments (~30-1,200 km²), an extensive calibration process was performed including several hundreds of simulation runs per catchment. The used CPUs ranged from 28 to 224, consuming up to 800 CPU/h per calibration run. The produced output can reach up to 125 GB per run for the largest catchment.

Decentralized retention basins are restricted to a volume of 5,000 to 50,000 m³ and a maximum water height of 4 m [4]. Therefore, the detection of such

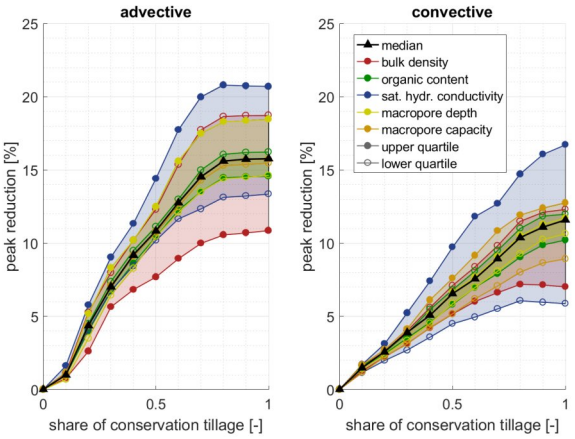

Figure 2: One-dimensional sensitivity analyses of the model parameters describing the variation of soil properties due to soil management changes for two different flood events with a return period of 20 years.

basins requires a very detailed digital elevation model (DEM) with a raster size of 1 m. The analysis of possible retention basin positions was done by performing a topographic analysis in MATLAB. Since several raster data are required for the evaluation (DEM, detailed land use map, river network, …), the analysis was separated into subcatchments to reduce the single memory demand. The detected potential retention basins (Figure 1) are included in supplementary efficiency analyses to calculate flood peak reductions.

Previous studies showed large variabilities in the peak reduction of land use and soil management strategies due to the dependency on the particular flood event, the catchment characteristics, the model structure and the selected model parameter values [5]. An extensive sensitivity analysis of several thousand runs has to be performed to quantify the uncertainties of the single parameters as well as their interaction. The analyses are performed based on single precipitation events, whereby the single simulation time is comparably low with about 20 min to 3 h using one single CPU. Therefore, a parallel execution of the *WaSiM* runs on one single node is done to get a better overall model performance. Figure 2 shows the sensitivities of the single parameters for different flood events for a continuously increasing share of conservation tillage on cropland sites for two different precipitation events (advective and convective) in the Glonn catchment. The variations strongly depend on the parameter and the flood event characteristics, highlighting the importance of a large number of simulation runs. The two events result in the same flood peak, however the advective event has a longer duration.

The calibration of the snow parameters in the small pre-alpine catchments was done with a Monte-Carlo-Simulation (n = 500). While rainfall events were reproduced in a good way, the simulation results of snow melt during rain-on-snow events and Foehn-events are inadequate. The complex interaction of different hydrological processes during these events require a more detailed and physically-based integration into the modeling framework. In consequence, new model parameters are included for which the spatial distribution can often only be estimated and thus, increase the parameter

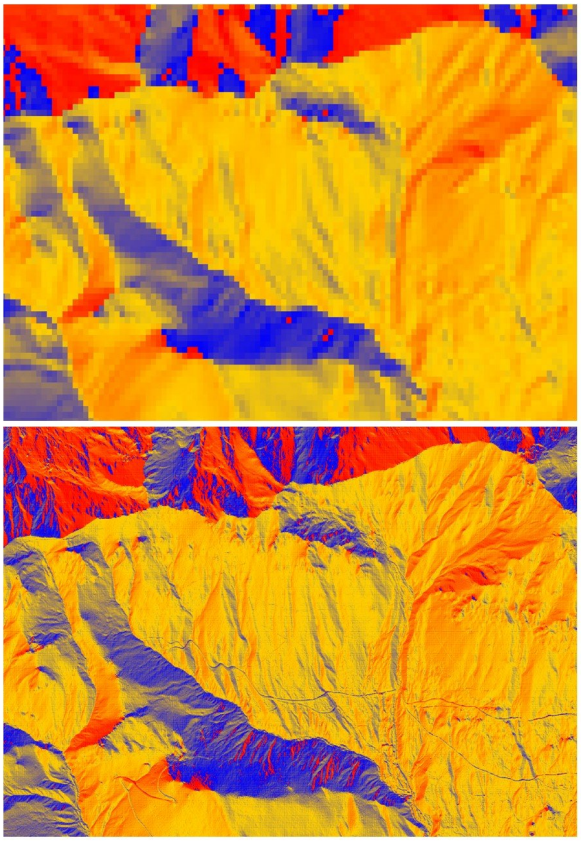

Figure 3: Map of the slope aspects of the Dreisäulerbach catchment based on digital elevation models with different raster resolutions; top: 25 m, bottom: 1 m.

uncertainties and the required number of simulation runs. Especially in steep and small pre-alpine catchments, the micro-topography plays a major role due to small flow paths, snow accumulation in depressions and a variable distribution of snow melt due to shading effects (Figure 3). The computational requirements of the selected catchments (~2 km²) is relatively low for a resolution of 25 m (~ 3,800 cells), but it largely increases for a higher resolution and smaller time steps, whereby an adequate compromise needs to be found.

On-going Research / Outlook

The simulations performed in one exemplary catchment already showed large sensitivities of the model parameters and, consequently, the range of possible efficiencies of land management changes. For more general statements, the developed methods are to be transferred to other selected catchments. Furthermore, a multi-parameter sensitivity analysis is required to gain information about the upper and lower limits of the possible efficiencies. After implementing a new method for simulating the snow accumulation and ablation by using the energy balance method including the effects of vegetation, an extensive sensitivity analysis of the additional model parameters needs to be performed to address the uncertainties.

References and Links

[1] https://www.hydrologie.bgu.tum.de/index.php?id=176&L=0
[2] https://www.hydrologie.bgu.tum.de/index.php?id=177&L=0
[3] Schulla (2017): Model Description WaSiM: Water balance Simulation Model. Zürich.
[4] DWA-M522 (2015): Kleine Talsperren und kleine Hochwasserrückhaltebecken.
[5] DWA-M550 (2015): Dezentrale Maßnahmen zur Hochwasserminderung.

High Engergy Physics

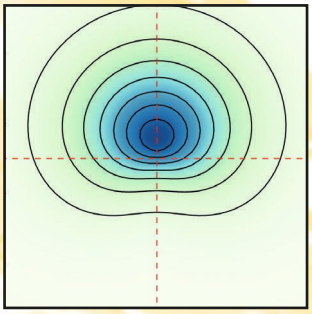

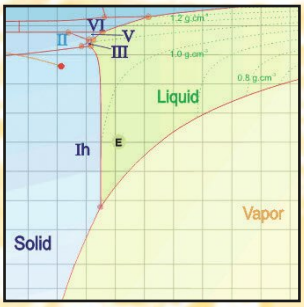

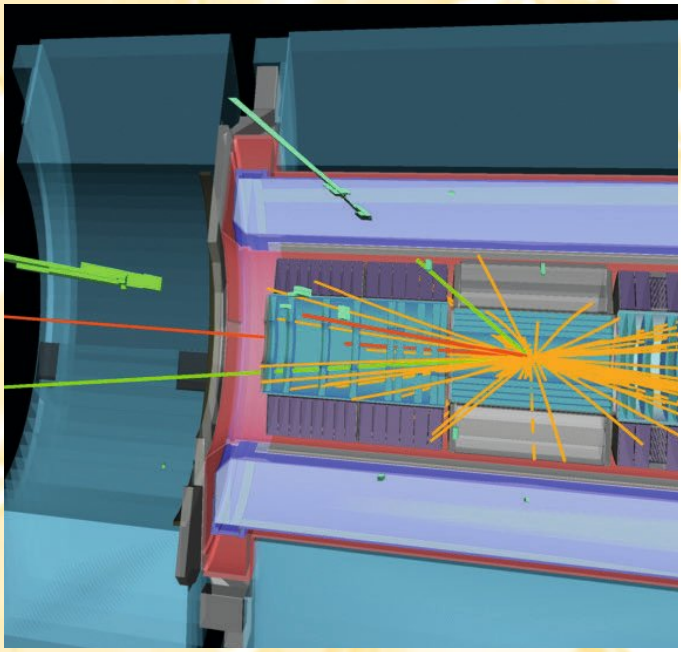

Numerical studies of anomalous transport and quantum chaos in strongly interacting gauge theories

Research Institution
Rechenzentrum der Universität Regensburg

Principal Investigator
Christoph Bauer

Researchers
Pavel Buividovich, Matthias Puhr, Semen Valgushev

5

Linux Cluster Project ID: b3101

We have used CPU time at the CoolMUC-2 cluster to study real-time dynamics and trans- port properties of strongly interacting gauge theories.

One of the studies was concerned with quantum chaos in dimensionally reduced super- symmetric gauge theory, the so-called Banks-Fischler-Stanford-Susskind (BFSS) model. Performing real-time simulations of the BFSS model on the CoolMUC-2 cluster, in the work [3] we have demonstrated the expected “scrambling” of quantum information as evidenced by the growth and eventual saturation of entanglement entropy, with saturation scale being related to the thermal von Neumann entropy. We further showed that Lyapunov exponents are in general smaller for quantum dynamics than for the classical dynamics at the same temperature/energy. We have also demonstrated that Lyapunov exponents vanish in the confining phase of the model at sufficiently slow temperatures.

Another set of simulations was concerned with anomalous transport effects in finite- density Quantum Chromodynamics (QCD). Anomalous transport phenomena originate from the chiral anomaly, a quantum effect that leads to the non-conservation of the axial charge.

In one of the projects, we have used CoolMUC-2 cluster to study numerically the Chiral Separation Effect (CSE), the generation of an axial current parallel to an external magnetic field in chiral media with finite chemical potential, in the context of quenched QCD on the lattice. While the CSE for free fermions was well understood before our study, little was known about the CSE in QCD. The main result of this work was the finding that the CSE does not get any non-perturbative corrections in both the confinement and deconfinement phases of quenched lattice QCD. For this project, we needed large amounts of computational resources and several TB of memory to store our results. The main numerical cost came from calculating matrix functions and the matrix inverse for large matrices with dimensions greater than 400,000 within the algorithm, which we have developed in [1,4]. The facilities at LRZ were essential for our study and enabled us to produce interesting results that were ultimately published in a prominent journal [2].

In another project, we have studied how anomalous transport phenomena affect the real-time dynamics of the plasma of chiral fermions, in particular demonstrating that the imbalance between left-handed and right-handed fermions in chiral plasma decays spontaneously at the expense of generating helical electric and magnetic fields [5]. To this end, we have for the first time, implemented chiral lattice fermions into real-time simulations based on the classical-statistical field theory approximation. Since the computational cost of such simulations scales as a square of lattice volume, the use of CoolMUC-2 cluster was essential to obtain results within a short time.

Acknowledgement

This work was financially supported by the S. Kowalevskaja award from the Alexander von Humboldt foundation.

References and Links

[1] M. Puhr and P. V. Buividovich, Comp.Phys.Comm. 208 (2016), 135. ArXiv: 1604.08057.
[2] M. Puhr and P. V. Buividovich. Phys. Rev. Lett. 118 (2017), 192003. ArXiv: 1611.07263.
[3] P. V. Buividovich, M. Hanada, and A. Schäfer. EPJ Web Conf. 175 (2018). Proceedings of Lattice 2017, 08006. ArXiv: 1711.05556.
[4] M. Puhr and P. V. Buividovich. PoS LATTICE2014 (2014), 047. ArXiv: 1411.0477.
[5] P. V. Buividovich and S. N. Valgushev. PoS LATTICE2016 (2016), 253. ArXiv: 1611.05294.

EPOS Simulation for ultra-relativistic ion-beam collisions

Research Institution
TUM, Physics Department, E62 institute for dense and strange matter

Researchers
Ante Bilandzic

Project Partners
ALICE Collaborations

Linux Cluster Project ID: t2321

Introduction

In modern particle physics it is mandatory to understand and describe all possible contributions in large and complex systems, like well-known Coulomb force to more arcane effects like anisotropic flow in heavy systems. With the help of modern and sophisticated Monte Carlo simulation packages, it is possible to model these complex systems and extract physical properties.

At the largest accelerator energies that are available at CERN's LHC a large amount of particles is produced and have to be tracked in the evolution of the system to the final state. These particles are then detected and reconstructed using the **A** **L**arge **I**on **C**ollider **E**xperiment (ALICE) detector setup.

The sheer number of interactions between all these particles results in a time and resource consuming theoretical calculation.

Therefore, a common desktop machine is not sufficient to meet these requirements, a clustered computing is necessary.

Results and Methods

The simulated data is being produced for the A Large Ion Collider Experiment (ALICE) detector setup. This experiment is located at the Large Hadron Collider (LHC) at CERN. Its most remarkable features are the size of 26 m length, 16 m height and 16 m wide with a weight of around 10,000 tons, as much as the weight of the Eiffel tower.

The simulation package which is used in this project is called EPOS, which stands for **E**nergy conserving quantum mechanical approach, based on **P**artons, parton ladders, strings, **O**ff-shell remnants, and **S**plitting of parton ladders.

The official description reads as follows: "EPOS is a sophisticated multiple scattering approach based on partons and Pomerons (parton ladders), with special emphasis on high parton densities. The latter aspect, particularly important in proton-nucleus or nucleus-nucleus collisions, is taken care of via an effective treatment of Pomeron-Pomeron interactions, referred to as parton ladder splitting. In addition, collective effects are introduced after separating the high density central core from the peripheral corona. EPOS is the successor of the NEXUS model." [1].

The open source framework which is used here is completely based on Linux, Bash and ROOT, and it is self-made by the researcher using the mentioned simulations package. As the framework is based on single jobs, first experiences could be made on a small local batch-farm, before migrating to the CoolMUC-2. This was necessary to get the knowledge of parallelization for these single jobs and estimate the needed resources for a large scale simulation.

A set of 250 proton-proton collisions at 7 TeV simulated with EPOS takes about 4 hours on one core. For a reasonable statistic a lower limit of 10 million events is necessary, which would result in running 18 years straight, without any parallelization.

With the help of the CoolMUC-2 85 million events have already been produced in a reasonable time. This results in a total size of 3.1 TB.

On-going Research / Outlook

Due to the positive experiences more complex system will be simulated in the future, like proton-lead or even lead-lead collisions. Here the number of contributing particles and partons increases tremendously and therefore also the resources for the simulations.

References and Links

[1] https://www.sciencedirect.com/science/article/pii/S0920563207007736

Life Sciences

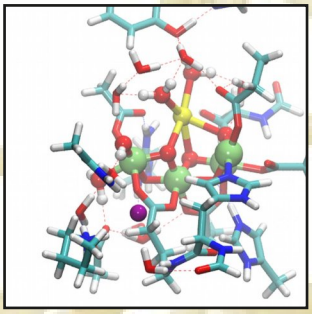

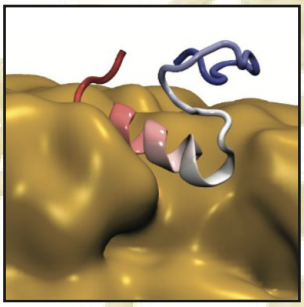

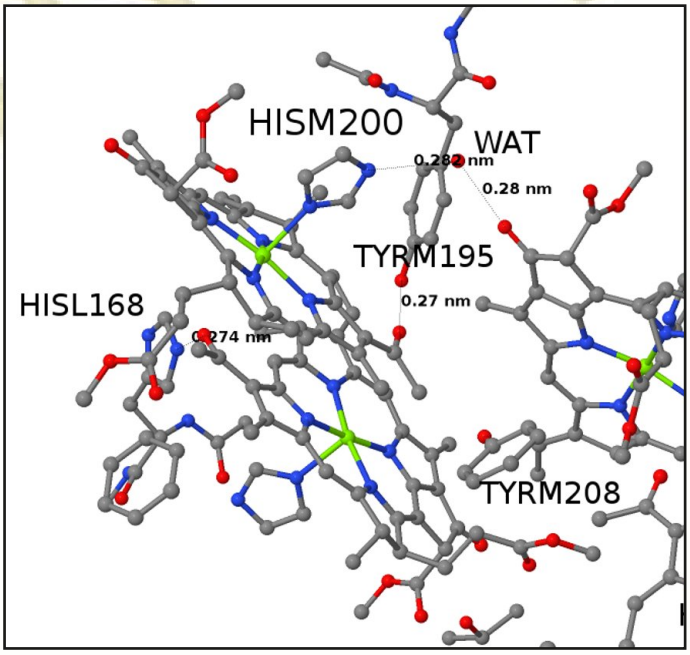

Studying protein dynamics to shed light on amyloidogenic diseases

Research Institution
Institute for Advanced Study, Technische Universität München, Garching, Germany

Principal Investigator
Carlo Camilloni

Researchers
Alexander Jussupow, Thomas Löhr

Project Partners
Program in Biophysics, Department of Chemistry, University of Michigan
Center for Integrated Protein Science Munich (CIPSM)
Department Chemie, Technische Universität München
Helmholtz Zentrum München

Linux Cluster Project ID: b1301

Introduction

The integrative structural biology lab focuses on developing and applying computational methods to provide accurate representation of biological molecules in motion [1, 2]. Protein molecules and the complex molecular machineries they build are in constant motion within their cellular environments. The biological functions of such molecules are indeed intimately dependent on their conformational dynamics. This aspect is particularly evident for disordered proteins, which constitute perhaps one-third of the human proteome. Experimental methods can only indirectly investigate the motion of biological molecules. There is no such microscope allowing us to peer into their tiny but incredibly important conformational changes. Computer simulations can show us how molecules may move, but this description is not always accurate and is limited to short time scales [3].

In this project we have first improved a recent methodology which integrates experimental information into computer models to make them as accurate as possible, and then applied this method to support the study of the interaction and interconversion of the human islet amyloid polypeptide (hIAPP) with membranes [4,5].

Membrane-assisted amyloid formation is implicated in human diseases, and many of the aggregating species accelerate amyloid formation and induce cell death. While structures of membrane-associated intermediates would provide tremendous insights into the pathology and aid in the design of compounds to potentially treat the diseases, it has not been feasible to overcome the challenges posed by the cell membrane. In this collaboration we used NMR experimental constraints to solve the structure of a hIAPP intermediate stabilized in artificial membrane nanodiscs. MD simulations helped to compare and visualize the interaction of the physiological conformation of the peptide with respect to that resulting from the interconversion preceding the amyloid formation.

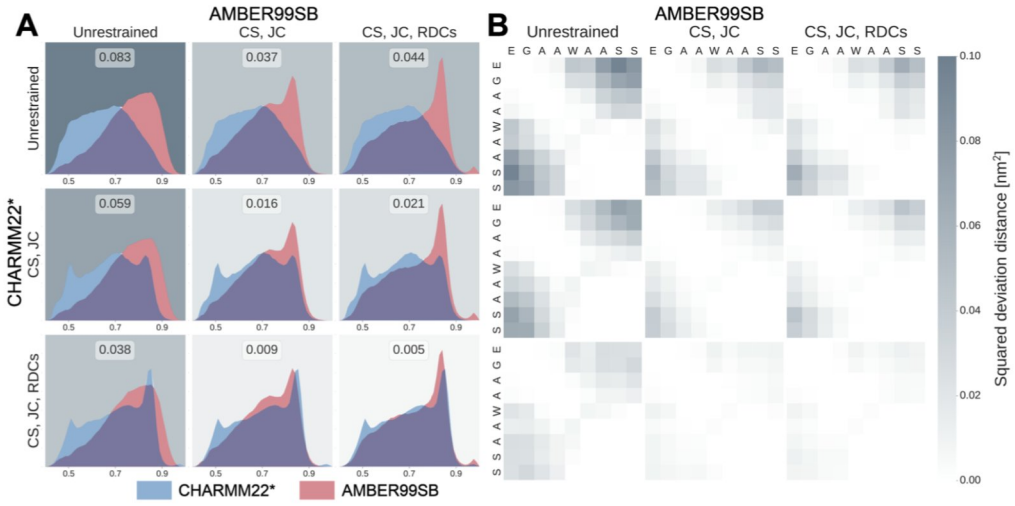

Figure 1. Convergence towards a unique dynamic. The two panels show two measures of dissimilarity. (a) The Jensen-Shannon divergence between the probability distributions of the peptide size for all pairs of simulations Transparent blue distributions represent results based on the CHARMM22*, while transparent red distributions represent results based on the AMBER99SB in TIP4P-D water. Lighter backgrounds indicate a lower divergence and thus higher similarity. (b) Squared-deviation amino-acids distance matrices between each pair of simulations. Lower distance deviations correspond to a higher degree of similarity.

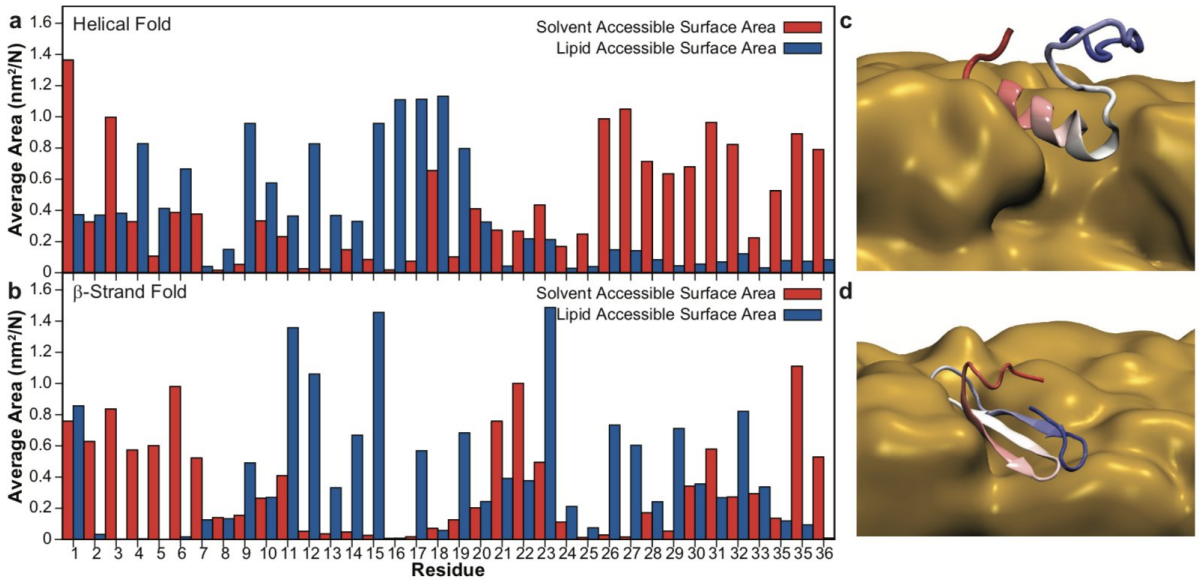

Figure 2: Electron mean free path for liquid iron alloys with 12.5 at% (Fe_7X) and 25 at% (Fe_3X) light element content for two cell volumes, near ambient pressure (left) and at conditions of the Earth's core (right), obtained by a Drude fit to optical conductivity. The mean free path approaches the Fe-Fe interatomic distance in the alloys (grey thick line) with increasing temperature, compression and impurity concentration. For Fe_3Si and Fe_3S at the smallest cell volume, the Ioffe-Regel condition is satisfied.

Results and Methods

The computational modelling of the dynamics of biological molecules is a challenging task that requires an accurate modelling as well as a thorough sampling of the system's conformational space. To address these challenges, we have recently introduced Metadynamic Metainference (M&M) which is publicly available in the Plumed. Metainference is a Bayesian framework that allows integrating multiple sources of information about a system and optimally balancing them. M&M simulations are run across in parallel multiple replicas requiring a high amount of computational resources, which superMUC can provide.

But what is the right amount of experimental data needed to make a simulation a good one? Our first goal was to study the disordered peptide EGAAWAASS making use of M&M, two state-of- the-art force fields from different families and integrated three different sources of commonly available experimental data, NMR chemical shifts (CS), 3J-couplings, and Residual Dipolar Couplings (RDCs). M&M allowed us to show that the dynamics for this peptide become robust with respect to the choice of the force field when employing these sources of data [4]. Figure 1 shows how simulations performed with different force field but the same experimental data become more and more similar the more data are employed.

To prove our point, we have run extensive MD simulations on CoolMUC-2, typically using hundreds of cores for many days guaranteeing a complete sampling of the conformational space.

Our approach has then been applied to characterize the interaction of the hIAPP peptide, whose aggregation is involved in type-II diabetes, with membranes. In this case the time scale associated with the binding process are so long with respect to what can be achieved by molecular simulations that we have make use of a simplified representation of our system. This representation, the MARTINI force field, is specialized to study protein-membrane interactions and has allowed us to characterize the interface of interaction between the physiological conformer of the protein and the nanodisc membrane environment as well as the interaction for the oligomeric intermediate state thus providing a molecular interpretation of the experimental observations [5]. In Figure 2 is shown the membrane bound state resulting from the simulations for the two conformers characterized experimentally.

On-going Research / Outlook

Thanks to CoolMUC-2 we have been able to first extend the development of new methods to perform accurate computer simulations of biomolecules. This can in principle provide faithful representations of the dynamics of these molecules in realistic environments. We have then applied our approach to shed light on the membrane driven interconversion of the hIAPP peptide from its physiological structure to a putative pathogenic intermediate. More work is going on to characterize peptides rationally designed to inhibit the formation of hIAPP amyloids fibrils. Currently we are working to expand the possibilities of M&M, so more types of experimental data can be used. In cooperation with several experimental groups at the TUM we are successfully applying this method in a wide range of biological systems: from linear polyubiquitin chains and the role they play in inflammation; to antibodies that aggregates and microRNAs recognition and processing in cell regulation.

References and Links

[1] http://www.compsb.ch.tum.de/
[2] http://sites.unimi.it/camilloni/
[3] Bonomi, M., Heller, G. T., Camilloni, C., & Vendruscolo, M. (2017). Principles of protein structural ensemble determination. Current Opinion in Structural Biology, 42, 106–116. http://doi.org/10.1016/j.sbi.2016.12.004
[4] Löhr, T., Jussupow, A., & Camilloni, C. (2017). Metadynamic metainference: Convergence towards force field independent structural ensembles of a disordered peptide. The Journal of Chemical Physics, 146(16), 165102–11. http://doi.org/10.1063/1.4981211
[5] Rodriguez Camargo, D. C., Korshavn, K. J., Jussupow, A., Raltchev, K., Goricanec, D., Fleisch, M., et al. (2017). Stabilization and structural analysis of a membrane-associated hIAPP aggregation intermediate. eLife, 6, 19. http://doi.org/10.7554/eLife.31226

Brain microstructure quantification with Bayesian inference and transient state magnetic resonance imaging

Research institution
Graduate School of BioEngineering, Technical University of Munich

Principal Investigator
Bjoern Menze

Researchers
Paula Orihuela, Pedro Gómez, Miguel Molina

Project partners
GE Global Research, Garching, Germany

Linux Cluster Project ID: pr28ve

Introduction

Historically, magnetic resonance imaging (MRI) has been a qualitative imaging technique. This means that images are created based on pixel intensities that are influenced by a several physical effects that cannot be interpreted separately. Contrary, quantitative images provide measurement of specific tissue parameters, enabling multi-study and multi-subject comparisons. However, these images require large collections of data and thus, long scanning times.

Recently, new image modalities have been proposed using the transient state of the MRI signal [1]. There are two main advantages derived from the use of the transient state: 1) since there is no need to achieve a steady state, scanning times can be significantly reduced; and 2) the MRI signal evolution in this regime depends on the tissue physical relaxation parameters (T1 and T2), which enables their estimation.

Every estimated parameter value comes with a level of uncertainty, that is not accounted in [1]. In the work implemented at the LRZ Linux cluster we introduced parameter estimation and uncertainty quantification together with transient state MRI to gain confidence on the goodness of the estimated values. To this end we used a Bayesian inference framework specifically designed for parallel computing [2].

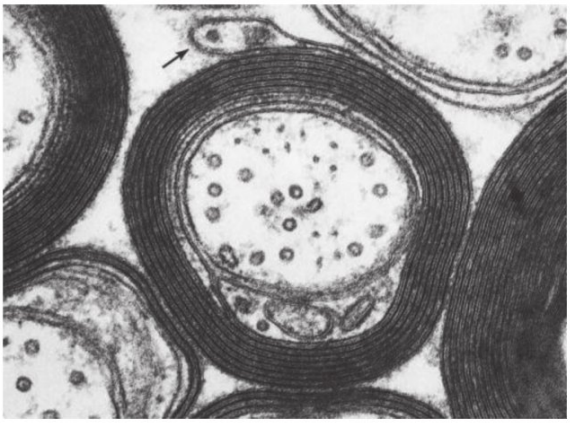

Figure 1: Electron micrograph of myelinated central nervous system axon. Reproduced from . Myelin packed in layers is shown in black surrounding the axon.

Finally, the parameter maps derived from transient state MRI are an over-simplification of reality. In fact, the brain tissue composition is more complex. One single pixel of the image contains millions of neurons, glia, and other components (Figure 1). We used a tissue model based on three different compartments: water trapped between the myelin layers; water inside and outside the axons; and cerebrospinal fluid (CSF); considering that each of them occupies a complementary volume fraction within the pixel. With

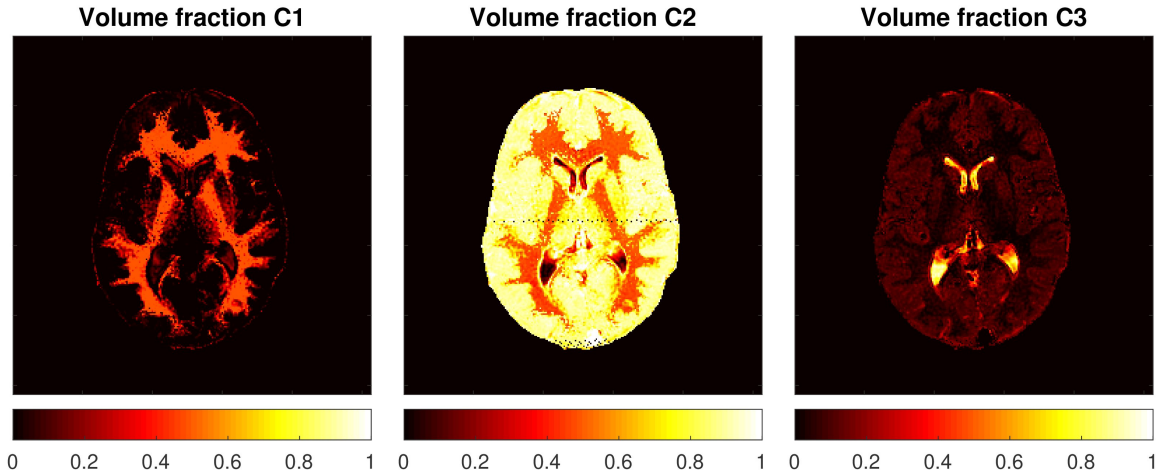

Figure 2: volume fractions of myelin water (C1), axonal water (C2), and CSF (C3). This parameters have clinical relevance since myelin volume fraction is highest in white matter as expected.

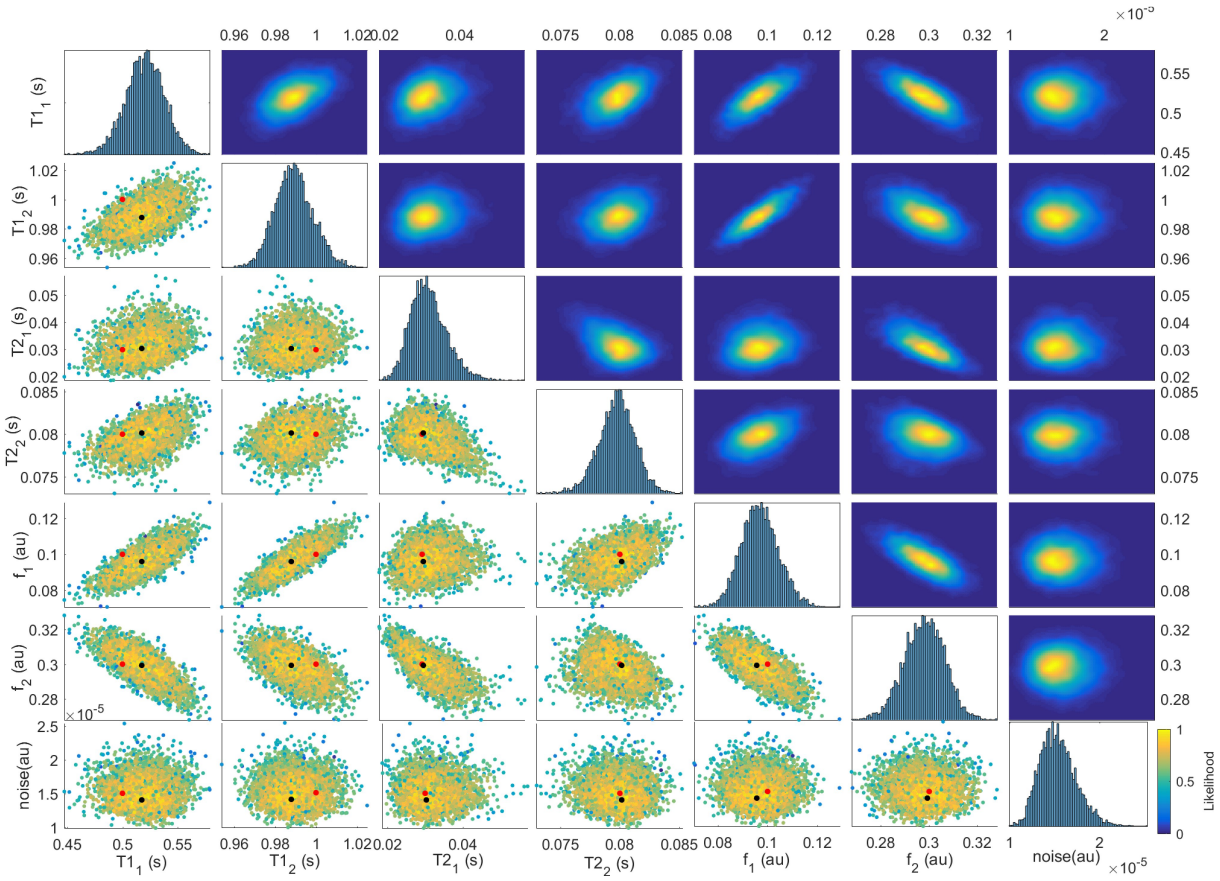

Figure 3: Parameter estimation and uncertainty quantification of the three compartments model parameters. Notice the good accuracy of the maximum-likelihood estimator (black point) regarding the ground truth (red point). The spread of the distribution of the estimations determines the uncertainty and thus, the precision of the estimated values.

this formulation we enabled the exploration of the microstructure organization beyond the image resolution.

Results and Methods

A volunteer was scanned using a transient state MRI protocol suitable for the three compartments model. This accounted for volume fractions, T1 and T2 of the c[3]ompartments mentioned before. They were inferred using a tool called π4U. This piece of software uses an hybrid approach to parallelization implemented in C combining OpenMP with MPI, enabling a hierarchy where the pixels where the first level of parallelization, reaching two more levels for the specific chains and tasks components of this method.

A single slide of the brain (Figure 2) required approximately 100 hours of computation time running in a full node (28 nodes and 64GB RAM). In average, 25MB in estimations were generated for each voxel. They were stored in SCRATCH summing up to 1.2TB.

The uncertainty quantification of the parameter estimations of our three compartments model for a single pixel are shown in Figure 3. One can interpret the accuracy and precision of the estimation in the following way. The closer the black and red points are, the better is the accuracy; and the lower is the spread of points across the space, the better is the precision. For each voxel in Figure 2, one can depict a representation like in Figure 3, to assess precision or uncertainty, but not accuracy, that can only be assessed through simulations.

On-going Research / Outlook

We have shown that sub-pixel information can be extracted from the transient state MRI signal, using the right model and the right tools. This is especially relevant to assess the impact of diseases like multiple sclerosis, that creates lesions in the white matter where the myelin volume fraction is reduced. Also, patients suffering from glioblastoma may profit from a quantification of the edema (CSF-like), that accumulates in the surroundings the tumor mass.

Although we have proven the feasibility and potential of this project. We are working on correcting some biases that we have identified in the estimations of the parameters. Moreover, we plan to extend the application space beyond brain, to reach other biological samples that will benefit from uncertainty quantification, and microstructural modeling.

References and Links

[1] D. Ma, V. Gulani, N. Seiberlich, K. Liu, J. L. Sunshine, J. L. Duerk, and M. A. Griswold, “Magnetic resonance fingerprinting.,” Nature, vol. 495, no. 7440, pp. 187–92, 2013.

[2] P. E. Hadjidoukas, P. Angelikopoulos, C. Papadimitriou, and P. Koumoutsakos, “Π4U: A high performance computing framework for Bayesian uncertainty quantification of complex models,” J. Comput. Phys., vol. 284, pp. 1–21, Mar. 2015.

[3] G. Siegel, B. Agranoff, and R. Albers, Basic Neurochemistry: Molecular, Cellular and Medical Aspects., 6th editio. 1999.

Statistical learning with (high-dimensional) biomedical data

Research institution
Institut für Medizinische Informationsverarbeitung, Biometrie und Epidemiologie, Arbeitsgruppe “Biometrie mit Schwerpunkt Molekulare Medizin”

Principal Investigator
Anne-Laure Boulesteix

Researchers
Riccardo De Bin, Silke Janitza, Roman Hornung, Heidi Seibold, Philipp Probst

Linux Cluster Project ID: pr87fi, pr74di

Introduction

In the context of the two LRZ projects pr87fi and pr74di, the Working Group „Biometry in Molecular Medicine“ (until Dec 2017: “Computational Molecular Medicine”) headed by Anne-Laure Boulesteix investigated and developed statistical learning methods at the interface between applied statistics, machine learning and biomedical applications.

Results and Methods

From a methodological point of view, the focus was on the following topics:

- the random forest algorithm for classification and regression;
- the boosting algorithm for classification, regression and survival analysis;
- the choice of tuning parameters for statistical learning algorithms (including but not limited to random forest and boosting);
- the design and analysis of benchmarking experiments.

For all these research topics, high-dimensional molecular data (“omics” data) are an important field of application. However, all methods can also be applied to other types of data.

This research was funded by the German Research Foundation (DFG) through individual grants to the PI Anne-Laure Boulesteix (BO3139/2-2, BO3139/2-3, BO3139/6-1, BO3139/4-1, BO3139/4-2). The group submitted and successfully published a number of papers on these topics. Some of them are briefly summarized in the following.

Probst et al. (2018a)
We developed a general framework and definitions regarding the tunability of a supervised learning algorithm (i.e. its capacity to yield – through appropriate parameter tuning - a performance better than the performance with default parameters). We also defined the tunability of specific parameters: this concept may be useful for users of the algorithms who want to know which parameters they should tune and which ones they can safely set to the default values (for example in cases where it is computationally intractable to tune all parameters). In this framework, we also addressed the choice of tuning ranges, i.e. intervals of the parameters that should be considered as candidate values for tuning. After defining these concepts from a theoretical point of view at the beginning of the paper, we present an estimation strategy to be applied when a large number of real datasets are available for benchmarking. The whole procedure is then illustrated through an application to six common supervised learning algorithms based on a large collection of 38 datasets from the OpenML database. The paper is available as a technical report and will be submitted in the next weeks.

Probst et al. (2018b)
In this project we focused on the special case of random forests. After an extensive but somewhat disappointing literature search on the choice of parameters of RF (disappointing in the sense that clear guidance is missing), we addressed this choice as a tuning problem that can be solved with modern tuning strategies. More precisely, we present a new R package for automatic tuning of RF as implemented in the R package ‘ranger’ using model-based optimization. The main result is that tuning can yield a slight performance improvement, but that RF is less tunable than most other algorithms investigated in Probst et al. (2018a). This paper is also submitted for publication and available as a technical report.

Probst & Boulesteix (2018)
In this project we focused our attention to the number of trees included in a random forest. In the literature, this parameter is sometimes considered as a tuning parameter that has to be carefully optimized, while other authors recommend simply setting it to the highest computationally feasible value. We investigated this problem systematically both from a theoretical point of view (by mathematically deriving

the expected error curve as a function of the number of trees for different performance measures) and from an empirically point of view (through a large scale benchmark study considering a much higher number of datasets than ever done in the literature in this context). The main result recommends setting the number of trees to a computationally feasible large number as long as classical error measures based on average loss are considered.

De Bin (2016)
Another project aimed at comparing and further developing two of the most widely used boosting regression techniques, model-based boosting (implemented in the package 'mboost') and likelihood-based boosting (implemented in the packages 'GAMBoost' and 'CoxBoost', the latter devoted to survival analysis). In addition to a more general comparison, the project focused on the handling of mandatory variables, i.e. variables that for a number of reasons must be included in a model, as is often the case for the clinical variables in clinical-omics combined model. In particular the study investigated the strategies implemented in the aforementioned R packages and showed how to modify the algorithms to explore different solutions for both the model-based and the likelihood-based boosting.

Seibold et al. (2017)
We investigated the influence of the resampling technique on model selection in the case of boosting regression techniques (keeping in mind that these results are largely valid for other methods). In biomedical research, boosting-based regression approaches have gained much attention in the last decade. Their prediction performance, however, highly depends on specific tuning parameters, particularly on the number of boosting iterations to perform. This crucial parameter is usually selected via cross-validation (CV). The CV procedure may highly depend on a random component, namely the considered fold partition. We empirically studied how much this randomness affects the results of boosting techniques for different CV types.

Janitza et al. (2016a)
This paper introduces a new computationally fast heuristic procedure for testing variable importances in the context of random forest based prediction. It is appropriate for high-dimensional data where many variables do not carry any information.

Couronné et al. (2017)
We conducted a large scale benchmark study using several hundreds of real datasets from the database OpenML and following good practice recommendations for benchmarking to compare the performances of logistic regression and random forest for binary classification. Most importantly, special attention was devoted to the effect of the datasets' characteristics. In particular, we performed extensive subgroup analyses, where the term "subgroup" refers to subgroups of datasets satisfying particular conditions. This paper is submitted for publication.

Hornung (2017)
In this paper, the ordinal forest method is introduced, a random forest based prediction method for ordinal response variables. Ordinal forests allow prediction using both low-dimensional and high-dimensional covariate data and can additionally be used to rank covariates with respect to their importance for prediction. This paper is submitted for publication.

Janitza et al. (2016b)
This paper presents a novel variable importance measure to assess predictor variables when the response variable is ordinal. In contrast to the ordinal forests presented in Hornung (2017), this variable importance measure is based on the standard random forest algorithm.

On-going Research / Outlook

Our current projects deal (among others) with:

- the development of improved variants of random forest, in particular to handle omics data
- the development and comparison of prediction methods to be used with omics predictors of multiple types
- the design of benchmarking experiments
- the quantification of the uncertainty due the choice of the analytical mode

References and Links

[1] P. Probst, B. Bischl, A.-L. Boulesteix, 2018a. Tunability: importance of hyperparameters of machine learning algorithmus. https://arxiv.org/abs/1802.09596.
[2] P. Probst, M. Wright, A.-L. Boulesteix, 2018b. Hyperparameters and tuning strategies for random forest. https://arxiv.org/abs/1804.03515.
[3] P. Probst, A.-L. Boulesteix, 2018. To tune or not to tune the number of trees in random forest? Journal of Machine Learning Research (accepted).
[4] R. De Bin, 2016. Boosting in Cox regression: a comparison between the likelihood-based and the model-based approaches with focus on the R-packages CoxBoost and mboost. Computational Statistics 31:513-531.
[5] H. Seibold, A.-L. Boulesteix, R. De Bin, 2017. On the choice and influence of the number of boosting steps for high-dimensional linear Cox-models. DOI: 10.1007/s00180-017-0773-8
[6] S. Janitza, E. Celik, A.-L. Boulesteix, 2016a. A computationally fast variable importance test for random forests for high-dimensional data. Advances in Data Analysis and Classification doi:10.1007/s11634-016-0270-x.
[7] R. Couronne, P. Probst, A.-L. Boulesteix, 2017. Random forest versus logistic regression: a large-scale benchmark experiment. Technical Report 205, Department of Statistics, LMU (submitted).
[8] R. Hornung, 2017 Ordinal Forests. Technical Report 212, Department of Statistics, LMU (submitted)
[9] S. Janitza, G. Tutz, A.-L. Boulesteix, 2016b. Random forest for ordinal response data: prediction and variable selection. Computational Statistics & Data Analysis 96:57-73.

Computational Biochemistry – A Molecular Microscope into the Biological World

Research Institution
Technical University of Munich

Principal Investigator
Ville R. I. Kaila

Researchers
Mona Baumgart, Ina Bisha, Andrea Di Luca, David Fischermeier, Ana P. Gamiz-Hernandez, Mikael P. Johansson, Alexander Jussupow, Sophie L. Mader, Max E. Mühlbauer, Mikko Muuronen, Daniel Riepl, Michael Röpke, Tapio Salminen, Patricia Saura, Shreyas Supekar

Linux Cluster Project ID: pr83ro

Introduction

Our research is focused on understanding molecular principles of enzyme function. Enzymes are biocatalysts that enable chemical reactions, by lowering the activation barrier for a chemical transformation. We are particularly interested in enzymes involved in biological energy conversion, i.e., enzymes that capture chemical or light energy, and transform this into other energy forms. Our recent LRZ-projects have focused on respiratory and photosynthetic enzymes, but also on artificial catalysts that mimic the function of natural enzymes. To address the function of the complex biochemical systems, we develop and apply computational multi-scale methods that range from ab initio quantum chemical techniques, hybrid quantum mechanics/ classical mechanics (QM/MM) to large-scale classical molecular dynamics simulations, as well as free-energy and continuum approaches (Figure 1). This allows us to probe the structure, dynamics, and energetics, on fs- µs timescales for systems comprising millions of atoms. Methods of computational biochemistry provide complementary information to many experimental techniques, and therefore offer powerful tools to probe mechanistic hypotheses at a molecular level. Our research aims to establish a fundamental understanding of nature's toolbox of catalytic elements, to elucidate how complex biochemical environments contribute to the catalytic effects, and ultimately to provide blueprints that can guide the design of man-made enzymes. The report describes our general research direction on LRZ Linux-Cluster during 2016-2017.

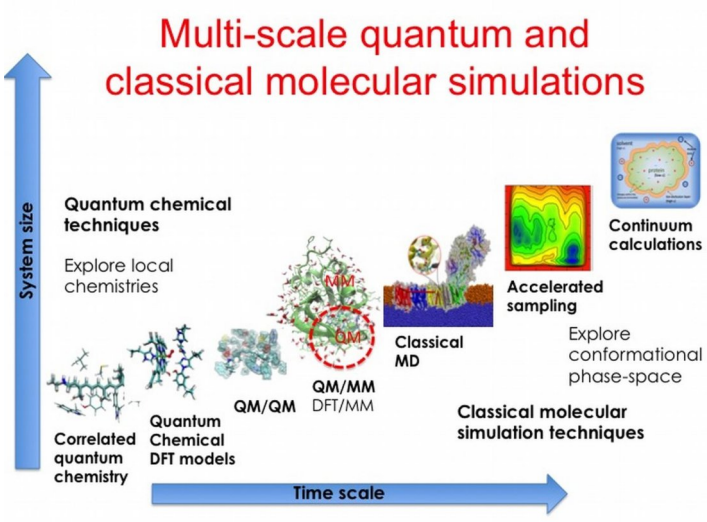

Figure 1: Multi-scale molecular simulations provide powerful techniques to address the structure, energetics, and dynamics of biomolecular systems on a broad range of time-scales and spatial resolutions. We develop and employ correlated QM-methods and DFT to explore local chemistries that we combine by QM/MM methods to classical molecular simulations techniques, which provide efficient ways to study the conformational phase-space of the molecules.

Results and Methods

In recent years, we have employed the LRZ-HPC Cluster to obtain a mechanistic understanding on how the molecular structure and dynamics are linked together with the biological function. Below we briefly describe our project related to enzyme catalysis and photobiological systems.

1. Molecular Mechanism in Enzyme catalysis
Energy conversion in nature is driven by enzymes that catalyze coupled transfer of protons and electrons or PCET-reactions. Two main PCET pathways establish the molecular basis of all life forms: the light-driven PCET of photosynthesis and the chemically driven PCET of respiratory chains. In recent years, we have focused on understanding the catalytic machinery of the redox-driven proton pumps cytochrome c oxidase and complex I that are central proteins in mitochondria, the power plants of our cells, as well as photosystem II, that captures sunlight and employs this to split and oxidize water into dioxygen, which is further released into the atmosphere (Figure 2). Computational treatment of these systems is challenging; these molecules are large membrane proteins with complex metal centers that are responsible for the chemical transformation processes. The system sizes range up to millions of atoms with active sites comprising several hundreds of atoms. To this end, we study the conformational dynamics of the systems using atomistic MD simulations, free-energy calculations and Poisson-Boltzmann continuum electrostatic calculations, whereas the PCET reactions in the metal-centers are modeled at density functional theory-level, often with hybrid QM/MM-methods. Although the studied proteins have very different

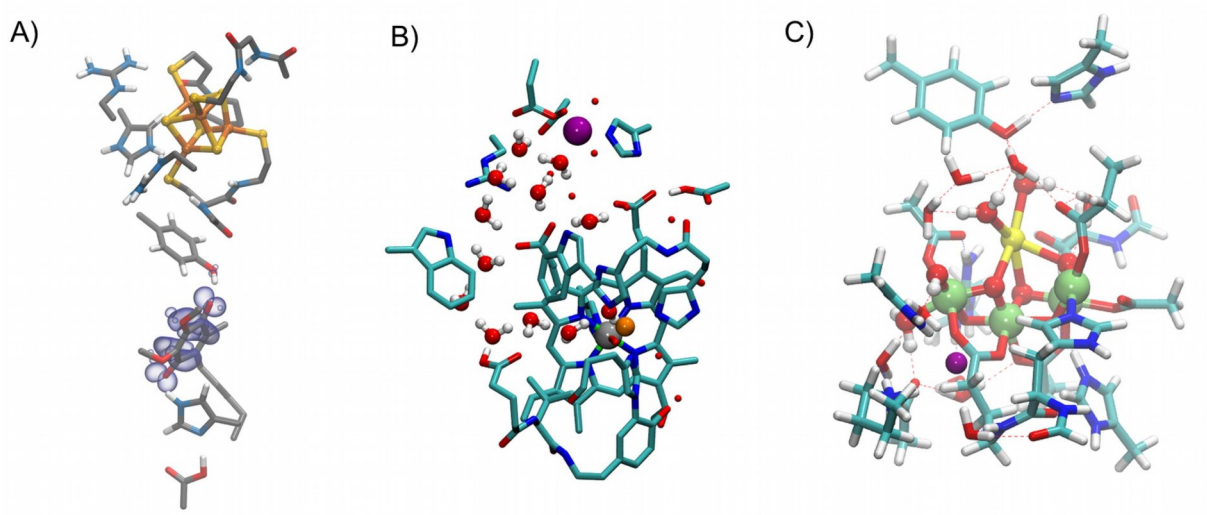

Figure 2: A) the active site of complex I with an iron-sulfur center and protein residues that catalyze quinone reduction; B) The active site of cytochrome c oxidase with a coupled heme-copper center that catalyzes oxygen reduction to water; C) The calcium-oxo-manganese center of photosystem II that catalyzes oxidation and splitting of water. All active centers were modeled at quantum chemical DFT-level.

molecular architectures, our computational work predicts that they nevertheless employ similar mechanistic principles, where the redox- or protonation changes trigger coupled electrostatic-, conformational-, and hydration-changes that establish the biological function (see references for central publications).

2. Computational Photobiology

As an important step towards understanding light-driven energy conversion, we study how different biological environments affect light-capturing properties of molecules by imposing electrostatic, mechanical strain, and/or polarization effects on the biochromophores. To computationally treat such effects, we have developed lower-order correlated quantum chemical methods (i.e. CC2 and ADC(2)) in combination with virtual space screening (RVS) approaches that allow us to perform accurate calculations for large biomolecular systems with several hundreds of atoms in combination with QM/MM methodologies. We have studied light-capturing mechanisms in natural and engineered retinal-proteins, type I- and II-photosystems, the lobster protein crustacyanin, and the photoactive yellow protein. Our work was also focused on characterizing how optical properties of light-driven ion-pumps are modulated by conformational changes in the protein structure, which we explored by large-scale classical simulations (see references for central publications). Our current work on photobiological systems is focused on the treatment of excited state dynamics in explicit surroundings by further developing QM/MM methodologies.

On-going Research / Outlook

The HPC offered by LRZ played a crucial role in the realization of our research projects by offering unique resources that enabled our simulations. The data produced on the LRZ cluster provided a starting point for our publications (see References). Our future and ongoing work is focused on deriving general mechanistic principles from the natural systems for the design of new artificial proteins.

References and Links

[1] http://villekaila.wordpress.com/
[2] Supekar S, Gamiz-Hernandez AP, Kaila VRI (2016) A Protonated Water Cluster as a Transient Proton Loading Site in Cytochrome c Oxidase. Angew Chemie Intl Ed 55:11940-11944.
[3] Ugur I, Rutherford AW, Kaila VRI (2016) Redox-coupled substrate water reorganization in the active site of Photosystem II. Biochim Biophys Acta – Bioenergetics 1857:740-748.
[4] Di Luca A, Gamiz-Hernandez AP, Kaila VRI (2017) Symmetry related proton transfer pathways in respiratory Complex I. Proc Natl Acad Sci USA 114:E6314-E6321.
[5] Fedor J, Di Luca A, Kaila VRI, Hirst J (2017) Correlating kinetic and structural data on ubiquinone binding and reduction by respiratory complex I. Proc Natl Acad Sci USA 114: 12737-12742.
[6] Gamiz-Hernandez AP, Jussupow A, Johansson MP, Kaila VRI (2017) Terminal Electron-Proton Transfer Dynamics coupled to Quinone reduction in Respiratory Complex I. J Am Chem Soc 139:16282-16288.
[7] Zhang Q, Catti L, Kaila VRI, Tiefenbacher K (2016) To Catalyze or not to Catalyze: Elucidation of the Subtle Differences between the Hexameric Capsules of Pyrogallolarene and Resorcinarene. Chem Sci 8:1653-1657.
[8] Suomivuori C-M, Lang L, Sundholm D, Gamiz-Hernandez AP, Kaila VRI (2016) Tuning the protein-induced absorption shifts of retinal in engineered rhodopsin mimics. Chem – Eur J. 22:8254-8861.
[9] Gamiz-Hernandez AP, Kaila VRI (2016) Conversion of light-energy into molecular strain in the photocycle of the photoactive yellow protein. Phys Chem Chem Phys. 18:2802-2209.
[10] Suomivuori C-M, Winter NOC, Hättig C, Sundholm D, Kaila VRI (2016) Exploring the Light-Capturing Properties of Photosynthetic Chlorophyll Clusters Using Large-Scale Correlated Calculations. J Chem Theory Comput 12:2644-2651.
[11] Suomivuori C-M, Gamiz-Hernandez AP, Sundholm D, Kaila VRI (2017) Energetics and dynamics of a light-driven sodium-pumping rhodopsin. Proc Natl Acad Sci USA 114:7043-7048.
[12] Luo Q, Boczek EE, Buchner J, Kaila VRI (2017) Conformational activation and Hsp90-dependence of c-Src and its oncogenic mutants. Sci Rep 7:43996.
[13] Wittwer M, Luo Q, Kaila VRI, Dames S (2016) Oxidative Unfolding of the Rubredoxin Domain and the Natively Disordered N-terminal Region Regulate the Catalytic Activity of M. tuberculosis Protein Kinase G. J Mol Biol 291:27062-27072.
[14] Supekar S, Papageorgiou AC, Gemmecker G, Peltzer R, Johansson MP, Tripsianes K, Sattler M, Kaila VRI (2017) Conformational Selection of Dimethylarginine Recognition by the SMN Tudor Domain. Angew Chemie. 57:486-490.

Proton Coupled Electron Transfer in the Reaction Center of Bacterial Photosynthesis

Research Institution
Physikdepartment der TU München

Principal Investigator
Sighart F. Fischer, EOE

Researchers
Philip O.J. Scherer

Linux Cluster Project ID: pr74ga, t2101

Introduction

Photosynthetic reaction centers perform light induced charge separation over a membrane with a high quantum yield of 95%. Since the structure of the membrane complex of the bacterial reaction center of Rps. viridis has been resolved, by Michel, Deisenhofer and Huber (Nobel prize 1985), it became a great challenge to resolve the observed dynamics on the basis of the structure information. The ongoing research in the field is motivated by the hope to learn from nature, how to improve the efficiency of artificial solar cells.

Even though it is possible to simulate the time dependence of many reaction centers including mutants within the frame of the step models or the superexchange model, there are fundamental shortcomings. Alternatively [1], we consider the adiabatic evolution of the state mixing driven by low frequency librational modes, which affect the hydrogen bonds over long distances. This approach incorporates specific structure properties of the dimer such as the C_2-symmetry and its dynamic breakage (see Fig. 1).

Results and Methods

We used the GAMESS [2] program package to perform quantum calculations on the HF and TDHF level, mostly with the 631G basis set. The TDHF method provided spectra (see Fig.2) which agree much better with experimental data than corresponding TDDFT calculations .

TDHF calculations on the full model (hexamer) required too much memory. Some calculations could be done within a test project on SUPERMUC . Most calculations were done on CoolMUC-2 for reduced models consisting of two to four of the chromophores. Calculations were limited by waiting times of typically one week and temporary problems with the scratch file system. So far we performed about 500 calculations. To obtain the maximum possible memory, only two tasks were used on each node, one for computation and one for data serving. Typically a job used 32 nodes and 7500 Mwords of memory as well as 1 to 20 Gbyte temporary disk space on each node. Wall time for one single point calculation was typically 1 day.

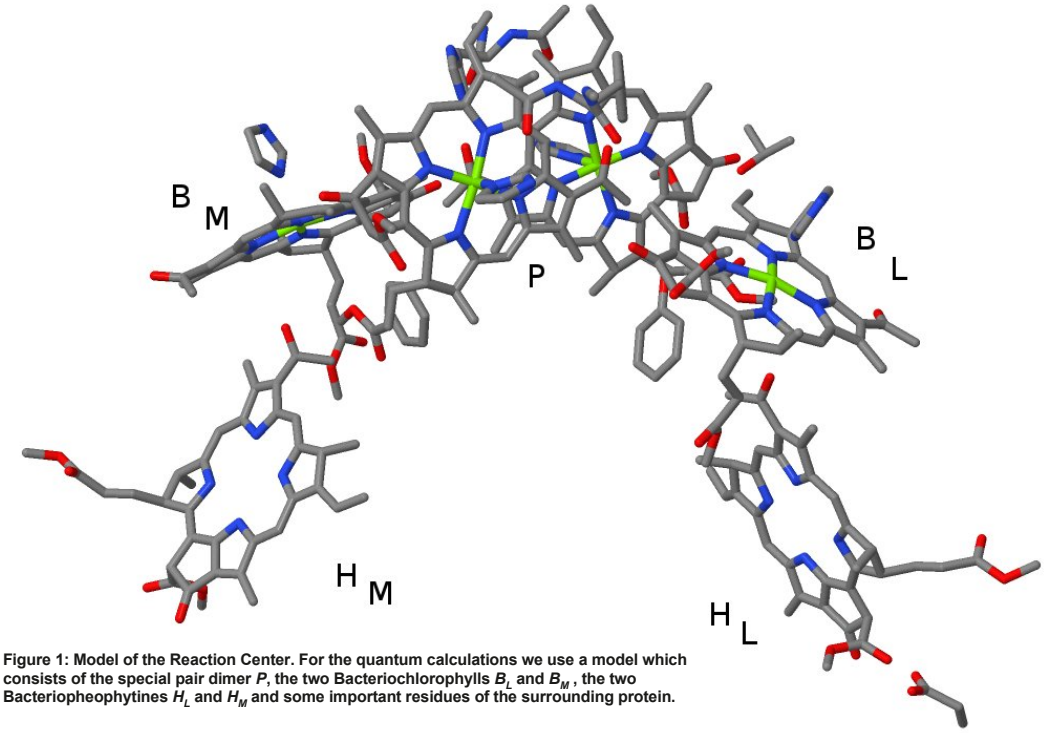

Figure 1: Model of the Reaction Center. For the quantum calculations we use a model which consists of the special pair dimer *P*, the two Bacteriochlorophylls B_L and B_M , the two Bacteriopheophytines H_L and H_M and some important residues of the surrounding protein.

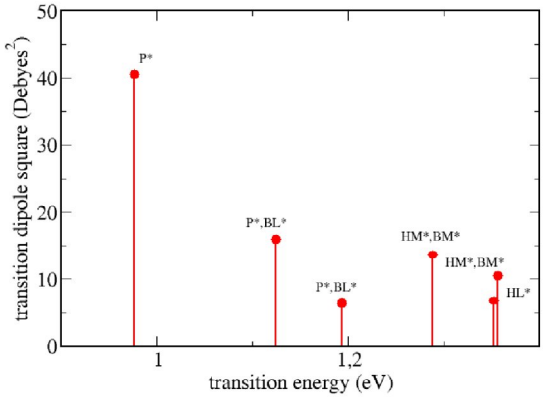

Figure 2: Calculated absorption spectrum of the reaction center model (Fig. 1).

The analysis of the eigenstates provides evidence for hole transfer via the excitonically coupled P^* and B_L^* states. We simulate the dynamics in the P^* state by the application of an electric field, which shifts the P+B_L-state in the energetic regime of the B_L^* state. The field mimics that way the high polarizability of the P^* state, which shows up in the Stark spectrum of the dimer. Apart from a proper field modulation we search for a reaction coordinate by varying hydrogen positions involved in H-bonding (Fig. 3), capable to lower the energy of the P+B_L-state in the presence of the P^* state. The participation in the proton dynamics is also documented by mutation and modifications of the structure.

On-going Research / Outlook

CoolMUC-2 gave us the possibility to perform a larger number of quantum calculations which need large amounts of memory but also much computing time. Due to the long waiting times and problems with the temporary file system we could not yet perform enough calculations to identify the relevant coordinates uniquely but we obtained a deeper insight into the spectral changes due to proton movements. We will continue this project and hope to interpret the recent experimental investigations on coherent oscillations with a refined model [1]. If possible, we will also make use of the new CoolMUC-3 system which provides even more memory but for the cost of longer computation time. So far problems with the temporary file system made GAMESS calculations impossible.

References and Links

[1] Philipp O.J. Scherer, Sighart F. Fischer, Theoretical Molecular Biophysics, 2nd edition, Springer Verlag 2017, chapter 28
[2] M.W.Schmidt, K.K.Baldridge, J.A.Boatz, S.T.Elbert, M.S.Gordon, J.J.Jensen, S.Koseki, N.Matsunaga, K.A.Nguyen, S.Su, T.L.Windus, M.Dupuis, J.A.Montgomery J.Comput.Chem. 14, 1347 (1993)

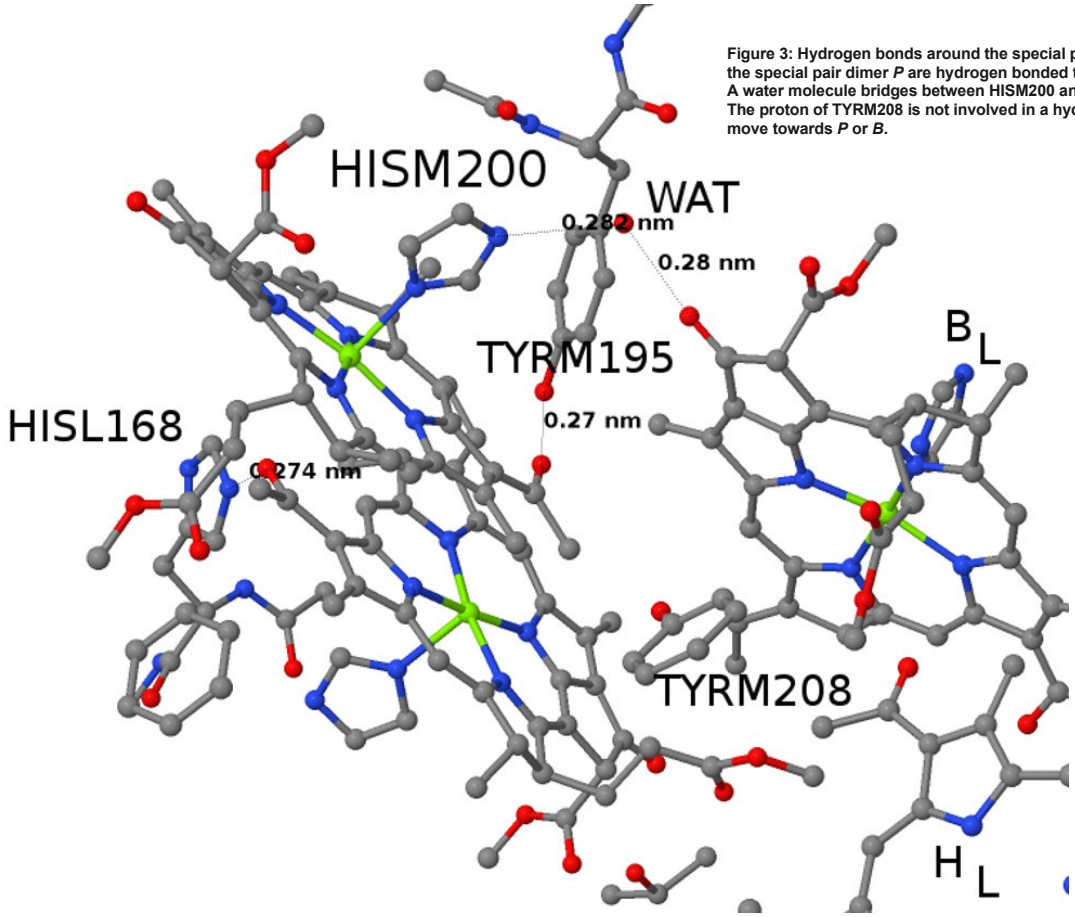

Figure 3: Hydrogen bonds around the special pair. The acetyl oxygens of the special pair dimer *P* are hydrogen bonded to HISL168 and TYRM195. A water molecule bridges between HISM200 and Bacteriochlorophyll B_L. The proton of TYRM208 is not involved in a hydrogen bond and can move towards *P* or *B*.

Comparative genomics and phylogenomics of non-bilaterian animals

Research Institution
Paleontology & Geobiology, Department of Earth and Environmental Sciences, LMU München

Principal Investigator
Gert Wörheide

Researchers
Sergio Vargas, Michael Eitel

Linux Cluster Project ID: uk213

Introduction

Comparative genomics and phylogenomics of early animals, i.e., the non-bilaterian phyla Porifera (sponges), Ctenophora (comb jellies), Cnidaria (jellyfish, corals), Placozoa (no common name), and their relationships to the Bilateria, to which we and the majority of all other animals belong, are important fields in evolutionary (geo)biology and one of the foci of our research [5]. Comparative genomics and phylogenomics utilize the ever increasing "big genome data", aiming to further our understanding about the (early) evolution of animals and their key traits, such as muscles, nervous systems, body axes, the gut, and visual systems. The basic foundation for such analyses is a well resolved phylogeny that displays the relationships among those five taxa. The current debate centers around two opposing scenarios: 1) the "Porifera-sister" hypothesis, where sponges are the sister group to all other animals (the classical scenario already derived from comparative morphology) and 2) the "Ctenophora-sister" hypothesis, where the comb jellies have this position instead. Both hypotheses have profound implications for our understanding of early animal evolution, but no consensus has been reached yet about those relationships. However, sponges are one of the best candidates for the sister group to all other animals and are, therefore, pivotal to early animal evolution research. In our research we address questions about early animal relationships, their genome architecture and evolution, as well as the interaction with their prokaryotic symbionts.

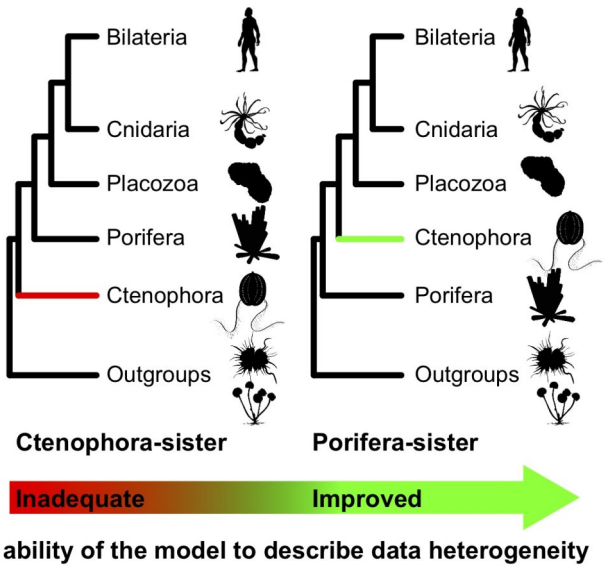

Figure 1: Changes in animal tree topology if the ability of the model to describe data heterogeneity is improved. From [1].

Results and Methods

To date, a limited number of genomes from non-model animals have been sequenced. From the (most likely) earliest branching animal lineage, the sponges, only three genomes have been published so far. Although these genomes have provided some first insights into the ancestral animal genome architecture and gene content, additional genomes from a diverse taxonomic range are urgently needed to understand genome and body trait evolution at the dawn of animals. One particular interest is to understand the diversification of gene families, since initial results indicate large-scale independent gene family expansions in sponges that are likely the basis for the variety of different bauplans we see in (modern) sponges. To enlarge the set of available genomic data for comparative genomics analyses, we assembled multiple genomes and transcriptomes of sponges and other non-bilaterians using large amounts of Illumina and Oxford Nanopore sequencing data. To generate the best possible assemblies we used genome assemblers such as SPAdes, CANU, bwise, among others, as well as the gold standard transcriptome assembler Trinity. So far we have assembled three sponge and one placozoan genome as well as dozens of transcriptomes from all four non-bilaterian phyla. These data are used for comparative genomics at various levels [2]: Genome synteny analyses, comparative gene family-, as well as phylogenomic (multi-gene amino acid gene alignments) analyses. Assemblies typically ran on 1-4 nodes (28-112 cores). Storage consumption depended on the amount of available date and ranged between a few and several hundred GB per analyses. The amount of files produced varied with programs. Some generated hundreds of temporary files (high I/O) while other generated a few, but large files (sometimes up to 80GB each).

The relationships at the base of the animal tree of life are still under intensive discussion. This is one of the most fiercely and controversial debates these days in evolutionary biology, due to the profound implications both Porifera-sister and Ctenophora-sister (see above) have on our understanding of early animal evolution. Not only our understanding of the

evolution of key animal traits, such as the nervous system is affected - single origin under Porifera-sister, maybe two independent origins under Ctenophora-sister – also our general understanding of how evolution proceeds is affected. The more classical Porifera-sister hypothesis is consistent with a relatively simple last common ancestor of all animals and a gradual progressive evolution from simple to complex animals. Under Ctenophora-sister, the last last common ancestor of all animals was likely much more complex than previously thought and likely there was no stepwise addition of more complex traits but a significant loss in complexity of sponges and Placozoa would have happened, in addition to a possible convergent evolution of a neural system in Ctenophora and the common ancestor of the Cnidaria and the Bilateria. We have addressed the question of whether the Ctenophora-sister hypothesis is real since nearly a decade with phylogenomic data, which has grown significantly in size, both in terms of taxa (leaves) and genes. Datasets we currently analyse easily can have sizes of >100 taxa x >500,000 amino acid positions. We have shown in multiple phylogenomic studies that the site-heterogeneous models of the CAT family, so far only implemented in the program Phylobayes-mpi, generally fit phylogenomic data much better than site-homogeneous models, such as GTR, WAG, LG, implemented in software like RAxML and MrBayes. Because it is necessary to use best-fit evolutionary models for phylogenetic analyses, we currently mainly use Phylobayes-mpi for such phylogenomic studies. However, analyses using the CAT models are computationally very intensive, but the code of Phylobayes-mpi is not fully optimized for parallel computing, it does not scale well above 100 cores. Consequently, a single chain of an analysis of a phylogenomic alignment can easily consume more than 500 hours of runtime on 112 cores on CoolMUC-2 (the typical number of cores used) to reach convergence, or, if too large, it can not be analysed on CoolMUC-2 due to memory restrictions and has to be jackknifed into smaller replicates to be computable. Only a few files are generated per analysis, but some of them (the .chain files) can reach sizes of more >25GB for each run (if -s option is chosen in phylobayes, necessary for many downstream analyses). In any case, a major restriction to carry out such analyses on CoolMUC-2 has been its walltime of 48 hours per analysis, necessitating multiple resubmissions and restarts, which can cause output file corruption. However, the analyses yet conducted on CoolMUC-2 in this context, published in high-profile journals such as Proceedings of the National Academy of Sciences of the USA [3] and Current Biology [1,4], have so far suggested that the Ctenophora-sister hypothesis very likely is a phylogenetic (tree reconstruction) artifact, caused by systematic error, such as evolutionary model misspecification and inadequate consideration of data heterogeneity, resulting in the so-called long-branch branch attraction artifact.

Sponges harbour numerous bacteria in their bodies. Some of these are symbiotic and play important roles in the nutrition of their sponge hosts. Despite their importance, the origin of most sponge symbionts, and of the symbiotic relationship per se remains to be determined. In order to provide an estimate of the age of a cyanobacterial sponge symbiont, we assembled a comprehensive sequence dataset of the phylum Cyanobacteria and inferred a phylogeny of this phylum using the program Phylobayes. Using this phylogenetic tree we estimated a time-calibrated phylogeny. The time calibrated phylogeny (chronogram) was inferred using the program BEAST 2.1 in combination with the library BEAGLE. BEAGLE allows for the parallelization of the likelihood computation and accelerates the estimation of chronograms in BEAST. For all analyses the alignment was analyzed using one computing node (28 cores), results can be obtained for relatively large datasets within weeks, instead of months. This allows for testing different parameter combinations and better explore the parameter landscape. The resulting chronogram will be used to infer the origin of symbiotic cyanobacteria in sponge and assess whether symbiosis in sponges is an ancient trait or a recent acquisition.

On-going Research / Outlook

The CoolMUC-2 system helps for all parts of these projects by providing access to fast multi-core computing infrastructure, including the large memory ‘hugemem’ nodes. Although our research would not be possible without this kind of computing power, one of the main restrictions to our analyses is the wall time of 48 hours (mpp2) to 168 hours (‘hugemem’), which is too short for many of the aforementioned analyses to complete without many time-consuming resubmissions/ restarts. In addition, some assembly and phylogeny tools lack any checkpointing functionality, making the use of the CoolMUC-2 only possible for relatively small datasets with these tools. Doubling, or better lifting completely, the wall time or allowing, for example, to allocate several ‘hugemem’ nodes to one run would greatly help us to complete some of our analyses in a more timely manner. In the future we will continue to use the CoolMUC-2 infrastructure for our research, also within the recently started Horizon 2020 Marie-Curie Innovative Training Network (ITN) “Comparative Genomics of Non-Model Invertebrates” (ITN-IGNITE.eu), of which the LRZ is a partner institution. This project aims to sequence, assemble and analyse an estimated 20 genomes, and the CoolMUC-2 system will be used widely and intensely to analyse this data.

References and Links

[1] Roberto Feuda, Martin Dohrmann, Walker Pett, Hervé Philippe, Omar Rota-Stabelli, Nicolas Lartillot, Gert Wörheide, and Davide Pisani. 2017. Improved Modeling of Compositional Heterogeneity Supports Sponges as Sister to All Other Animals. Curr. Biol. 27, 24 (December 2017), 3864–3870.e4.

[2] Warren R. Francis and Gert Wörheide. 2017. Similar Ratios of Introns to Intergenic Sequence across Animal Genomes. Genome Biol. Evol. 9, 6 (June 2017), 1582–1598.

[3] Davide Pisani, Walker Pett, Martin Dohrmann, Roberto Feuda, Omar Rota-Stabelli, Hervé Philippe, Nicolas Lartillot, and Gert Wörheide. 2015. Genomic data do not support comb jellies as the sister group to all other animals. Proc. Natl. Acad. Sci. U. S. A. 112, 50 (November 2015), 15402–15407.

[4] Paul Simion, Hervé Philippe, Denis Baurain, Muriel Jager, Daniel J. Richter, Arnaud Di Franco, Béatrice Roure, Nori Satoh, Éric Quéinnec, Alexander Ereskovsky, Pascal Lapébie, Erwan Corre, Frédéric Delsuc, Nicole King, Gert Wörheide, and Michaël Manuel. 2017. A Large and Consistent Phylogenomic Dataset Supports Sponges as the Sister Group to All Other Animals. Current Biology 27, 7 (April 2017), 958–967.

[5] Gert Wörheide. 20110410. Molecular Geobiology and Palaeobiology Lab. Molecular Geo- and Palaeobiology Lab, LMU Munich. http://www.geobiology.eu

Solid State NMR for Large Biomolecules

Research Institution
Bavarian NMR Research Center

Principal Investigator
Bernd Reif

Researchers
Zdenek Tosner, Matthias Brandl, Riddhiman Sarkar

Linux Cluster Project ID: pr86gi

Introduction

Solid state NMR for biological samples has seen tremendous advancements in the last decade. However, sensitivity of solid-state NMR experiments always suffers from a number of parameters. One of them is inhomogeneous radio frequency (RF) profile across the sample volume. In general, the sample in solid-state NMR resides in a rotor that is placed within a solenoidal coil. RF fields are applied through such solenoidal coils that excite nuclear spins. It has been observed that the RF field distribution is not homogeneous, which leads to imperfect excitation of NMR signals in the sample volume. It is shown that by using Optimal Control theory, it is possible to design NMR pulses that are largely insensitive towards RF inhomogeneity. This leads to a gain in sensitivity of NMR experiments by a factor that is not achievable by conventional means.

Results and Methods

We are using SIMPSON (a simulation package for solid-state NMR) for the optimization of radio frequency (RF) pulses using its Optimal Control functionality. In addition, these pulses are computationally characterized and compared to conventionally used, non-optimized pulses. Large scale pulse optimizations (including all computationally expensive complications) generally run for approx. 4 wall hours on 50 cores, followed by approx. 16 wall hours on 420 cores, on the CoolMUC-2 cluster. About 15 of these large-scale optimization jobs were run in the past year. Pulse characterizations average at approx. 1 wall hour on 150 cores, with on the order of 50 jobs in the past year.

On-going Research / Outlook

We continue to develop Optimal Control based RF pulse sequence design by using the Linux clusters for various steps in NMR experiments.

References and Links

[1] Tosner et al., Overcoming volume selectivity of dipolar recoupling in biological solid state NMR, Angewandte Chemie Int. Ed (2018). https://doi.org/10.1002/ange.201805002

Appendix: System Description

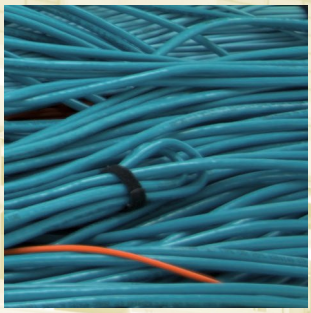

CoolMUC: System Description

The CoolMUC-1 system was installed by Megware in 2011 as a significant extension of the Tier-2 high performance infrastructure. The machine had 178 dual socket nodes, based on AMD Magny Cours processors with 8 cores per socket and Infiniband QDR interconnect. The system also served as a research platform for energy efficiency and cooling technologies, since a large part of it was water-cooled on the system board level with a high inlet temperature (>38 °C), and a smaller part of it was air-cooled with absorption cooling technology. On the software side, the SLURM scheduler was deployed to process user jobs, and Par-Tec's Parastation MPI supported execution of large scale distributed memory parallelism.

In the fall of 2015, the LRZ started user operation of CooLMUC-2. The hardware of the system was identical to SuperMUC Phase 2, offering 384 dual socket nodes with Intel Haswell processors and Infiniband FDR interconnect, which was also used to connect to the parallel GPFS file system of SuperMUC. This allowed users to switch more easily between the different HPC resources at the LRZ, since they could access their data from both systems. Just like CoolMUC-1, CoolMUC-2 was a prototype system for the next-gen LRZ cooling solution. Lessons learned from operating CoolMUC-1 influenced the new design to make it even more efficient. Together with SorTech AG, a manufacturer of adsorption chillers, IBM Research Zürich, and Lenovo Germany, a new concept was developed: The hot outlet water was used to drive six adsorption chillers that generated refrigerated water, which was then used to cool about 90% of SuperMUCs disk storage systems.

Two years later, in the fall of 2017, Megware installed CoolMUC-3, with 148 nodes based on Intels Many-Core architecture Knights Landing. As with previous CoolMUC systems, CoolMUC-3 is used to research future HPC architectures and programming models. On the infrastructure side, the power supplies are now also cooled using warm water, allowing a thermal isolation of the rack and thus reducing heat exchange to air. Additionally, possibilities for fine-granular control of applications are also being investigated in order to further reduce energy consumption.

Within many applications, there are often performance degrading factors that are particularly noticeable on modern processors; unfortunately, these factors are often deeply embedded in the design of the data layout, so that the amount of work required to solve the problems can be considerable. To a certain extent, the development environment provided by Intel provides support for systematic optimization, such as conversion from an (usually non-vectorizable and therefore unfavorable) array-of-structures layout to structures-of-arrays, or for the identification of serially running code areas that can then be converted to multi-threading.

Technical details about all three systems can be found in the table on the next page.

Figure 1: CoolMUC-1 (front) and adsorption chiller (back). Picture: Megware, CC-BY-SA 4.0.

Figure 2: CoolMUC-2 (left) and adsorption chiller (right). Picture: Michael Klinksik.

	CoolMUC-1	CoolMUC-2	CoolMUC-3
Begin of operation	2011	2015	2017
End of operation	2017		
Processor type	AMD Opteron 6128HE ("Magny Cours")	Intel Xeon E-2697 v3 ("Haswell")	Intel Xeon Phi 7210-F ("Knights Landing")
Number of nodes	183	385	148
Cores per node	16	28	64
Threads per core	1	2	4
Core frequency	2.0 GHz	2.6 GHz	1.3 GHz
Memory per node	16 GB (DDR3)	64 GB (DDR4)	96 GB (DDR4), 16 GB (MCDRAM)
Interconnect	Infiniband QDR	Infiniband FDR14	Intel Omnipath 1
Peak performance	22.7 TFlop/s	366.4 TFlop/s	394 TFlop/s
Operating system	SUSE Linux Enterprise Server		
Batch scheduler	Slurm Workload Manager		

Figure 3: CoolMUC-3.

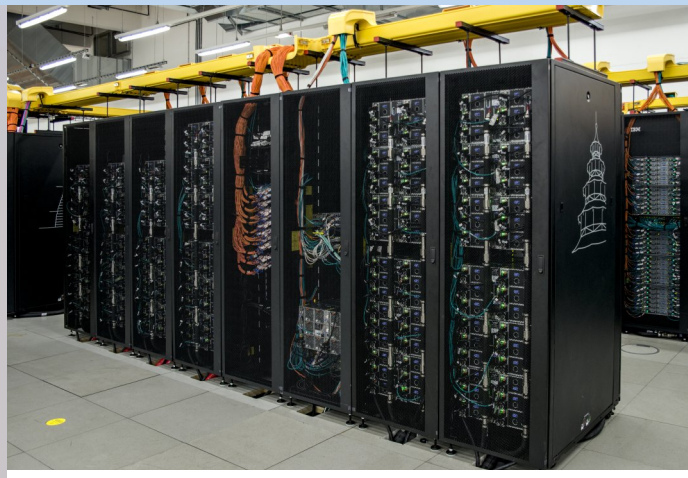

In this book, the Leibniz Supercomputing Centre (LRZ) reports on the results of numerical simulations, performed in the period 2015–2018 on the high performance systems CoolMUC-1, CoolMUC-2, and CoolMUC-3. The 44 project reports give an impressive overview of the utilization of the CoolMUC machines, the Tier-2 systems of the Bavarian Academy of Sciences and Humanities.

CoolMUC-1 (left) began user operation in Mid-2011, **CoolMUC-2** (top right) started early 2015, and **CoolMUC-3** (bottom right) became operational by the end of 2017. A detailed system description can be found in the appendix.

The articles provide an overview of the broad range of applications that use high performance computing to solve challenging scientific problems. For each project, the scientific background is described, along with the results achieved and the methodology used. References for further reading are included with each report.

ISBN 978-3-9816675-3-0
https://www.lrz.de/hpcbooks